# Weather Forecast Review Project
# for
# Operational Open-water River Forecasting

**A report prepared for**
Alberta Environment and Sustainable Resource Development
**River Forecast Centre**
**By**
**AMEC**
**June 2014**

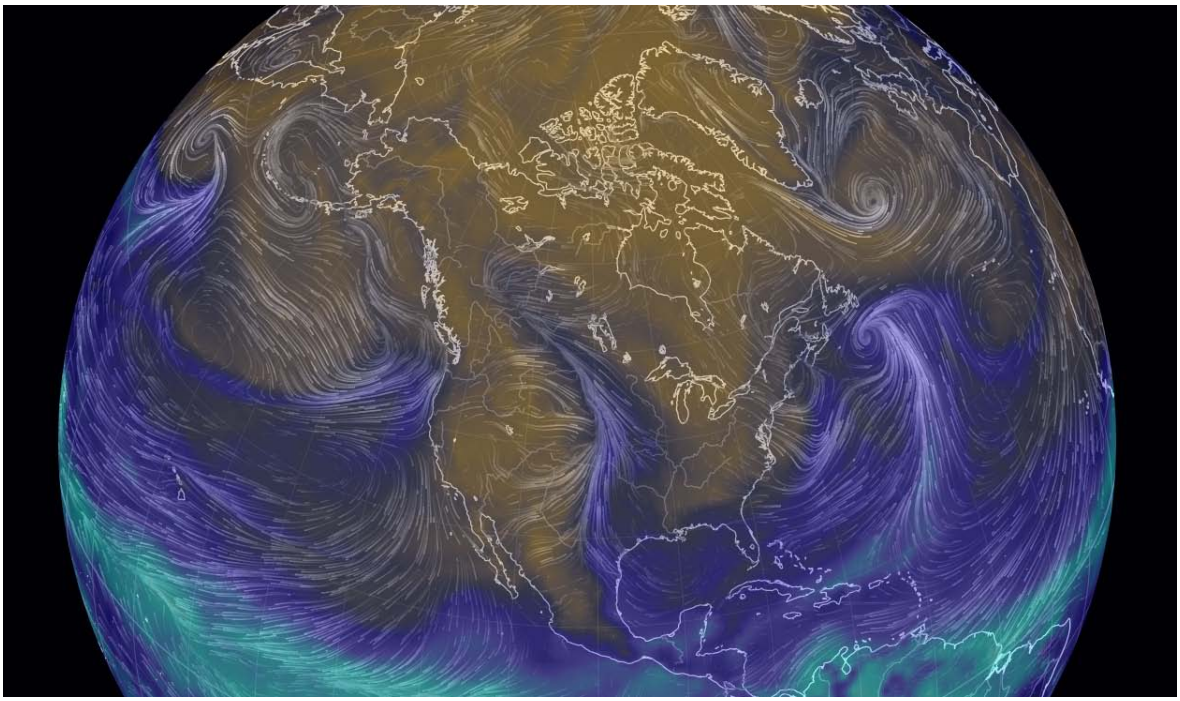

Cover Photo: Total Atmospheric Precipitable Water and Surface Winds, showing a plume of moisture from the Gulf of Mexico being carried into southern Alberta (20140423-18UTC)
http://earth.nullschool.net/

# TABLE OF CONTENTS

**PAGE**

## TABLE OF CONTENTS (*cont*)

**PAGE**

## LIST OF FIGURES

## LIST OF TABLES

## Glossary of Abbreviations

| | |
|---|---|
| ARPS | Advanced Regional Prediction System |
| ARW | NCAR Advanced Research WRF |
| CAPE | Convective Available Potential Energy |
| CLASS | Canadian Land Surface Scheme |
| CMC | Canadian Meteorological Centre |
| CP | Convective Parameterization |
| DTC | Developmental Test Center. |
| EC | Environment Canada |
| ECMWF | European Center for Medium range Weather Forecasting |
| EPS | Ensemble Prediction System |
| ETS | Equitable Threat score |
| ESMF | Earth System Modeling Framework |
| ESRD | Alberta Environment and Sustainable Resource Development |
| FAR | False Alarm Ratio |
| FIM | Flow-following finite-volume Icosahedral Model |
| IBC | Insurance Bureau of Canada |
| GDPS | Global Deterministic Prediction System |
| GEFS | Global Ensemble Forecast System |
| GEM | Global Environmental Multi-scale Model |
| GFS | Global Forecast System |
| GPLLJ | Great Plains Low Level Jet |
| GSI | Grid-Point Statistical Interpolation |
| HIRESW | High-Resolution Window Forecast System |
| HRDPS | High Resolution Deterministic Prediction System |
| IFS | Integrated Forecast System |
| ISBA | Interaction Soil-Biosphere-Atmosphere |
| LAM | Limited Area Model |
| LES | Large Eddy Simulation |
| LLJ | Low Level Jet |
| MCS | Meso-scale Convective System |
| MLCOL | Mid-level Cold Low |
| MRB | Meteorological Research Branch |
| MSC | Meteorological Service of Canada |
| MSLP | Mean Sea Level Pressure |
| NAM | North American Meso-scale forecast system |
| NAVGEM | Naval Research Laboratory Navy Global Environmental Model |
| NCAR | National Center for Atmospheric Research |
| NCEP | National Center for Environmental Prediction |
| NAEFS | North American Ensemble Forecast System |
| NEMS | NOAA Environmental Modeling System |
| NMM | Non-hydrostatic, hybrid vertical coordinate mesoscale model |
| NMM-B | Non-hydrostatic Multi-scale Model B-grid version |
| NMSM | National Meteorological Service of Mexico |
| NOAA | National Oceanic and Atmospheric Administration of the USA |

| | |
|---|---|
| NUOPC | National Unified Operational Predication Capability |
| NWP | Numerical Weather Prediction |
| NWS | National Weather Service of the USA |
| PBL | Planetary Boundary Layer |
| PELLJ | Prairie Easterly Low Level Jet |
| POD | Probability of Detection |
| PTP | Perturbations of Physics Tendencies |
| PV | Positive Vorticity |
| QPF | Quantitative Precipitation Forecast |
| RDPS | Regional Deterministic Prediction System |
| REPS | Regional Ensemble Prediction System |
| RFC | River Forecast Centre |
| RH | Relative Humidity |
| RPN | Recherche en Prévision Numérique |
| RRTMG | Rapid Radiative transfer model |
| RUC | Rapid Update Cycle model |
| SL | Surface Low |
| UTC | Universal Coordinated Time |
| WRF | Weather Research and Forecasting Modeling System |
| WRFEMS | Weather Research and Forecasting Environmental Modeling System |

## 1.0 EXECUTIVE SUMMARY

The purpose of this project was to develop an understanding of the uncertainties in weather forecasting and propose a method of how the River Forecast Centre (RFC) can manage those uncertainties when modeling rainfall scenarios and issuing flood advisories. The ultimate needs of any RFC are accurate forecasts of rainfall amount, location, timing, and intensity. This project was designed to assess how well these rainfall forecast requirements are currently being met by the current suite of popular numerical weather prediction (NWP) models, for the extreme events in Alberta, when they are needed the most. Specifically discussed is exactly how well the existing NWP models perform in these severe flood situations and what their variability is leading up to the event.

Extreme rainfall events that affected Albertans in 2013, 2012, 2011, 2010, 2007, 2005, and 2002, were analyzed in order to:

- Document the specific meteorological factors that caused the extreme rainfall amounts;
- Assess the performance of several NWP models in their ability to forecast the amount, location, and temporal and spatial variability of the precipitation; and
- As a function of forecast lead time.

The four NWP models analyzed for this project were the Canadian global environmental multi-scale (GEM) Global model, GEM Regional model, and the global forecast system (GFS) and North American meso-scale forecast system (NAM) models from the USA. Between 2011 and 2013, all the operational NWP models have received upgrades and improvements to their physics parameterizations and their horizontal and vertical resolution. Due to these recent changes to the NWP models, more emphasis was placed on the analyses and assessments of model performance for the most recent 2013 events, which occurred after the latest changes.

Numerical prediction of summertime convection over Alberta is very challenging due to the spatial distribution of the convective precipitation and orographic effects. High resolution model details can look amazingly realistic; however, the entire event may be misplaced, occur sooner or later, or may not occur at all. Careful examination of the situation is required to assess how plausible the prediction is, and other model runs, even coarser-resolution runs with less detailed physical parameterizations may give a sense of how likely an event is to occur or where and when it is more likely to occur.

A major obstacle to accurate weather forecasts, especially in western Canada, comes from the lack of observational data to provide adequate and accurate initial and boundary conditions for the input to the weather models. If a weather model is incorrectly initialized at a certain location, advection will transport this faulty situation downwind. The lack of detailed upper-air observations off the Pacific Coast and the coarse network of upper atmosphere sounding stations in western Canada is a serious limitation for proper modeling of the extreme events in Alberta, especially evident at the longer forecast lead times that are desired by hydrologic modellers. Upper air soundings are available only two times a day at 0 UTC and 12 UTC (5 pm and 5 am MST). It is very evident that the model forecasts at 06 UTC (11 pm MST) and 18 UTC (11 am MST) have greater and significant variability, most likely associated with the lack of

updated radiosonde data at 06 UTC and 18 UTC for their initialization conditions. Surface station observations are also sparse in the mountains and foothills, northern Alberta, and Saskatchewan; therefore, there is a general lack of data to provide the necessary initial and boundary conditions required to achieve optimal model performance.

Verification of quantitative precipitation forecasts (QPFs) presents many scientific challenges that are associated with the characteristics of the forecasts as well as the observations. Precipitation is a highly discontinuous variable in both time and space. Statistics were computed for average depths over target precipitation zones (sub-basins) used as inputs for the hydrological modeling, using thresholds more representative of potentially dangerous amounts (e.g., >25 and >100 mm).

All of the NWP models did a relatively poor job in forecasting the most extreme observed precipitation amounts, locations, and their spatial and temporal variability more than 24 hours in advance. Automated, high-resolution temporal, and spatial QPF forecasts that may be automatically input into operational hydrologic models are now possible; however, this study indicates that this level of sophistication may not lead to improved flood forecasts and warnings more than 24 hours in advance. For example, none of the NWP models accurately forecast the June 2013 extreme rainfall amounts and extent in southern Alberta. Burns Creek reported ~350 mm rainfall over a 72 hour period for this event. The GFS model forecast 72 hour accumulations for that area of ~320 mm, 5 days in advance; however, subsequent model forecasts were all less and highly variable, thereby reducing the confidence in the earlier forecast. The GFS and NAM models forecast the most rain; >150 mm, 48 hours before the start of the 3-day flood event, within the target basin. However, the NAM forecast greater amounts in other sub-basins, and their forecasts at 6 and 18 UTC fluctuated considerably, with significantly lower values, which once again lowers the confidence in the higher amounts at the time they were forecast. The GFS model produced the most consistent high values of precipitation extending out to 48 hours lead time. Precipitation >100 mm was consistently forecast 72 hours (3 days) in advance over the sub-basin near the Burns Creek station; however, there were also significant deviations at the 6 hour intervals. The Global Deterministic Prediction System (GDPS) model had one high (~290 mm) forecast value 3.5 days in advance, and then consistently forecast about 100 to 150 mm (<50% of the maximum observed) in the period 2 to 3 days before the event. The Regional Deterministic Prediction System (RDPS) model is limited by its maximum 48 hour forecast period, and consistently forecast the lowest precipitation the day before the event started.

The latest, advanced version of the Weather Research and Forecasting Modeling System (WRF) was run for the June 2013 event. The forecasts of total 72-hour precipitation, 2 days in advance and 1 day in advance were disappointing. There were no obvious differences or advantages to using the WRF, in spite of its very high spatial resolution (4 km) and explicit convection. The WRF simulation was conducted in the same manner in which it would have been run in real-time, with initialization using the available GFS model data at 48 hours lead time for initial and boundary conditions. The WRF model results in this study suffered from the errors and limitations introduced by the erroneous real-time GFS initialization.

We must conclude that considerable uncertainty is inherent in the current state-of-the-art precipitation forecasting process. Quantifying this uncertainty is important to the decision making processes associated with flood forecasting. This study supports the current trend in using ensemble-based approaches. Using ensembles is popular because they allow effects of a wide range of "inherent" uncertainties to be incorporated. The main sources of modeling uncertainty are associated with the following main groups:

- Random or systematic errors in the model input boundary and initial conditions;
- Uncertainties due to less than optimal model parameter values; and
- Uncertainties due to incomplete or biased model processes.

Small differences in the initial state of the atmosphere have been shown to result in large differences in the forecast, especially during extreme events. Therefore, forecasting precipitation should be thought of in terms of probabilities. Ensemble statistics from several models can be used to provide a better estimate of the likelihood of future events. The best recommendation is that QPF should be probabilistic, especially at longer projection times.

Ensemble approaches appear to hold the greatest potential (at this time) for operational hydrologic forecasting. As demonstrated with atmospheric ensemble forecasts, the estimates of predictive uncertainty provide forecasters and users with objective guidance about the level of confidence that they may place in the forecasts. In summary, when assessing forecast uncertainty, the departure of each individual model from the ensemble mean is an indication of higher uncertainty. Ensemble spread is an indication of predictability and confidence:

- Small ensemble spread indicates higher confidence and higher predictability.
- Large ensemble spread indicates lower confidence and lower predictability.

The ensemble distribution should be considered when assessing possible scenarios as it can provide insights into the probability of occurrences of extreme events given that the ensemble mean may not always provide the best forecast. The end users can decide to take action based on the probability of occurrence, and prioritized according to their risk tolerance, on an event by event basis.

## 2.0 INTRODUCTION

Southern Alberta is no stranger to flooding, especially in June, typically the wettest month of the year and a time when mountain snowmelt usually intensifies to compound the problem. Alberta Environment and Sustainable Resource Development's (ESRD) RFC has the mandate to provide Albertans with information related to current and future river conditions to enable Albertans to make decisions related to water supply and emergency response planning.

Alberta's major flood that occurred 19 to 22 June 2013 prompted the largest evacuation across Canada in more than 60 years with up to 100,000 Albertans told to leave their homes. It was also the costliest insured natural disaster in Canadian history (Insurance Bureau of Canada [IBC] Media Release 23 September 2013). Economists project damage losses and recovery costs from the flood to exceed $6 billion, including a record $3 billion in insured losses (IBC estimate). In its wake, the flood caused significant infrastructure losses from destroyed roads and hundreds of washed-away bridges and culverts. Among insured losses were thousands of cars and homes demolished and damaged by backed-up sewers and raging torrents of water.

Although high and low forecast precipitation scenarios are currently used to estimate potential flows prior to an event, the actual uncertainty surrounding weather models, documented after a meteorological review of all the data, is required to assist in the enhancement of river forecasting processes. Based on the events in southern Alberta this past June (2013), there is a need to document weather forecast and NWP variability in order to assess the total impact of the uncertainty associated with forecast precipitation totals and rainfall intensities, which in turn impacts the uncertainty associated with forecast river flows.

### 2.1 Primary Project Objectives

The purpose of this project is to develop a better understanding of the uncertainties in weather forecasting and propose a method of how the RFC can manage those uncertainties when modeling rainfall scenarios, providing flood forecasts, and issuing flood advisories and warnings to the public and municipalities in the future. Based on the identified variability in weather forecasts, the report shall include a discussion of the possible changes to the current RFC decision making process that would help manage this variability for improved river forecasts in the future.

## 2.2 Primary Project Tasks

The following list summarizes the tasks mandated by the project:

- For a set of historical flood events, for each of the 5 days prior to the onset of precipitation, document the five day temporal changes in the precipitation forecasts as indicated by the GEM regional and global weather models (from Environment Canada [EC]) and the NAM and GFS models from National Oceanic and Atmospheric Administration of the USA (NOAA). Parameters to be assessed are total precipitation amount, temporal distribution of the precipitation, precipitation intensity and geographic location. The historical flood events shall include the following:
  - 2013 May (Ft McMurray).
  - 2013 June (Central - Southern Alberta).
  - 2012 (Bow Valley, Central Alberta).
  - 2011 (Central Alberta).
  - 2010 (Cypress Hills).
  - 2007 (Swan Hills).
  - 2005 (Central - Southern Alberta).
  - 2002 (Southern Alberta).
    - The NWP data is no longer available for 2002, but the study still reviews the meteorological characteristics.
- Document the variability between the forecasts reviewed in item one and the meteorological data recorded after the event.
- Document the general causes of weather model output variability.
- Document the specific meteorological, spatial, topographical, other factors that affect the range of forecast variability.
- Determine what degree of uncertainty is introduced when taking current weather model precipitation output and transforming it into 6-hourly or hourly hydrological model inputs.
- Based on this identified variability in weather forecasts, propose possible changes to the current RFC decision making process that will help manage this variability when providing flood forecasts and warnings to the public and municipalities.

# 3.0 GENERAL CAUSES OF EXTREME PRECIPITATION EVENTS

## 3.1 Synoptic Features

Heavy precipitation requires the presence of a favourable environment of synoptic and meso-scale forcing that can maintain a sustained high rainfall rate (Doswell et al, 1996). Heavy rainfall is often associated with a well-developed surface cyclone coupled with a cold core low (or a deep trough) aloft. The transport of humidity is often found in the moist warm surface flow or the low level jet (LLJ). At the mid-levels (500 hpa) cyclonic vorticity maxima (or vortices) accentuate a favorable synoptic pattern for significant widespread precipitation (Lin et al, 2001). This pattern provides convergence of the incoming moist airstream, where the moist air can be lifted to the condensation level and develop precipitation.

The spatial organization of rain is often categorized into three types based on the synoptic system background:

- Air-mass precipitation;
- Frontal precipitation; and
- Cyclonic precipitation.

It is also divided into two types based on the intensity and duration:

- Steady precipitation (or stratiform precipitation), which lasts longer with lesser intensity variation; and
- Showery precipitation (or convective precipitation), which has shorter duration with greater intensity variation.

## 3.2 Orographic Effects

Topography plays an important role in the atmospheric circulation as mountainous terrain intensifies cyclonic weather systems on all scales of atmospheric motion (Chung et al., 1976; Lin et al., 2001). The topography of Alberta has a significant influence on the weather of the province. It provides some preferred regions of convective development caused by differential slope heating, orographically forced convergence, and thermally driven upslope winds (Reuter and Nguyen, 1993; Smith and Yau, 1987).

There are two major precipitation enhancement processes due to orography influences:

- Lee Cyclogenesis; and
- Orographic Lifting.

Lee Cyclogenesis is defined as synoptic-scale development of an atmospheric cyclonic circulation on the downwind side of a mountain range. Orographic Lifting is defined as ascending airflow caused by mountains. Both of these dynamic processes contribute to the convergence of the moist air.

## 3.3 Convective Storms

For heavy convective rainfall, convective instability is required. The convective instability provides the energy released by the latent heat due to cloud condensation. The thermal energy is converted to upward kinetic energy providing the lifting for the precipitation formation.

## 3.4 Atmospheric Moisture

The moisture supply is a basic ingredient and is crucial for flood-producing rainstorms (Lin et al, 2001). Without a large amount of moisture, synoptic systems, orographic effects, and conditional instability alone cannot produce long-lasting, widespread, and heavy precipitation in Alberta. Previous water transport studies indicate that it is possible that water vapour originating in the Gulf of Mexico can be carried northwards into Alberta by a LLJ stream (Brimelow and Reuter, 2005). However, there are other sources of atmospheric moisture such as the eastern Pacific Ocean and Hudson Bay. Furthermore, local sources of abundant moisture may exist in the form of transpiration from agricultural fields during the active summer growing season.

## 3.5 Climatology of Extreme Rainfall Events (1921 to 1978)

Verschuren and Wojtiw (1980) compiled a climatology of Alberta rainfall events that had local rainfall amounts exceeding 50 mm. Their data covered the period 1921 to 1978. From this inventory of cases they selected all storms that produced accumulated rainfall amounts exceeding 150 mm during their lifetime. These extreme events had the following characteristics:

- Alberta storms with >150 mm rainfall are relatively scarce. During the 58 years (1921 to 1978), 27 cases occurred, although there is some evidence to suggest that these extreme events may be occurring more frequently as a result of recent climate change.
- Alberta storms with >150 mm rainfall occurred primarily during spring and summer. The monthly occurrences were June (12), August (7), July (5), April (2), and May (1). During the 58 years, no cases occurred during the 7 month period from September to March.
- Alberta storms with >150 mm rainfall typically lasted from 3 to 5 days. Only one storm lasted for 2 days.

It is interesting to note that between 1921 up to May 2005, Alberta never had two storms with rainfall amounts exceeding 150 mm within the same month. June 2005 was the first month ever when two 150+ mm storms occurred, and this was repeated in June 2013.

Historical rainstorms with rainfall of 200 mm or more during their life time in southern Alberta were recorded only five times since 1921. Four out of the five extreme events occurred in the foothills. The Oldman and Bow river basins were the regions with the highest frequency of extreme rainfall in excess of 200 mm. The rainstorm during 5 to 9 June 2005 ranked third in terms of its peak rainfall at the time. That was exceeded again in 2013.

Warner (1973) analyzed in detail the weather system causing the flood of 7 to 8 June 1964 in the Oldman and Milk river basins. The severe rainstorm was a cross-border flood event that covered the eastern slope of the Rocky Mountains of southwestern Alberta, Canada, and

northwest Montana, United States. The affected area in Alberta was near Waterton Lakes Red Rock in the Oldman River basin. It was primarily attributable to an extreme rainfall of 252 mm. It was also affected by the pre-existing saturated moisture condition due to the above normal precipitation in May and below normal temperature during late spring delaying the usual peak snowmelt-runoff into early June. The formation of a low pressure system in the eastern foothills region of the mountains (Lee-side Cyclogenesis) caused upslope flow, sustained the ascending motion by vorticity advection, and channelled moisture from far south (Warner, 1973).

Similar synoptic conditions were identified during the 17 to 20 June 1975 rain storm that caused flooding in the Oldman River Basin. Reuter and Nguyen (1993) investigated the 17 July 1986 rainstorm that caused wide-spread flooding along the banks of the North Saskatchewan, Red Deer and Athabasca rivers. Again Lee Cyclogenesis deepened the upper cold low when the system crossed the Rocky Mountain range. Brimelow and Reuter (2005) analyzed the atmospheric moisture transport for three extreme rainfall events (22 to 23 June 1993; 18 to 19 June 1996, and 28 to 29 July 2001). For all three cases, the moisture trajectories originated near the Gulf of Mexico. The time required to complete the journey varied between 6 and 10 days. The transport of modified Gulf of Mexico moisture to Alberta was realized when northward extension of the Great Plains LLJ to the Dakotas occurred in sync with rapid cyclogenesis over Alberta. In this way, modified low-level moisture from the Gulf of Mexico arrived over the northern Great Plains at the same time as strong southerly flow developed over the Dakotas and Saskatchewan, in advance of the deepening cut-off upper low over Alberta. The moist air was then transported over Saskatchewan and finally westwards over the Athabasca River Basin, where strong rainfall occurred.

A very intense rainstorm occurred on 6 to 7 June 1995 causing extensive flooding that affected mainly the Oldman River Basin. The peak rainfall of 310 mm was recorded at Spionkop Creek, located just north of Waterton Lakes Park. In addition to the heavy rainfall, the 1995 flood was once again compounded by mountain snowmelt runoff.

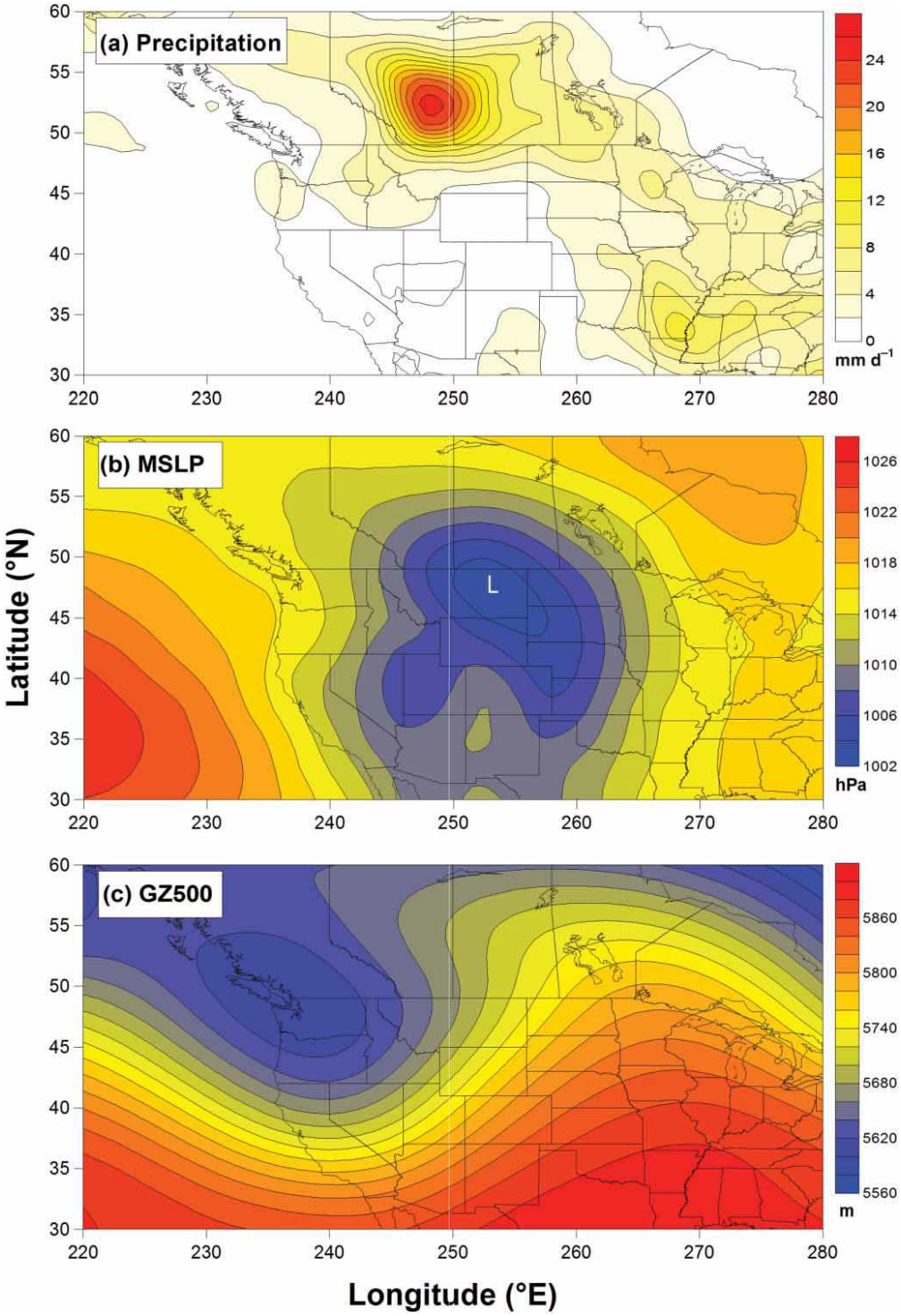


(a) precipitation (mm/day), (b) mean sea-level pressure (hPa), (c) geopotential height (m)

**Figure 1: Composite Storm Characteristics of Highest 15 Extreme Precipitation Events That Occurred Over Western Prairies (South of 55°N and West of 252.5°E) 1950 to 2005**

## 3.6 Common Features of Long-lived Extreme Rain Events (1950 to 2005)

A review of the above climatology of extreme rainfall events in Alberta reveals several common ingredients. Szeto et al. (2011) presented common storm characteristics of the highest 15 extreme precipitation events that occurred over the western prairies (south of 55$^{o}$N and west of 252.5$^{o}$E) during the period 1950 to 2005. The detailed analysis of the 2005 southern Alberta event and other similar events allowed them to identify atmospheric conditions and features critical for the development of an important class of long-lived extreme rain events on the Canadian prairies. Such critical features include enhanced background baroclinicity and north-south atmospheric moisture gradients for surface cyclone development and associated enhanced moisture transport, a broad high pressure area in western and central Canada that blocks the eastward movement of the cyclone and enhances the south–north pressure gradients over the southern prairies, a strong mid-level shortwave or cut-off low that approaches the continent near the international border where it could couple effectively with the surface front for effective cyclogenesis, and dry air in the prairies that facilitates the enhanced sub-cloud evaporation and associated cloud-scale dynamic feedbacks. The synoptic scale weather patterns for these critical features are summarized on **Figure 1** (Szeto et al., 2011).

# 4.0 CASE STUDIES OF ALBERTA FLOODS

## 4.1 June 2002

Szeto et al. (2011) presented a detailed case study analysis of the June 2002 catastrophic rain event that occurred in southern Alberta. Interestingly, the extreme rainfall event occurred during a major drought over the northern United States and Canadian prairies in early June 2002. The storm brought record-breaking rainfall and major flooding to many locations in the region. The detailed analysis revealed several key synoptic and topographic features that affected the development of the extreme rain event.

### 4.1.1 Key Synoptic, Topographic, and Meso-scale Feedback Processes

On 7 June 2002, a shortwave trough with an embedded cut-off low entered the west coast of North America just north of the Canada–United States border. The cut-off low moved south and coupled to a weak surface low (SL) that was developing along a strong quasi-stationary front located over the midwestern United States on 8 June. The coupled system remained almost stationary and significant baroclinic development occurred during the following 2 days. The strong cyclonic flow induced by the deepening SL conveyed moisture from the moist southern and central United States to the western prairies and forced powerful uplifting at the foothills to produce enduring heavy precipitation. In conjunction with the onset of the orographic precipitation, a strong easterly LLJ developed rapidly over the southern prairies, which further facilitated the moisture transport and orographic precipitation. Simultaneously, the SL, along with a high pressure ridge sitting over the eastern United States, induced a strong southerly flow which acted in concert with the Great Plains LLJ to transport a tremendous amount of moisture from the Gulf of Mexico into the central northern United States. Strong updrafts and moisture flux convergence occurred between late evening and the early morning hours when the enhanced LLJ encountered the quasi-stationary surface front located near the international border and this triggered the development of severe diurnal meso-scale convective systems (MCSs) over the eastern prairies during the following 2 days.

First, on the synoptic scale, the upper-level positive vorticity (PV) anomaly induced by the latent heating associated with the orographic clouds and precipitation intensified classic baroclinic growth of the parent system by both enhancing the PV anomalies of the upper level low and slowing its eastward propagation. Second, mesoscale lower-level pressure perturbations induced by differential latent heating and cooling in different regions of the orographic precipitation caused the synoptic scale pressure gradients to be focused into the area of precipitation which in turn enhanced the easterly LLJ and associated moisture transport and orographic precipitation. The storm features were; therefore, phase locked to the Rockies resulting in the slow storm propagation and longevity of the precipitation.

A conceptual model of the synoptic and meso-scale features that affected the development of the June 2002 extreme rain event is given on **Figure 2** (Szeto et al., 2011).

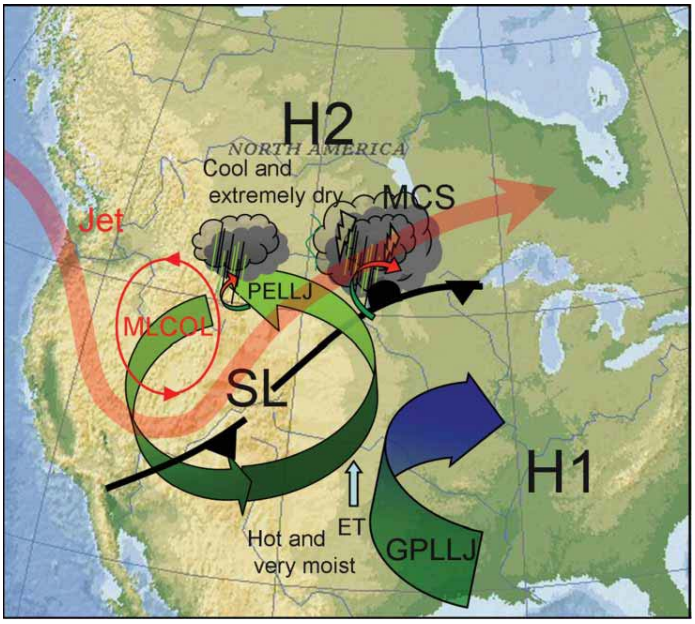


Upper-level features are shown in red and lower-level features in green. MLCOL denotes the mid-level cut-off low, SL the surface low, ET is evapotranspiration, PELLJ the Prairie easterly low-level jet, GPLLJ the Great Plains LLJ, and H1 and H2 the high pressure ridges located east and north of the region, respectively.

**Figure 2: A Schematic Summary of the June 2002 Extreme Rain Storm**

Key features of the conceptual model that are common to these types of extreme rainfall events are the mid-level cold low (MLCOL) and the coupled, long-lived circulation of the SL and the two high pressure systems H1 and H2. The resultant strong, sustained southerly flow, forms the great plains low level jet (GPLLJ) stream and the prairie easterly low level jet (PELLJ) stream, which are able to “funnel” large amounts of moisture from the Gulf of Mexico and Pacific Ocean into southern Alberta, which is then pushed up against the Rocky Mountains, creating upslope precipitation along the mountains and foothills, and enhanced MCS rainfall across southern Alberta. The upper level ridge of high pressure to the east prevents the low pressure precipitating system from moving quickly towards the east thereby further increasing the precipitation accumulation within individual basins.

### 4.2 June 2005

In June 2005, extensive rainfall caused flooding in southern Alberta. A total of 16 Albertan municipalities declared states of emergency for river flooding. Thousands of people were forced to leave their homes. Hundreds of houses were damaged and many farms were flooded. An estimated $400 million of damages in total, and 4 lives were claimed. This devastating flood was described as a “1-in-200-year event” (Dartmouth University, 2005).

To improve our understanding of the meteorological development of these events, Ou (2008) documented the synoptic and mesoscale evolution of the June 2005 Alberta flood events. Weather maps for this event showed a cold low at 500 hPa, and a well-defined moisture tongue at 850-hPa, PV advection at 500 hPa, combined with a surface quasi-stationary inverted trough or trowal (trough of warm air aloft) east of the Rocky Mountains. Once again, these are common

features for these types of extreme rainfall events in southern Alberta. The analysis also suggested that the rainfall was strongly influenced by the underlying orography.

### 4.3 June 2013

The June 2013 super flood in southern Alberta, which extended from Canmore to Calgary and beyond, started in the headwaters of the Bow River watershed on 19 June, 2013 and featured an intense, slow-moving moist upper low pressure system that parked itself over southern Alberta, delivering 3 days of heavy rain. What was not typical was that it stalled and sat over the mountains for days due to a massive high-pressure ridge to the northeast that blocked it from moving east and pushed it up against the Rocky Mountains. The stationary, wide-ranging low drew in warm, moist air from the Pacific Ocean and the Gulf of Mexico, before drenching the Rockies watershed in southeastern British Columbia and southern Alberta. Beginning late on 19 June, the rain in southwestern Alberta started, and poured for 15 to 18 hours. The slow moving low, with embedded thunderstorms, kept drenching the mountains, melting the snowpack but not thawing appreciably the partially frozen ground. The already saturated soil on thinly covered steep slopes could not hold any more water.

Calgary received 68 mm rain over 48 hours, but the rainfall west of the city in the elevated headwaters of the Bow and Elbow rivers was exceptionally heavy. Rainfall rates from this storm were 10 to 20 mm/hour in the higher elevations, with several stations reporting 50% to 70% of their storm rainfall in the first 12 hours. Totals averaged 75 to 150 mm over 2.5 days, with Burns Creek (west of High River at 1,800 m elevation) recording a phenomenal 345 mm (Phillips, 2013). At Canmore, over 200 mm of rain fell – ten times that of a typical summer rainfall. Also contributing to the flood, the warm air and rain melted the remaining snowpack.

The 500 hPa (approximately 5 km MSLP) upper-air meteorological analysis on 20 Jun 2013 is shown on **Figure 3**. The dominant feature is a very large, cold, cut-off low along the United States-Canada border, stretching from Vancouver Island to the Saskatchewan border, and a ridge of high pressure extending from Kansas, across Saskatchewan, to northern Alberta and British Columbia.

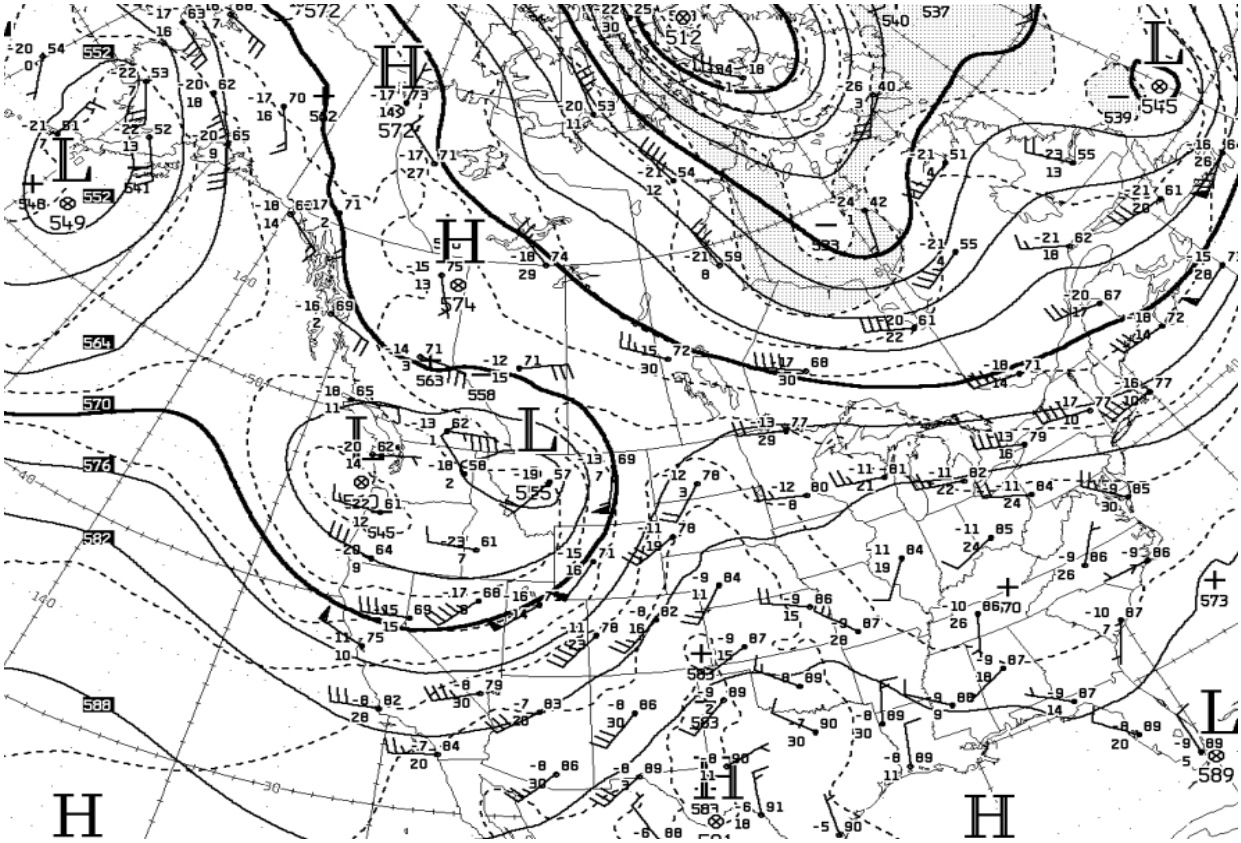

Courtesy A. Liu - Environment Canada

**Figure 3: 500 hPa Analysis Map at 12 UTC 20 June 2013, with 500 hPa Geopotential Height in Solid Line, 1000-500 hPa Thickness in Dashed Line**

The surface map on 20 June 2013 is shown in **Figure 4**. An intense low located in southern Alberta, and its associated counter-clockwise circulation, helped to funnel warm, moist air from the midwestern United States into southern Alberta, and force it up against the foothills and mountains west of Calgary, releasing its convective instability and associated precipitation.

A surface map showing the location of lightning strikes on 20 June 2013 is shown on **Figure 5**. The trace of accumulated precipitation and time of lightning strikes at Burns Creek are shown on **Figure 6**. The convective storms with associated lightning were accompanied by high intensity rainfall, with significant accumulation (approximately 100 mm) over a relatively short time period (6-hour) duration on the evening of 19 June, followed by continuous non-convective rainfall for another 12 hours on 20 June 2013.

A summary of the total rainfall amounts and the rain associated with thunderstorms for stations in the Bow River sub-basin are shown on **Figure 7**.

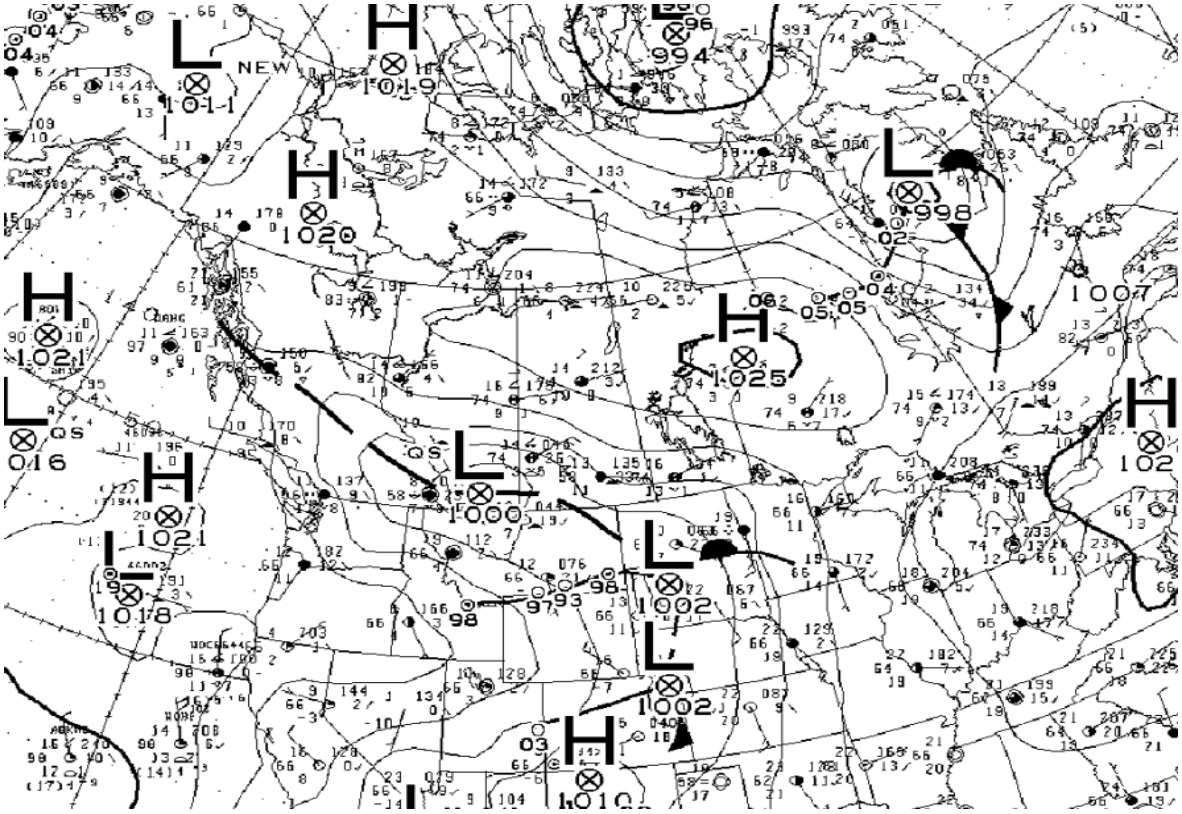

Courtesy A. Liu - Environment Canada

**Figure 4: Surface Analysis Map at 12 UTC 20 June 201, with MSLP in Solid Line**

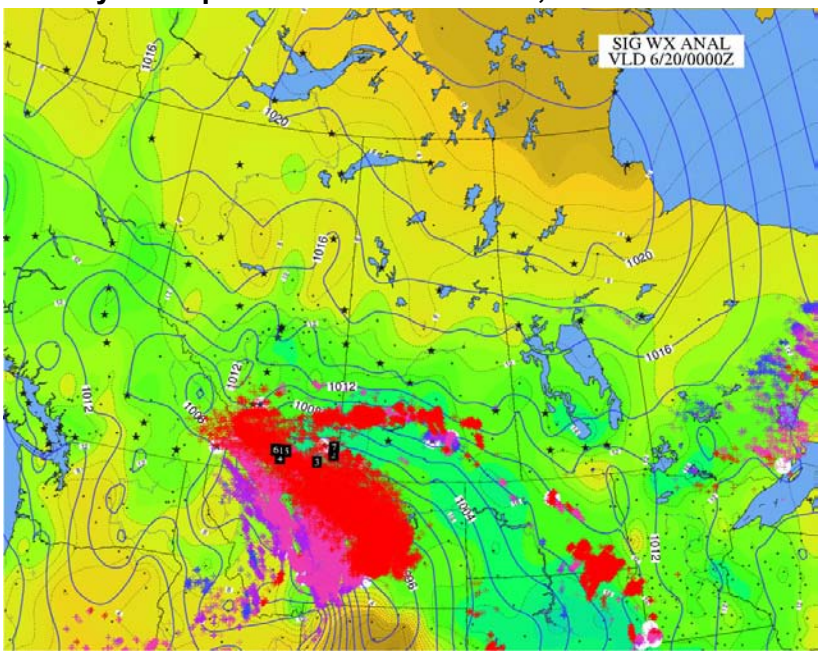


Courtesy B. Kochtubajda, Environment Canada

**Figure 5: MSLP at 00 UTC 20 June 2013, Lighting data from 18 UTC 19 June 2013 to 06 UTC 20 June 2013 (18-21 UTC Blue; 21-00 UTC Purple; 00-03 UTC Pink; 03-06 UTC Red)**

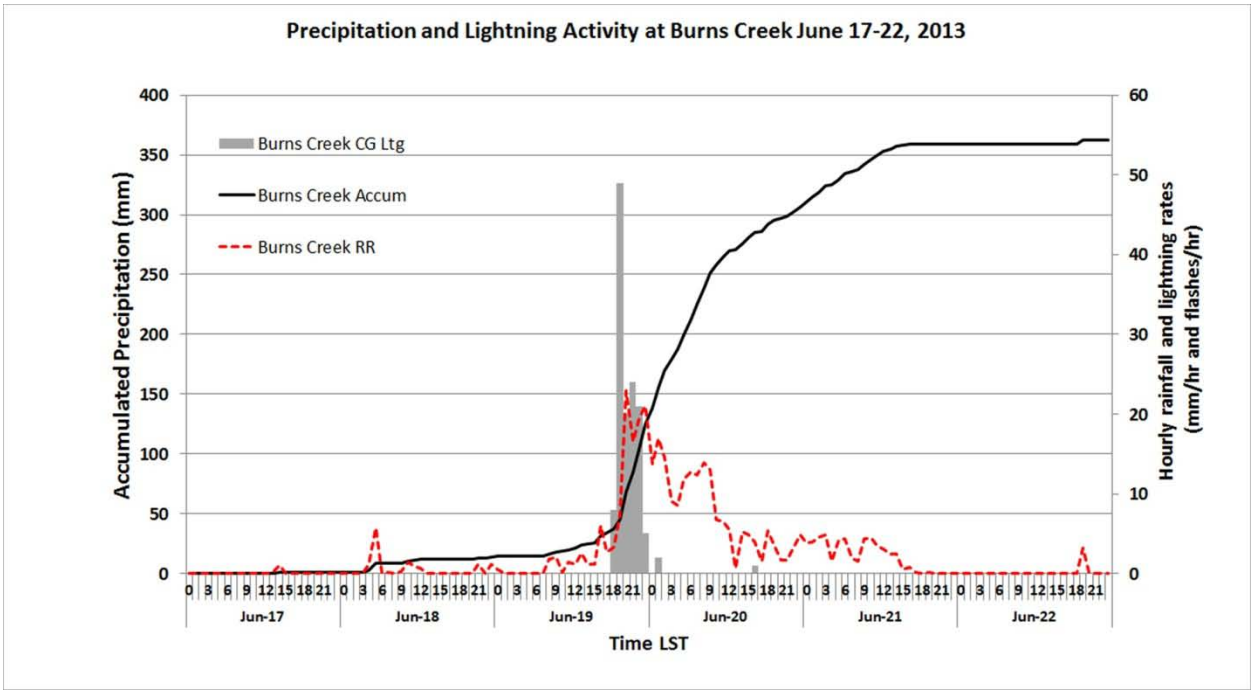


Courtesy A. Liu and B. Kochtubajda, Environment Canada

**Figure 6: Precipitation and Lightning Activity at Burns Creek, 17 to 22 June 2013**

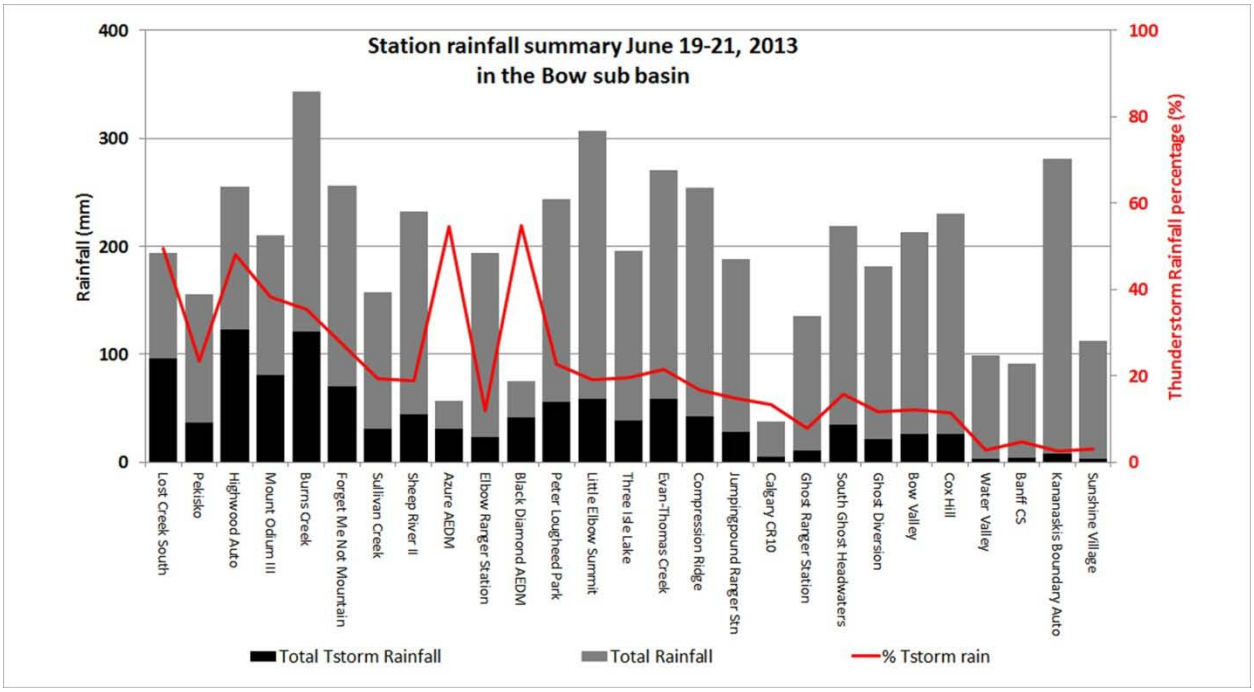


Courtesy B. Kochtubajda, Environment Canada

**Figure 7: Total Rainfall and Rain(%) From Thunderstorms for stations in the Bow River Sub-basin**

The 2002, 2005, and 2013 case studies reveal many common synoptic and mesoscale features, and suggest that both the orographic precipitation and its feedback effects onto the parent storm

need to be accurately represented in models before the numerical predictions of these extreme rainstorms can be accurately represented. These synoptic-mesoscale-topographic feedback processes are responsible for compounding the already extreme situation, and constitute the biggest challenges for NWP and precipitation forecasting.

### 4.3.1 Precipitation Forecasts for the June 2013 Event

The original rainfall forecast early in the week (Monday, 17 June 2013) was for 80 to 160 mm over 48 hours on 19 to 20 June for the Red Deer and Bow river basins, with maximum 12-hour intensities of up to 50 mm corresponding to a 1/5 to 1/10-year rainfall event (ESRD private communication). This forecast did not change significantly until after the rain started on Wednesday night (19 June when EC issued their first warning). EC updated the forecast on the afternoon of 18 June and predicted that rainfall accumulations no greater than 125 mm were expected through 21 June (ESRD private communication). Other forecasts (e.g. from the NOAA) predicted 60 to 70 mm in 12 hours, once again less than the amounts experienced from 19 June around 6 pm to 20 June 6 am (as high as 140 mm). NOAA predicted 148 mm over 72 hours which was about half of the actual measured rainfall amounts.

The June 2013 flooding in Alberta has provided the motivation for the ESRD RFC to investigate why the precipitation for such a severe flood was under predicted by today's weather prediction models. Specifically questioned was exactly how well the existing NWP models perform in these severe flood situations and what their variability is leading up to the event.

## 5.0 NUMERICAL WEATHER PREDICTION - UNDERSTANDING THE PROBLEM

The NWP involves integrating current weather conditions through mathematical models of the atmosphere-ocean system to forecast future weather. Over recent years the forecast skill of NWP systems has been continuously improving (Palmer et al., 2007). Rodwell et al. (2010) showed that over the period 1995 to 2008, the European area-averaged precipitation forecasts gained approximately 2 days at lead times of 3 to 9 days, with the gains due to forecast system upgrades.

One of the underlying objectives of this study is to use the rainfall forecasts from four state-of-the-art global NWP models currently used in Canada and the United States to evaluate their ability to capture the extreme rainfall for the recent extreme flood events in Alberta. The main questions to be addressed are:

- Are the current NWP models capable of providing a realistic depiction of area-averaged rainfall amounts and the location of the area most affected by the extreme rain event?
- What is the dependence of the forecast accuracy on lead time and spatial averaging scale?

In natural systems there exists variability and randomness. A certain amount of uncertainty will always be present within a natural system. Uncertainty is an inevitable outcome of incomplete or imperfect knowledge. Stated another way, it is impossible to describe exactly an existing condition or set of conditions. More than one possible outcome always exists. Our goal is to reduce the uncertainty.

Some key questions related specifically to the problem in this study are as follows.

- Are QPF errors due to bias, or are the errors more random?
- Do the model QPFs show skill?
- How well do the models perform during the extreme high-impact events?
- How much does lead time impact QPF performance?
- At what lead time do the QPF errors become unacceptably large for hydrologic forecasts?

One of the challenges for hydrometeorological data is to take point measurements for single value forecasts and, in turn, apply this information to areas. Complicating this effort is that these forecasts are space and time dependent. A level of uncertainty is involved whenever the space or time scale changes. Just as forecasts are scale dependent, so is the verification.

As an example, consider an areal forecast for 24-hour precipitation. A forecast for a 24-hour period typically has a higher skill than 6-hour forecasts for the same location. This is because it is easier to say that precipitation can occur anywhere within a 24-hour window and more difficult to forecast precipitation within a narrower 6-hour window. In a similar way, the same occurs for a forecast over a large area as compared to smaller areas. The larger area represents a larger “window” in which the precipitation may occur and thus allows a higher skill metric. A smaller area is a smaller “window” and will likely have a lower forecaster skill metric.

Verification of QPF presents many scientific challenges that are associated with the characteristics of the forecasts as well as the observations. Precipitation is a highly discontinuous variable in both time and space. Small forecast errors in timing and spatial distribution may lead to large errors in some verification measures. To choose the most appropriate verification measures, the verification objective needs to be clearly defined. The quantity being verified and the data characteristics need to be part of the definition. Also, QPF can be for points, it can be for grid bins with a gridded product, or it can represent areal averages, such as average precipitation for a given basin. Furthermore, verification results are affected by variations in forecast resolution - both spatial and temporal - and lead time. The QPF verification tools and methodologies should consider the various data resolutions.

Any specific verification measure is not likely to capture all aspects of QPF performance. A variety of verification measures is typically needed to describe the different aspects of the forecast performance. These may look at quantitative error, bias, forecast discrimination, forecast reliability, and forecast skill to name just a few.

## 5.1 General Causes of Weather Model Output Variability

The basic physical equations governing the behaviour of fluids are well known. For fluids which are sufficiently dense to be a continuum, do not contain ionized species, and have velocities small in relation to the speed of light, the momentum equations are the Navier–Stokes equations for Newtonian fluids, which are non-linear differential equations that describe the flow of a fluid whose stress depends linearly on velocity gradients and pressure. Water and air are examples of Newtonian fluids for all practical purposes. Thus, in principle, meteorologists should be able to solve these equations to provide weather forecasts, but only for the last 60 years have practical, although imperfect, computed forecasts been made on a daily basis. Even today, some weather elements, such as heavy precipitation, fog, and local storms, are often poorly forecast with operational NWP models (e.g. Roebber and Bosart, 1998). There are several obstacles to accurately obtaining prognosis using the physical-mathematical modeling approach. First, the mathematical equations that describe air motion, thermodynamic processes, and precipitation microphysics are complex non-linear partial differential equations, which cannot be solved simply by analytical methods. Instead, numerical approximation techniques, which are extremely laborious and require an immense number of computations, must be used. The numerical computations require a fine spatial and temporal resolution; however, there are always important smaller scale features such as turbulent air motion, which are unable to be resolved.

Currently, no single model covers all the required temporal and spatial scales associated with meteorological applications. Examples of the suite of numerical models within EC, shown with their representative time scales and horizontal spatial scales are shown on **Figure 8**. The models cover a time-space range from decades and hundreds of kilometres for global climate prediction to minutes and meters for high resolution modeling of the atmospheric flow around buildings or complex terrain. The current names of the operational models within EC are shown on **Figure 9**.

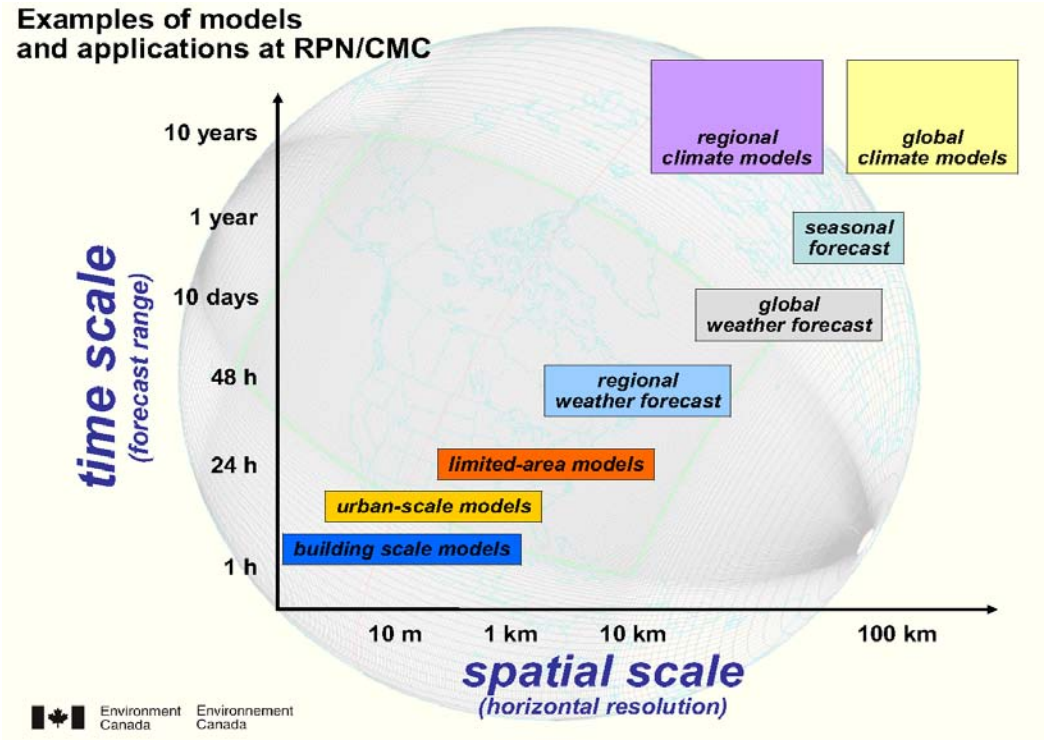


Courtesy J. Milbrandt -Environment Canada

**Figure 8: Examples of Model Applications and Their Representative Temporal and Spatial Scales**

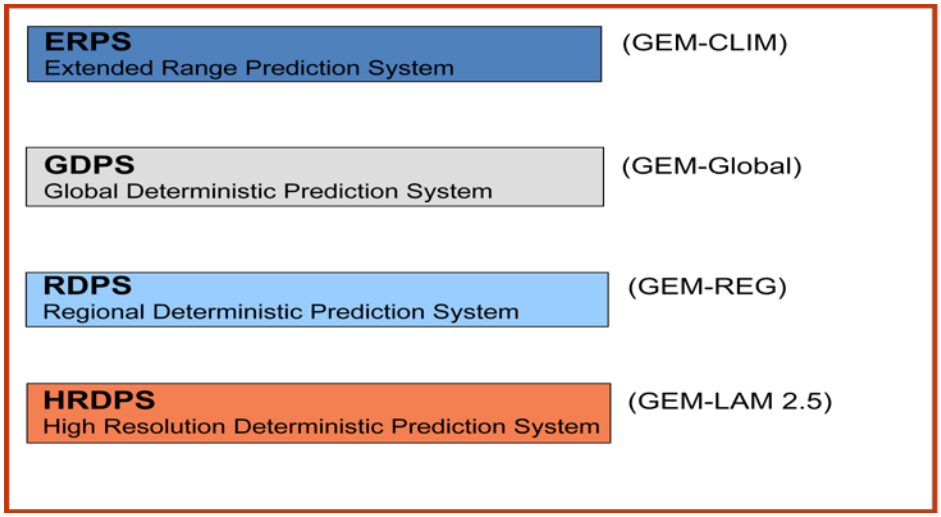


Courtesy J. Milbrandt - Environment Canada

**Figure 9: Current Names of Operational Models at EC**

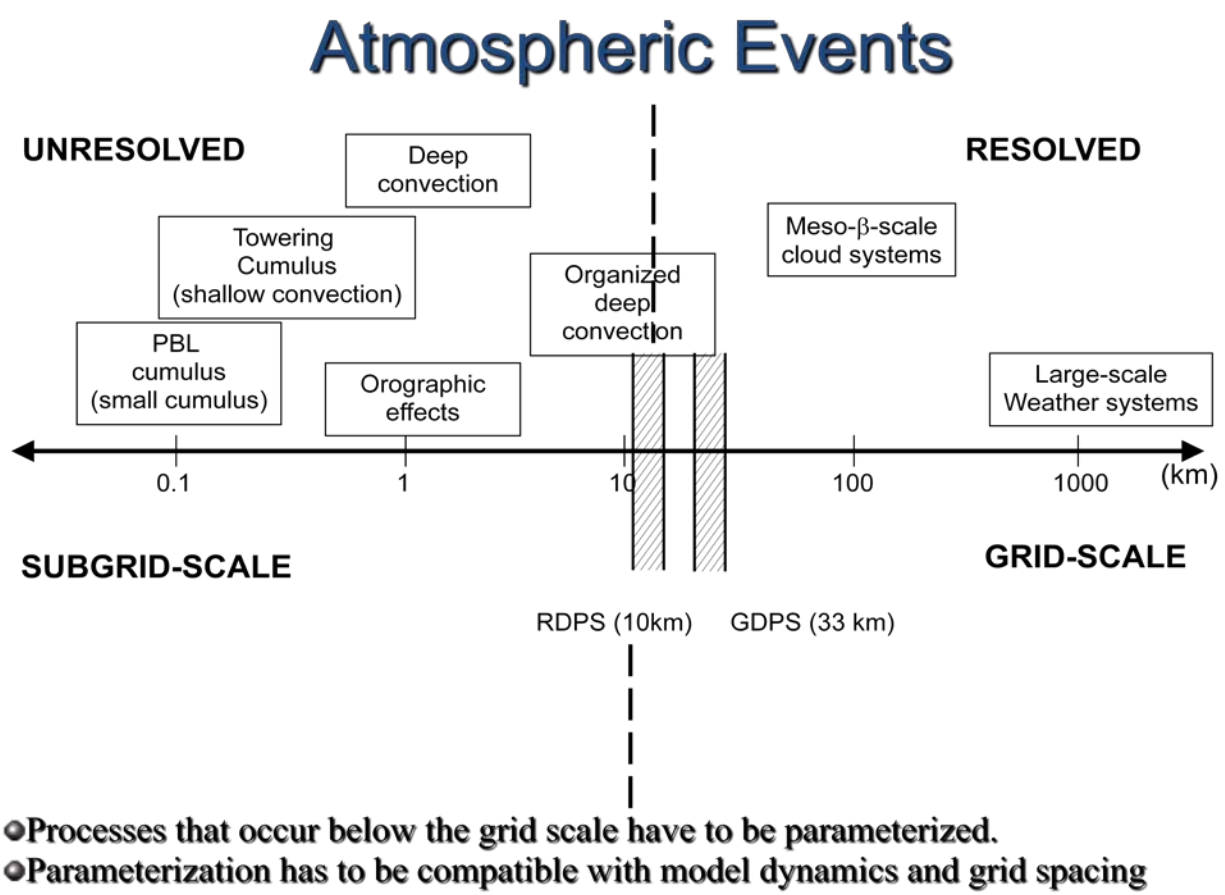


Courtesy R. Goodson – Environment Canada

**Figure 10: Characteristic Spatial Scales of Atmospheric Events Represented Within NWP Models**

The characteristic spatial scales of important atmospheric events and phenomena that are simulated by the NWP models are shown on **Figure 10**. For each type of model, the processes that occur below the spatial grid scale of the model must be parameterized or approximated by simplified relations. These parameterizations must be compatible with the model dynamics and spatial grid spacing, which is often difficult to approximate in a realistic manner. Of particular note are the spatial scales of thunderstorms (deep convection) and orographic effects (localized upslope) which occur on scales of 1 km and; therefore, typically involve parameterization schemes.

A second obstacle to accurate weather forecasts comes from the lack of observational data to provide adequate initial conditions for the input to the weather model (e.g., if a weather model is incorrectly initialized colder than reality at a certain location, advection will transport this faulty coldness downwind). In addition, small initial errors tend to magnify in nonlinear differential equations. Third, most of the time the net force acting on any part of the atmosphere is very small compared to each of the individual forces acting on it (e.g., minute differences in vertical forcing cause significant variation in cloud condensation and precipitation formation).

The data flow chart and spatial and temporal down-scaling of atmospheric processes modeled by operational NWP is shown schematically on **Figure 11**. The flow chart shows that observations play a key role in the data assimilation conducted in the initialization of synoptic and mesoscale NWP models. Upper-air radiosonde atmospheric soundings are collected twice daily (00 and 12 UTC) around the globe. Atmospheric soundings play a major role in the initialization operation. This also means that the data assimilation stage for model runs that are conducted every 6 hours, do not have the luxury of assimilating updated radiosonde data.

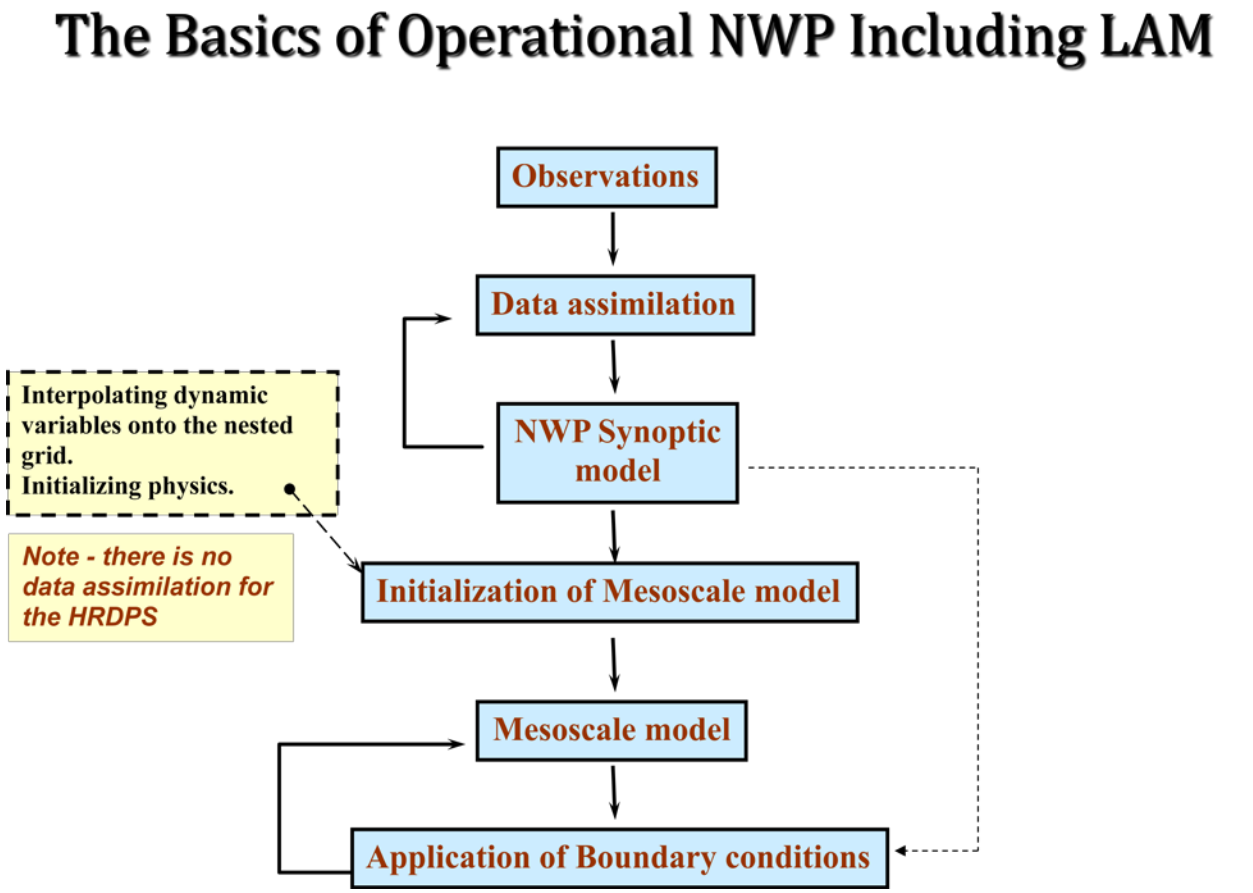


Courtesy J. Milbrandt - Environment Canada

**Figure 11: The Flow Chart of Initialization Data in a Sequence of NWP Models Operating at Different Spatial and Temporal Scales**

Numerical prediction of summertime convection over Alberta can be challenging, particularly due to the spatial distribution of the convective precipitation and orographic effects. Erfani et al. (2003) used the GEM model in a non-hydrostatic configuration to simulate a convective storm over central Alberta. While the simulated storm structure and intensity resembled radar observations, the simulated storm track deviated significantly from the observed storm track. Milbrandt and Yau (2006) used a mesoscale model to simulate a severe convective storm forming over Alberta. Despite the fine spatial resolution of the nested grid, the simulation did not coincide with the observed radar echoes. Summer storms that can produce extensive precipitation continue to present a challenge for accurate simulation.

In summary, the quality of model forecasts is critically dependent upon the following:

- The correctness of the initial conditions:
  - 3-D atmospheric variables.
  - 2-D surface fields.
- Whether the model resolution is appropriate to represent adequately the scale of the critical processes of the primary phenomena of the day.
- How well the parameterization schemes handle the processes which cannot be explicitly modeled.
- The inherent predictability of the weather phenomena.

Even for high resolution models (e.g., 1 to 2 km scales or less), the following issues are important.

- The quality of the boundary conditions of the larger, driving model incorporated into the higher resolution model.
- How often information is transferred from the larger driving model to the higher resolution model.
- How accurately the information transferred is incorporated into the higher resolution model.
- The frequency and quality of added sources of data, and the associated method used, for their assimilation into the domain.
- Errors in initial conditions of high resolution models tend to magnify and compound much more quickly than coarser resolution models (data quality is always a problem).

## 6.0 NUMERICAL MODEL INITIALIZATION

Initialization is the process by which observations are processed to define the initial conditions for a model's dependent variables. The process infers taking observations, performing quality control, assimilating the observations, and ensuring that the final analysis is balanced and representative of the real atmosphere. There are two types of model initialization:

- Static Initialization: interpolation (or downscaling) of data to a model grid and subsequent adjustment as necessary to meet a desired balance condition (e.g., using another model's initial analysis as initial conditions for a limited area model [LAM] simulation).
- Dynamic Initialization: use of a numerical model during a preforecast period to assimilate data, ensure balance, and to spin-up small-scale features.

Currently, initial observations may consist of in-situ observations or remotely sensed observations. All measurements are associated with observational error inherent to the observing platform. In addition, retrieval algorithms inherently introduce observation uncertainty due to sensitivities in their formulations to specific atmospheric constituents (e.g., satellite-based remote sensing platforms are great for measuring upper atmospheric conditions). However, they are often strongly impacted by clouds and precipitation. This can limit their ability to gather observations in the lower to middle troposphere. Also, since the observation is a point observation, it may be of local variability that is not representative of the atmosphere as resolved by the numerical model.

The most common sources of data for initialization of NWP models are surface observations and upper-air radiosondes. However, radiosondes are typically released only twice daily (0 and 12 UTC), and the network of radiosonde stations in Canada is particularly sparse and none are located in the Pacific Ocean upwind of western Canada. The operational network of radiosonde stations is shown on **Figure 12**, and the network in the United States is shown on **Figure 13**. The only regular radiosonde station in Alberta is in Edmonton and there are no stations in Saskatchewan. This network may be sufficient for most typical weather systems; however, the spatial and temporal coverage is almost certainly insufficient to cover the most extreme, dynamically active weather systems over western Canada and systems located offshore the west coast. Unfortunately, this is when the increased data coverage would be of the most value.

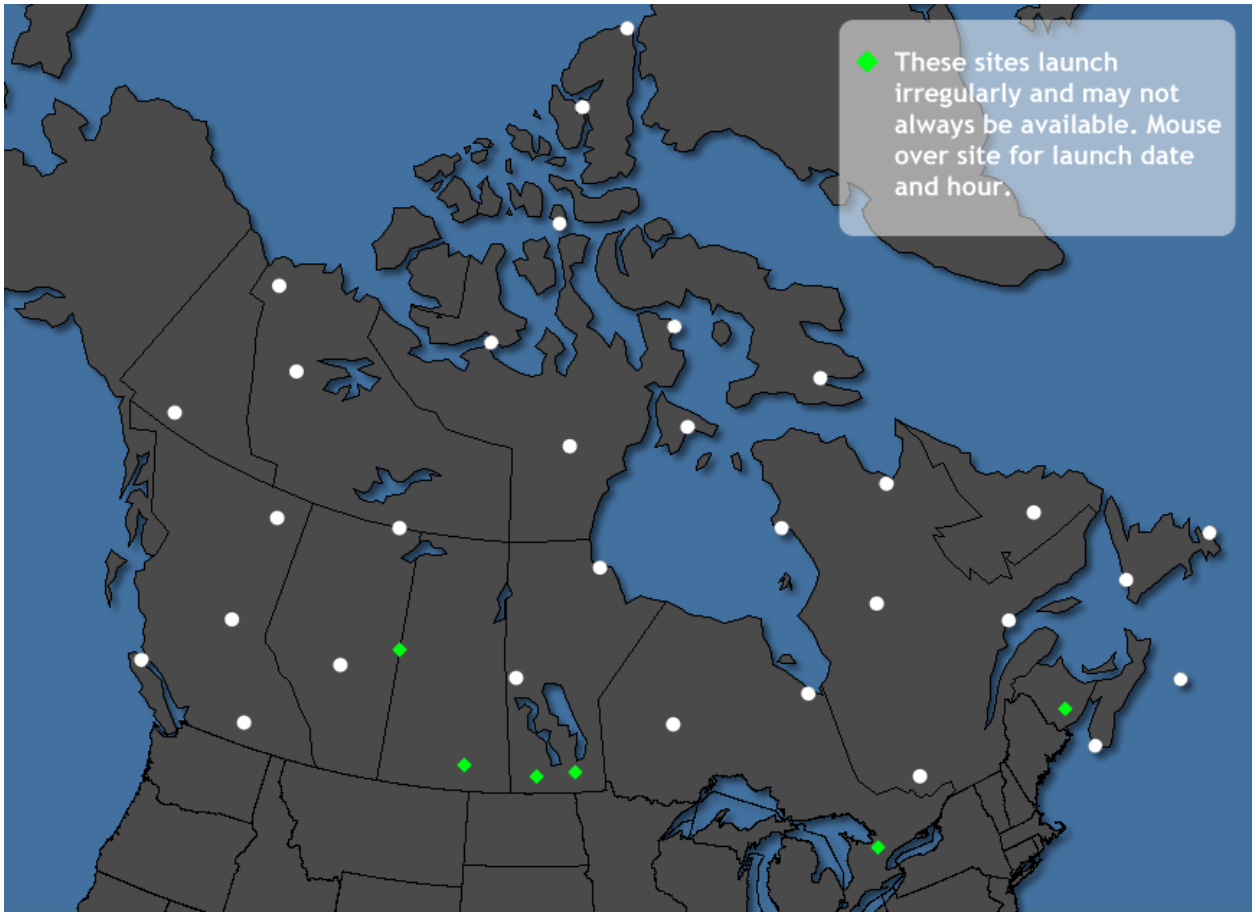


**Figure 12: Observation Network of Regular Radiosonde Releases in Canada**

Quality control protocols are used to ensure that a given observation is of sufficiently high quality to be used within a numerical model analysis. There are many possible means by which an individual observation may be erroneous, independent of inherent observational error or uncertainty. An observation may be rejected due to improper errors introduced during data transmission, systematic errors (improper instrument calibration), or random errors (instrument malfunction). An observation may also be rejected due to climatological limits which test to see if the value is within the range of previously-observed values at that station. This test has resulted in the rejection of some data for rare events. The erroneous discarding of a good observation can have as much of a negative impact upon an initial atmospheric analysis as keeping a bad observation.

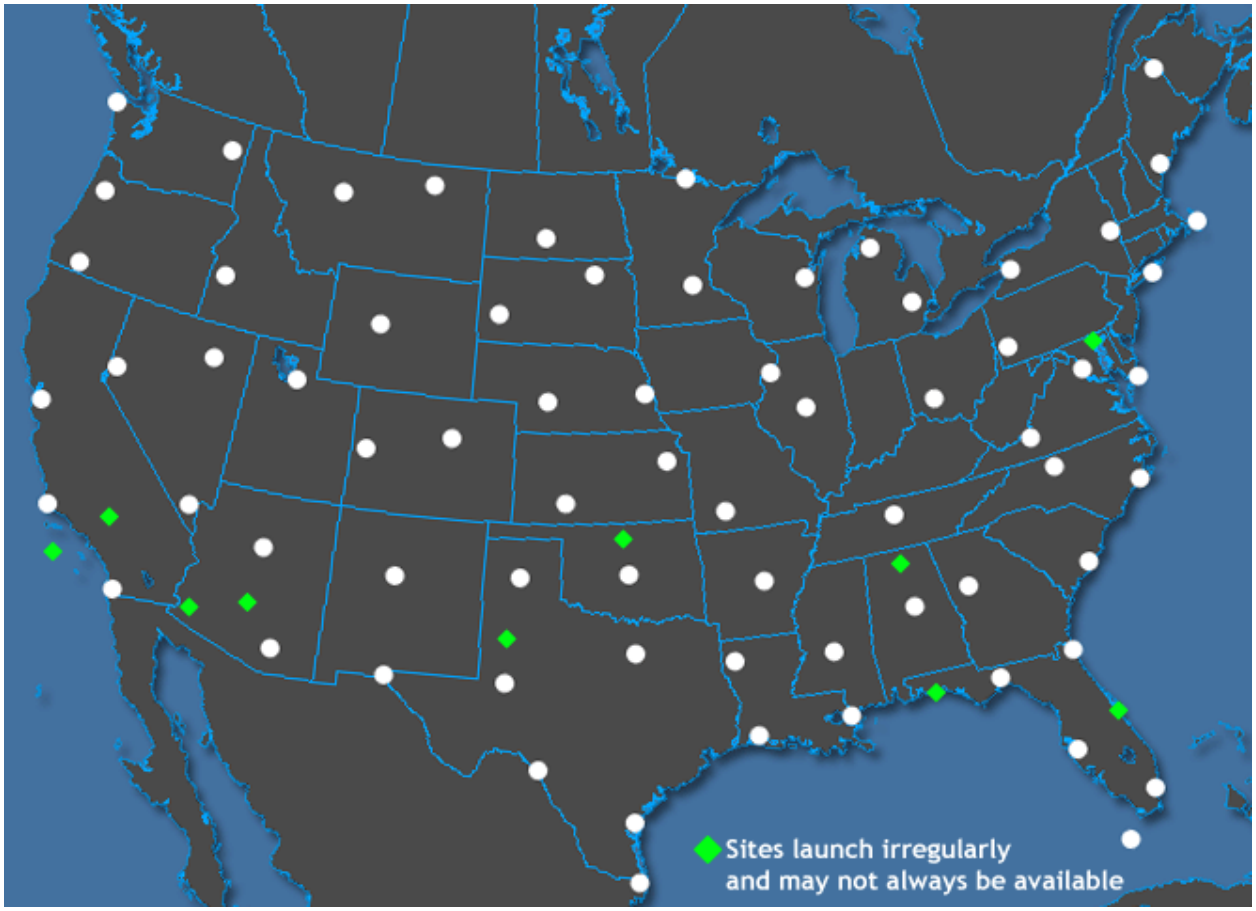


**Figure 13: Observation Network of regular Radiosonde Releases in the United States**

Once the model begins its forecast period, it will generate atmospheric variability. However, it takes time for the variability to mature (e.g., become physically-realistic and balanced). The process by which such variability is generated is known as model spin-up. The time taken to generate such variability is the model spin-up period, which typically can take approximately 6 to 12 hours (cold start). To reduce this time, dynamical initializations are utilized, whereby a pre-forecast integration period is coupled with data assimilation at the end of that period. The current-generation NWP models typically include only kinematic features in the dynamic initialization and no precipitation is active at the model start.

## 7.0 NUMERICAL WEATHER MODEL PHYSICS

The next step in gaining a better appreciation for the challenges of NWP is to have a closer look at the key atmospheric processes and the model physics. The phrase "model physics" generally refers to all processes other than dynamics, convection, and cloud and precipitation microphysics treated in numerical models. Ultimately, these processes primarily relate to model treatment of incoming solar (shortwave) and outgoing terrestrial (longwave) radiation, both in the atmosphere and at the surface.

The effects that model physics parameterizations attempt to simulate are generally unresolvable at grid scales and can be categorized as follows.

- Shortwave (solar) and longwave (terrestrial) radiation in the atmosphere. This includes the effects of clouds, water vapor, trace gases, and aerosols.
- Land and sea surface characteristics and their impact on how incoming radiation affects surface energy and water balances. This includes the effects of vegetation type, soil type, soil moisture quantities, snow, water bodies, and land and sea ice.
- Mechanical transfer of heat, moisture, and momentum between the ground and the planetary boundary layer (PBL) and between the PBL and the free atmosphere by turbulence. This is affected by the treatment of radiation in the atmosphere and at the ground.

The influence of model physics on the forecast of sensible weather varies significantly depending upon the meteorological situation. In general, its influence is:

- Important when dynamic forcing is weak or when physical processes are strong, such as near the center of a high-presssure system or during a clear, calm night; and
- Reduced when dynamic forcing is strong, such as during a frontal passage or near a developing low-pressure system.

Physics effects typically dominate when:

- The diurnal cycle of solar radiation is strong (summer);
- Parcels are very near to the ground, and thus can be sensibly heated or cooled; or
- Precipitation processes are significant (latent heating and evaporative cooling).

Even if a radiation model were perfect, model forecasts would be subject to errors in:

- Initial analyses of moisture and cloudiness;
- Predicting the location and thickness of clouds;
- Predicting the amount of moisture, aerosols, and trace gases in the atmosphere; and
- Analyzing, predicting, and/or prescribing the land and/or ocean surface state.

Model emulation of land surface processes, including the evolution of soil moisture conditions, often falls victim to systematic model biases and errors, which can result in model feedbacks

that exacerbate the original bias. Such feedbacks may become inconsequential when model dynamics are strong and physical forcing is weak (for example, during the winter season) but become very important when model physics dominates the dynamics.

## 7.1 Short-wave (Solar) and Long-wave (Terrestrial) Radiation

In the real world, the Earth's surface interacts with incoming solar radiation that remains after scattering, reflection, and absorption by the atmosphere. The resulting surface energy balance depends upon surface albedo, availability of water to evaporate from the surface and/or its vegetation, roughness of the surface, surface type (soil, water, or ice), presence of snow, and other characteristics. The net surface energy balance directly determines surface temperatures and characteristics of the atmospheric layer directly influenced by the earth's surface (PBL).

The important elements of the surface energy balance are shown on **Figure 14**.

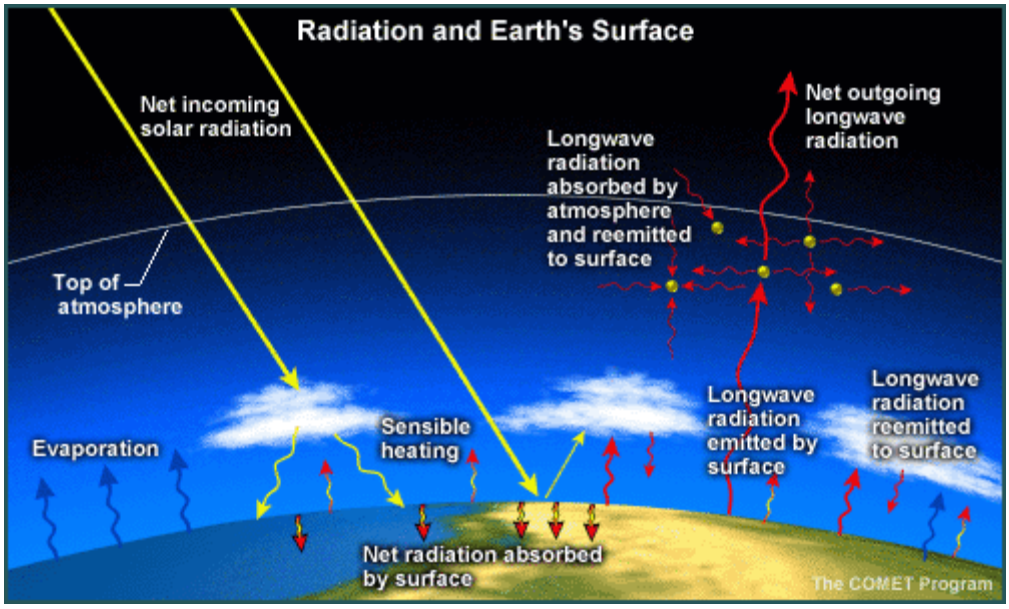


**Figure 14: The Important Elements of the Surface Energy Balance (COMET program).**

The key elements of the surface energy balance include:

- Net incoming solar radiation absorbed at the surface (determined by the solar angle and surface albedo).
- The amount of long-wave radiation emitted by the surface and reemitted by the atmosphere back down to the surface (net long-wave radiation).
- The amount of absorbed energy used to heat the surface (sensible heating) and for evaporation and sub-surface soil heating (ground heat flux).
- Ease with which the surface sheds its heat through sensible and latent heat flux.

- The actual absorption of solar radiation and subsequent exchange of sensible heat, moisture, and momentum between the surface and the atmosphere (and from the surface into the ground) is affected in reality by a detailed configuration of the:
  - Type of surface (land, water, or ice).
  - Type and amount of vegetation (through albedo, evapotranspiration characteristics, and amount of live vegetation, known as vegetation fraction).
  - Type of soil (which determines porosity and thermal properties).
  - Surface roughness (determined by vegetation and topography over land and by wind velocity over water).

Since the surface water balance is determined in part by precipitation minus evaporation, energy and water budgets at the earth's surface are linked through evaporation. Evaporation from the surface is affected by the:

- Amount of available incoming solar energy;
- Amount of soil moisture available for evapotranspiration through vegetation;
- Amount of water held on vegetation leaves for re-evaporation; and
- Existence and mass of snow cover.

In NWP models, earth surface parameterizations emulate the interaction of the surface with incoming radiation to exchange heat, moisture, and momentum between the surface and atmosphere, and to drive the PBL.

Errors in emulating surface processes result in errors in near-surface temperature and moisture forecasts, and stem from:

- Incorrect amounts of short- and long-wave radiation reaching Earth due to incorrect forecasts of cloud and atmospheric moisture, etc.; and
- Incorrect surface albedo due to errors in surface representation.

Common surface representation errors:

- The vegetation type and vegetation fraction prescribed in the land surface part of the model may not be representative of an area at forecast time;
- The soil type (coarseness and albedo) may not be representative;
- Snow cover in winter may not be accurately predicted or prescribed;
- Incorrect evaporation from soil moisture errors, precipitation errors, or errors in surface condition representation of vegetation amount or soil type or from incoming energy errors; and
- Feedbacks from other errors (e.g., incorrect evaporation may result in cloudiness errors, which will result in net solar radiation errors, which will amplify existing surface temperature errors).

## 7.2 Turbulent Processes

Heating of the atmosphere by radiation occurs primarily through the transport of heat, moisture, and momentum from the earth's surface to the PBL and free atmosphere. This is accomplished mainly through turbulent mixing at numerous small time and space scales by mechanically and buoyantly driven eddies. Turbulent processes produce these vertical transports many times more efficiently than molecular processes such as conduction. Among other things, these processes result in the modification of polar air masses as they move toward the equator over warmer surfaces, development of diurnal convection, and frontogenesis along the horizontal edges of surfaces with contrasting characteristics such as land/sea boundaries.

The PBL exhibits strong diurnal, synoptic (3- to 5-day), and seasonal variations. In general, PBL depth depends upon:

- The amount of sensible and latent heating from the surface, which determines static stability and the growth of turbulent eddies; and
- The amount of vertical wind shear, which determines the amount of mechanical turbulence available to grow turbulent eddies.

The accuracy of vertical transports from the model surface through its PBL and into the free atmosphere is based in part on the accuracy of predicted model skin temperature and near-surface grid-scale model temperature, moisture, and wind. Local errors that result from deficiencies in PBL and other model physics parameterizations may accumulate and feed back onto the larger synoptic scales over time. Model PBL errors can be caused by errors that result in incorrect model surface energy balance and thus model skin temperature, including:

- Cloudiness errors;
- Snow cover errors;
- Soil moisture errors;
- Soil heat diffusion errors;
- Surface characterization errors, for example vegetation type and amount, and snow cover and water equivalent;
- Wind forecast errors;
- Incorrect prescription of model surface roughness;
- The moisture and/or heat fluxes in the soil model;
- The assumed or diagnosed profile of wind, temperature, and moisture near the surface;
- An over- or under-active shallow convection parameterization (either within the PBL scheme or separately) mixing heat, moisture, and momentum; and
- The mismatch between the actual size of turbulent eddies and closure assumptions (local versus non-local closure).

## 7.3 The Effects of Snow

Snow is a common phenomenon in Alberta and is highly variable in its depth, density, and area over the plains and mountains of Alberta in the spring. Its importance deserves special attention in any description of model physics. The presence of snow in a forecast model directly affects predicted surface and boundary-layer temperatures, moisture, and other forecast variables. It is important to consider how snow cover and snow depth in a forecast model are determined.

The emulation of snow cover within models mainly affects the amount of incoming solar radiation available to the surface for heating (through differences in albedo). Model snow cover and snow depth are determined using various methods, two examples of which are listed below.

- Initial snow cover and water equivalent snow depth are incorporated from available analyses. Water equivalent snow depth is forecast through a simple snow budget, which requires diagnosis of precipitation type and water equivalent amount of snow accumulation, snow sublimation, and/or snowmelt over the forecast period. This method was used (e.g., in the GFS) starting in 2009. Effects of snow aging on albedo and snowmelt, and the insulating effects of snow with respect to the ground are not accounted for.
- Initial snow cover and water equivalent snow depth are incorporated from available analyses, but also snow density is diagnosed based on first atmospheric layer temperature as the snow accumulates. Snow melt and rain falling into snow pack are partially stored in the snow pack up to a critical snow density, beyond which all water runs off. This method is used in the WRF-non-hydrostatic, hybrid vertical coordinate mesoscale model (NMM) starting in 2009.

Some models base the albedo of a snow-covered grid square on model snow depth relative to model-prescribed surface and topographic roughness. This estimates the effect of potentially bare surfaces, such as trees, hilltops, and rock outcroppings, on overall model surface albedo. Some models also account for the effect of patchy snow when snow cover is thin. In both cases, the albedo ranges between the prescribed albedo for the underlying surface (such as grassland) and that for totally snow-covered surfaces.

Some second-order effects include increased evaporation (because snow surfaces are treated as water surfaces for calculating evaporation rates) and the constrained model skin temperature in the presence of snow (cannot exceed 0°C until model snow vanishes, though where there is patchy snow, some models have a mixed bare ground/snow-covered temperature that may slightly exceed 0°C).

## 7.4 Surface Soil Layer Moisture

Surface soil and vegetation canopy water errors generally affect forecasts for short time periods (hours at most for canopy, a few days at most for surface soil layer). If model feedbacks result from these errors (such as too much triggering of convective precipitation), their impact may last for longer periods. These errors may result in errors in estimates of incoming solar radiation, evaporation, humidity, wind speed, and precipitation.

## 7.5 Convective Parameterizations

In nature, convection serves not only to produce precipitation, but also to transport heat upward, redistribute moisture, and thereby stabilize the atmosphere. If enough convection occurs over a large enough area, it can also create outflow jets and mid-level vortices and drive larger atmospheric circulations that affect weather in distant locations. The convective processes that must be simulated within a NWP are shown on **Figure 15**. Models must try to account for the various types of convective effects. Given the scale at which convective processes occur (typically <10 km), though, current operational models cannot predict them explicitly and must do so via parameterization.

Convective parameterization (CP) schemes are primarily designed to:

- Account for the vertical transport of latent heat, which drives the general circulation in the tropics.
- Reduce thermodynamic instability so the grid-scale precipitation and cloud parameterization (microphysics) schemes do not try to create unrealistic large-scale convection and overly active low-level cyclogenesis. The CP schemes reduce instability by rearranging temperature and moisture in a grid column.

To accomplish both tasks, each scheme must define the following, using information averaged over entire grid boxes:

- What triggers convection in a grid column;
- How convection, when present, modifies the sounding in the grid column; and
- How convection and grid-scale dynamics affect each other.

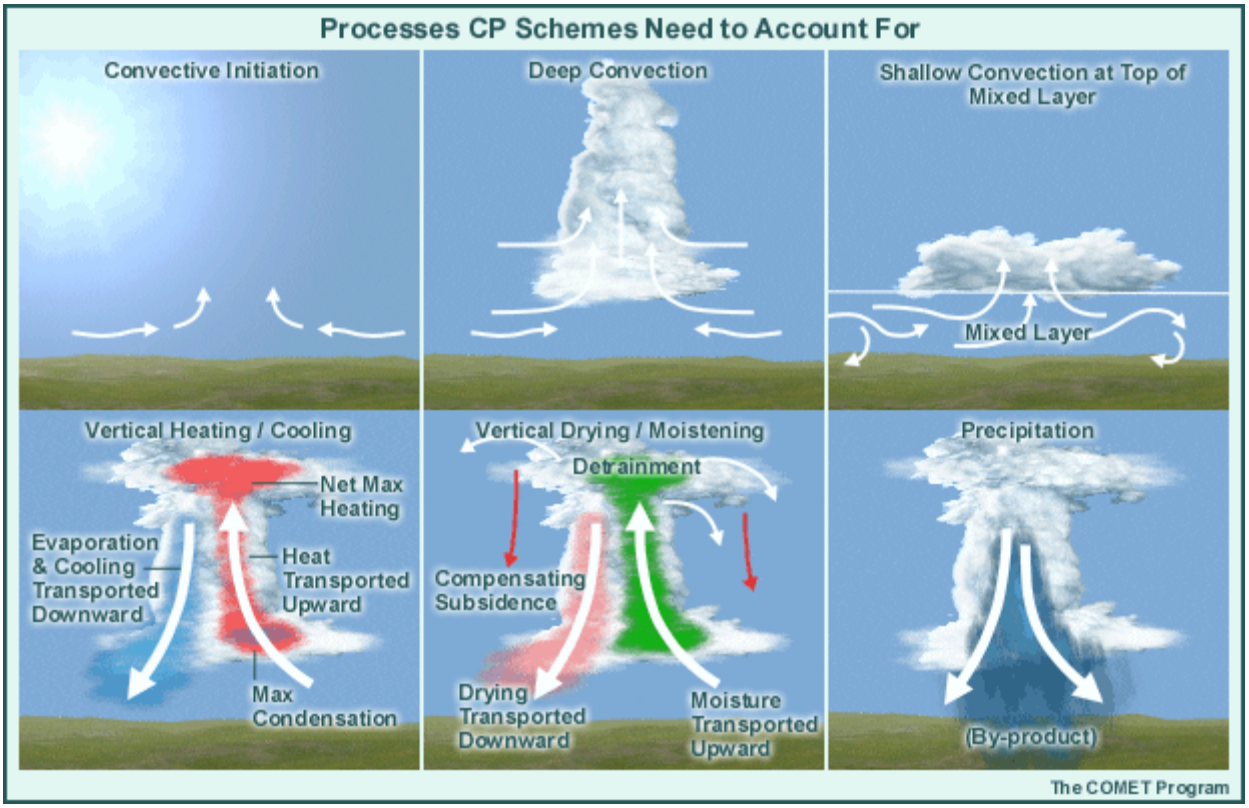


**Figure 151: Convective Processes That Must be Simulated within an NWP (COMET Program)**

The manner in which a scheme handles these processes can limit its effectiveness. Furthermore, the parameters used in the assumptions are adjusted to optimize the scheme's overall performance in all situations. As such, they may work well for some locations and situations but work poorly for others. It is unlikely that NWP models are designed or tuned to perform at their best in southern Alberta during the spring time; therefore, it is important for forecasters to understand the physics of the models in order to better understand their limitations during extreme events at certain times of the year.

### 7.5.1 Legacies of Early Convective Parameterization Schemes

Some of the characteristics of current CP schemes contain legacies of early schemes, the first of which were developed to account for the diabatic heating in tropical convection that drives planetary circulations in very coarse global models. For example:

- The primary emphasis in CP schemes is on heating rates; therefore, precipitation is merely an incidental by-product.
- Changes made to forecast soundings by CP schemes are most appropriate for the tropics.
- The triggering mechanisms and links to large-scale dynamics work better for longer time and space scales than mesoscale weather.

- The CP schemes assume that convection occupies only a small fraction of the grid column. This was fine for older, coarse-resolution, global models, but not for many of today's higher-resolution models.

As model resolution improves to grid spacings of 1 to 2 km, cloud-scale updrafts and downdrafts will be sufficiently well modeled that CP schemes will no longer be used. More will be discussed on this topic later.

The forecast impacts of convection parameterizations in a model are profound, just as are the impacts of actual convection in the real atmosphere. It is important to remember the following:

- Model convective precipitation is only created as a by-product of the CP scheme rearranging heat and moisture, yet it affects the model's precipitation forecast and the model's soil moisture availability, which can then affect evaporation and subsequent boundary-layer dew points and continued convective instability.
- Incorrect timing, placement, and amount of model precipitation causes errors in the simulation of the temperature-humidity profile, and many other forecast variables; therefore, these effects are advected to the downstream weather due to the previous errors in modeled precipitation.
- Model convective precipitation forecasts have notoriously poor skill.
- Many CP schemes have been designed for the large-scale tropics and tuned with data from tropical oceanic convection.

### 7.6 Microphysics Schemes

Microphysics refers to the model emulation of cloud and precipitation processes that remove excess atmospheric moisture directly resulting from the dynamically driven forecast wind, temperature, and moisture fields. Microphysics schemes have commonly been referred to as grid-scale precipitation schemes.

The microphysics parameterization scheme is considered less important than the forcing parameters (winds, vertical motion, moisture, and temperature advection) because it is essentially driven by them. In fact, these forcing fields are considered critical to precipitation forecasts. If they are in error, the model's precipitation forecast cannot be accurate. In some NWP models, cloud and precipitation hydrometeors from microphysics parameterization are cycled back into the data assimilation scheme to reduce spin-up time needed to regenerate clouds and precipitation. This becomes more important in the high-resolution models that are currently being implemented (e.g., GEM regional LAM).

While the large-scale forcing and associated water budget generally govern how much water will fall out of a given weather system, the microphysics parameterization determine exactly how model precipitation will be distributed both in space and time.

Models handle vertical motion differently from wind, moisture, and temperature advection in that vertical motion is a derived quantity, directly resulting from interactions between these

parameters. In this sense, models do not typically represent the placement or strength of vertical motions as accurately as they do wind, moisture and temperature advection. Accordingly, model errors in the vertical motions fields often lead to precipitation forecast errors.

Although models can generally forecast the forcing fields quite well, the forecasting of precipitation timing, location, and amounts is often quite poor. Remember that the model is best at forecasting the dynamics of the atmosphere (temperature, heights, moisture, and winds), while its skill with physics of all sorts, especially precipitation processes, can be erratic at best.

Given the complexity of real precipitation processes in the atmosphere, understanding how models handle them is among the most difficult challenges for forecasters and modellers alike. As model resolution has increased, more detail has been needed for microphysical processes occurring in clouds. Additionally, some mesoscale convectively driven motions can be resolved. These have been achieved, in part, by:

- Developing microphysics schemes that contain hydrometeor information; and
- Linking the microphysics and CP schemes more directly so the CP scheme can pass microphysical information resulting from convective processes to the microphysics scheme.

This provides for more realistic precipitation processes and better links between the model microphysics and radiation schemes. As of 2009, all operational NWP models at minimum predict cloud water. Other more complete versions of these microphysics schemes are used in some operational models and most research/quasi-operational models. Work continues to incorporate these more sophisticated schemes in operational models.

The CP scheme accounts for the effects of sub-grid cloud scale updrafts and downdrafts by removing the instability, dropping some precipitation immediately, and changing the vertical profile of heat and moisture. Convective changes in heat and moisture distribution stimulate the microphysics scheme to make hydrometeors and additional precipitation. The microphysics scheme and dynamics become closely coupled, generating resolved mesoscale motions. Evolution of organized convective systems is then simulated through this coupling between the CP and microphysics schemes.

Cloud-scale updrafts, parameterized by CP, create moistening and heating in the middle to upper troposphere, leading to grid-scale ascent as model dynamics respond to the heating. The microphysics scheme creates hydrometeors where vertical motion and moistening result in supersaturation, releasing latent heat, leading to further grid-scale vertical motion. Coupling between dynamics and microphysics becomes the dominant response, generating mesoscale circulations driven by latent heating above and melting and evaporation below.

Evaporative cooling of the air from falling precipitation takes place in sub-saturated layers below where precipitation is formed. Over time, these feedbacks onto model forecast variables may further strengthen the circulation that initially produced the model clouds and precipitation. The strengthened circulation may increase the precipitation and latent heating, which in turn,

may result in additional feedbacks. These types of feedbacks were identified as being important in the intensification of the June 2002 flood event in southern Alberta by Szeto et al. (2011).

### 7.6.1 Schemes Using Simple Clouds

The GFS model uses a simple cloud scheme. Characteristics and impacts of simple cloud schemes include the following:

- Easy to diagnose moisture field initialization since cloud water is predicted.
- Good at forecasting precipitation location and timing because the scheme advects cloud water, diagnoses cloud ice, has realistic precipitation processes.
- Scheme driven by large-scale forcing.
- Many microphysical processes not accounted for.
- Unrealistic instantaneous fallout of precipitation.
- Cloud forecasts use a sub-saturated critical level to account for relative humidity (RH) variability within the grid column.
- Condensation increases temperature and decreases water vapor mixing ratio. Therefore, model layers initially too moist and above the saturation threshold may have too much condensate and layers that are too warm
- Evaporation of falling precipitation decreases temperature and increases water vapor mixing ratio. Model layers that are too dry will cool too much.

### 7.6.2 Schemes Using Complex Clouds

These are schemes that predict clouds and precipitation based on RH by directly predicting precipitation hydrometeors and accounting for internal cloud processes. These schemes are only used in higher-resolution models because they require sufficient model resolution to resolve small-scale features affecting microphysical processes. The Rapid Update Cycle model (RUC) and WRF-NMM use schemes with complex cloud (cloud liquid, cloud ice, rain, snow, graupel). The GEM regional LAM uses a complex cloud scheme.

The strengths of schemes using complex clouds are the following:

- Models can directly predict precipitation type reaching the surface and amounts of each type.
- Direct prediction of graupel improves precipitation forecasts.
- Precipitation forecasts may be improved over those from schemes that only include cloud water and ice.
- Can directly predict cooling from evaporating and/or melting precipitation.
- Occurs over time as precipitation takes time to fall.
- Can realistically predict snow to blow far downwind from regions where it is generated.
- Can depict convective system anvil extent and stratiform rain region.

- Development and areal coverage of cirrus anvils is improved. This is important because of the effect of ice clouds on radiation in the atmosphere.
- Cloud cover and areal coverage/duration of precipitation from a convective system is improved through the inclusion of multiple major hydrometeors.
- Assimilation of remote sensing data is further improved.
- Can include satellite-derived information on some hydrometeor types.
- Can incorporate radar data into the assimilation process.
- Can verify forecast precipitation type using surface observations.
- Can directly forecast aircraft icing based on the existence of supercooled water in clouds and precipitation.
- Environmental RH fields are more realistic because some water or ice is held in clouds.
- Since more hydrometeor types are accounted for, cloud interaction with radiation is further improved over simple cloud schemes.

The limitations of schemes using complex clouds are:

- They can become prohibitively expensive (in model run time and memory requirements) to implement.
- Require sufficient model resolution to resolve small-scale variability features affecting microphysical processes. For example, precipitation bands in cyclonic storms occurring on a scale of 20 to 30 km require a horizontal resolutions of under 10 km to predict the motions producing them.
- Can be difficult to determine which cloud hydrometeors are most important for different situations and applications, such as aircraft icing.
- Although cloud data can be used in data assimilation systems, direct measurements of hydrometeor types and concentrations are not normally available.
- Data for verifying hydrometeor concentrations do not exist for the full depth of the observed cloud.
- Because data for initial concentrations of cloud and precipitation hydrometeors are typically not available, the microphysics scheme has to "spin up" until equilibrium is reached between the hydrometeors and the forecast moisture, temperature, and wind fields. This results in the under prediction of clouds and precipitation early in the forecast.
- Spin up problem mitigated somewhat if using the short-range forecast "first guess" values for hydrometeors in model data assimilation scheme, though lack of observed hydrometeor data is still a problem.

In addition to simulating precipitation processes more faithfully, more complex microphysics schemes may have a large, indirect influence on precipitation forecasts by improving dynamical variable forecasts. This is accomplished through better forecasts of the vertical distribution of diabatic heating and cooling affecting mesoscale and synoptic scales; more realistic linkage of the model atmosphere water and energy cycles through the use of predicted clouds in the model's radiation scheme; and the ability to assimilate additional types of satellite data. These

improvements in data assimilation and forecasts of precipitation-forcing mechanisms result in additional improvements in precipitation forecasts.

## 7.7 Convective Parameterization Schemes in Current Operational Numerical Weather Prediction Models

### 7.7.1 Betts-Miller-Janjic Scheme

The Betts-Miller-Janjic Scheme is currently used in the NAM model. The strengths of this scheme are:

- Often works well in moist environments with little or no capping inversion.
- Treats elevated convection better than other CP schemes (although still not well).
- Implicitly includes the effects on cloud layers of downdrafts, latent heat of fusion from freezing in updrafts, melting of falling precipitation, and many other complicating natural features.
- Runs quickly; does not require much computing resources.

The limitations of this scheme are:

- Reference profiles are fixed based on climatological observations rather than being flexible for every forecast situation; as a result, they may eliminate important vertical structure.
- Is only triggered for soundings with deep moisture. This is a potential problem in arid environments and for loaded-gun soundings.
- When triggered, the scheme often rains out too much water, either because the reference profile is too dry for the forecast situation or the transition to the reference profile is too rapid. This leaves too little water vapor behind for precipitation occurring later or downstream.
- Does not account for the strength of cap-inhibiting convective development.
- Does not account for any changes below cloud base.
- Makes no attempt to simulate gust fronts and their associated mesohighs.
- Only affects surface conditions indirectly, such as through the evaporation of precipitation and the reduction of solar heating from cloud cover.

### 7.7.2 Arakawa-Schubert Scheme

Variations of the Arakawa-Schubert scheme are used in the GFS, the National Center for Environmental Prediction (NCEP) Regional Spectral Model, and some climate and research models. This is a complex scheme that includes the effects of moisture detrainment from convective clouds, warming from environmental subsidence, and convective stabilization in balance with the large-scale destabilization rate.

To trigger convection, the scheme requires some boundary-layer CAPE. Although it varies in specific implementations, the general formulation requires the presence of large-scale

atmospheric destabilization with time. The process by which the scheme attempts to assess destabilization is complex; for example, it must account for the effects of entrainment and clouds of various depths.

The strengths of the scheme are:

- Accounts for the influences of entrainment, detrainment, and compensating subsidence around clouds.
- Can account for a cap inversion, depending on the specific implementation details.
- Some implementations can account for saturated and/or unsaturated downdrafts, tilting of updrafts so rain falls through cloud or is ejected outside the tower, and/or microphysical processes occurring in convection.
- This is a complex scheme that deals with a variety of cloud depths and is capable of providing complex sounding changes corresponding to many forecast situations.

The limitations of the scheme are:

- May not sufficiently stabilize the model atmosphere.
- May produce rain later (not immediately) or result in a prolonged period of weak convection, especially if destabilizing advection or surface fluxes counteract the modest convective scheme stabilization.
- May result in grid-scale convection. This represents a major failure of the CP scheme, since it's supposed to prevent the microphysics scheme from trying to make convection the size of an entire grid box; if this happens, many serious negative forecast impacts can occur, including dramatic changes to the model's mass fields.
- Is not designed for elevated convection.
- Assumes that convection exists over only a very small fraction of the grid column, which may not be appropriate at today's higher-resolution models.
- Assumes that convective updrafts entrain through the sides, whereas observations of cumulus and towering cumulus indicate entrainment mainly through cloud top. This affects scheme rainfall and heating profiles, which feed back onto the resolved motions.
- Takes longer to run than other schemes.

### 7.7.3 Kain-Fritsch Scheme

The Kain and Fritsch (1993) scheme is currently used by the GEM regional model. Strengths of this scheme are:

- Suitable for mesoscale models and coupling with microphysics schemes that use clouds.
- The assumption about consuming convective available potential energy (CAPE) is most appropriate for short time and space scales.
- It accounts for microphysical processes in convection; can be set up to feed hydrometeors to the microphysics scheme.

- May perform better in cases of severe convection.
- Physically realistic in many ways.
- Has the most realistic treatment of trigger and cap (although it still fails if the model boundary-layer forecast is bad).
- Accounts for entrainment and detrainment more realistically than Arakawa-Schubert schemes.
- Handles elevated convection.
- Like the Arakawa-Schubert scheme, can vary its response to different forecast scenarios.

The primary limitations of this scheme are:

- Tends to leave unrealistically deep saturated layers in post-convective soundings (the microphysics scheme will then activate simulating post-convective stratiform precipitation, which may be overdone).
- Takes longer to run than simpler schemes.
- Model fields may look "splotchy" from convection triggering in scattered grid boxes. Other schemes tend to have a smoother clustering of grid boxes where convection is triggered. Although this may be more realistic, it can make the interpretation of model fields more difficult.

### 7.7.4 Effects of Too Much Convection in a Model

Some convective schemes are susceptible to removing too much instability and moisture even when the large-scale fields are well predicted and convection is initially triggered at the correct location and time. When the predicted forcing to which the CP scheme responds is too strong or the scheme is triggered excessively for any reason, the CP scheme sometimes removes too much moisture and instability. When this occurs, the CP scheme is referred to as overactive.

Forecasters are often asked to compare the model versus the observed atmospheric profile or sounding in order to assess how well the model is simulating the current situation. This is a problem in Alberta since there is only one upper air station, located near Edmonton (CWSE). This does, however, allow comparison at one point of the model versus observed atmospheric profile of temperature, humidity and wind, which still can provide an indication of how accurately the model is handling the current weather situation, while the situation is unfolding. As an example, **Figure 16** shows the observed sounding at CWSE at 0 UTC on 20 June 2013, compared with the NAM model 24 hour forecast sounding for CWSE for the same time. In general there is excellent agreement; however, upon closer inspection one can see some subtle differences, that the modeled sounding is slightly warmer and more moist in the lower levels, and the surface winds are more easterly in the model. These subtle differences can potentially have far reaching effects regarding the forecast of precipitation.

In the above example, the warmer and moister lower levels could suggest more convection than reality. In this case, if the model has an overactive CP scheme, the following effects may result:

- Excessive rains where convection originates and too little downstream resulting in the early demise of convective systems;
- The atmosphere is dried out too much and too quickly, both at and downstream from the location of the CP error;
- The microphysics scheme produces too little cloud and overrunning precipitation; and
- CP sounding adjustments are excessive and then advect downstream.

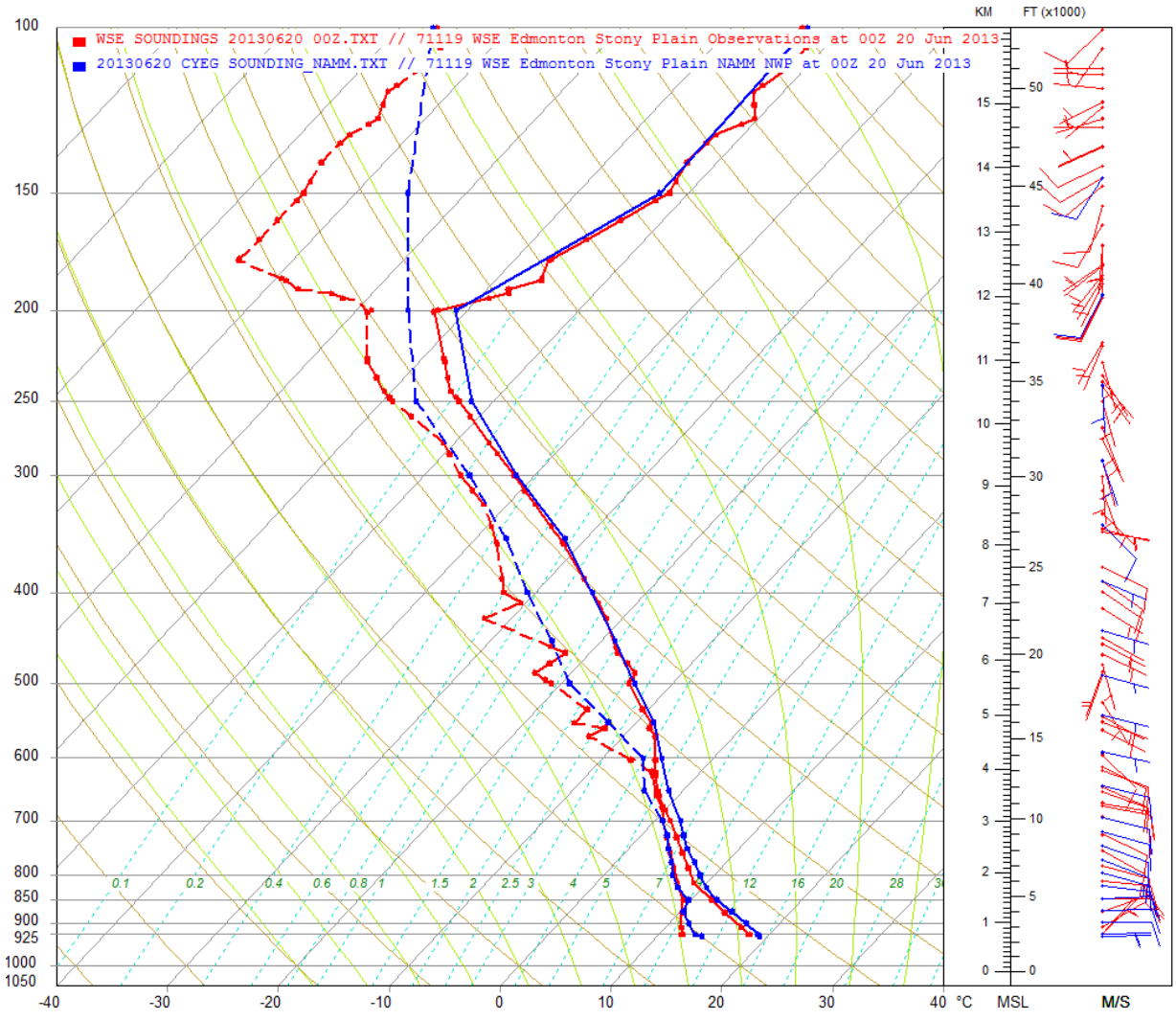


**Figure 16: The Observed Sounding (red) at CWSE at 0 UTC on 20 June 2013 is Compared with the NAM Model 24-hour Forecast Sounding (blue) for CWSE for the Same Time**

If the large-scale dynamics correctly supply enough moisture to compensate for the excess drying caused by the CP, prolonged intense rainfall may actually occur, although predicted amounts may still be too concentrated in the upstream direction.

When a CP scheme fails to remove enough moisture and instability, perhaps because the large-scale forcing or triggering conditions are not well predicted, the scheme is said to be underactive. Effects of an underactive CP scheme are:

- Precipitation onset is delayed as the model waits for the microphysics saturation threshold over the entire grid box instead of "triggering convection" immediately.
- The microphysics scheme produces grid-scale low-topped precipitation with too much low- and mid-level clouds and precipitation, and too little high cloudiness.
- Too moist at low and mid levels
- Too little instability removed from the grid column
- Too much latent heat is released in the lower to middle troposphere from the microphysics scheme. This leads to an over deepening of low-pressure systems the cause of "convective feedback bull's eyes")

This is just one example of the complexity and challenges of the NWP process.

## 7.8 Explicit Convection

The CPs are used in current operational hydrostatic models to account for the effects of convection since the model cannot resolve convective motions explicitly. However, high-resolution (1 to 2 km) nonhydrostatic models can be run without CP schemes because the grid spacings are small enough to begin to resolve convective motions. For example, the resolution can be fine enough that entire grid boxes can be filled with updraft air and condensate while others are filled with downdrafts. Explicit convection is currently used in the WRF Model and will be used in the new generation GEM Regional-LAM (High Resolution Deterministic Prediction System [HRDPS]-PanCanadian 2.5 km model).

A rapid and tight coupling between the dynamics and the microphysics scheme results in:

- Explicitly simulated updrafts strong enough to lift hydrometeors up to the equilibrium level
- Explicitly simulated downdrafts and their accompanying gust fronts

This allows a more realistic redistribution of heat and moisture than when a CP scheme is used. It also enables the winds and vertical motion to be modified directly by the convection. Explicit convection ultimately provides a direct prediction of convective precipitation. Remember that CP schemes can only indirectly predict convective precipitation as a by-product of removing instability and often do a poor job.

Explicitly predicted model convection has become an operational reality, so its capabilities and limitations are important to recognize. The strengths of explicit convective schemes are:

- Convective modes, such as isolated cells, bow echoes, long lines, or large amorphous clusters, are often well predicted, especially when there is agreement among several different models or model runs.

- Explicitly predicted storm characteristics, such as identifying areas where storms will have strongly rotating updrafts or strong straight-line winds, seem to be well represented, though research on this is continuing.
- Convective initiation in strongly forced cases is often good, although typically a couple hours too late for models run with a grid spacing of around 4 km as it takes extra time for the model to build updrafts spanning several grid boxes, much wider than observed updraft widths.
- Typically better with timing, placement, and shape of precipitation areas than predicted by models using a CP, even if amounts are poorly predicted.
- Interpreting output statistically over a radius around each point can help build a probabilistic forecast, such as the probability of a thunderstorm in a one-hour period based on the percentage of area covered by a 40 dBZ echo within 40 km of a point at any time during the 1-hour time period.

Limitations of an explicit convective scheme are:

- Precipitation in some models is frequently excessive along predicted cell tracks, several times maximum observed amounts.
- Convective initiation in weakly forced cases is often poor, resulting in realistic-looking storms in the wrong times and places.
- Resolutions of 1 km or finer are often needed to simulate internal convective cloud structures and evolution, as well as second-generation cell initiation by gust fronts. This impacts precipitation timing, intensity, and spread, and affects downstream cloud, temperature, and wind.
- Running a model at 1 km or finer grid spacing takes a very large amount of computing resources, restricting the size of the domain which can be covered. The adverse influence of the model boundary conditions too close to the area of interest may exceed the benefits of finer resolution.
- If initial conditions come from a coarser-resolution model, a several-hour spin-up period is required. The best forecast is more likely to come from hours 9 to 18 than from hours 0 to 6.
- If initial conditions directly utilize observations of small-scale features such as assimilating real-time radar reflectivity data, the best storm-scale forecast is likely to be in the first few hours, as the mesoscale details assimilated quickly lose influence during the model integration.

Mesoscale details can look amazingly realistic, including rear-inflow jets, trailing stratiform regions, isolated cells ahead of a squall line, splitting cells, and so on. However, the entire event may be misplaced or may not occur at all. Careful examination of the situation is required to assess how plausible the prediction is, and other model runs, even coarser-resolution runs with parameterized convection, may give a sense of how likely an event is to occur or where and when it is more likely to occur.

## 8.0 THE GLOBAL ENVIRONMENTAL MULTI-SCALE MODEL

We often refer to EC's global model or regional model. In fact, there is only one model and it is the GEM model which is run in two configurations; regional and global configurations.

The GEM is an integrated forecasting and data assimilation system developed in the Recherche en Prévision Numérique (RPN), Meteorological Research Branch (MRB), at the Canadian Meteorological Centre (CMC). Along with the National Weather Service of the USA's (NWS) GFS, which runs out to 16 days, the European Center for Medium range Weather Forecasting's (ECMWF) Integrated Forecast System (IFS), which runs out 10 days, the Naval Research Laboratory Navy Global Environmental Model (NAVGEM), which runs out to 8 days, and the UK Met Office's Unified Model, which runs out to 6 days, it is one of the five predominant synoptic scale medium-range models in general use in the world.

The GEM model is currently operational for the global data assimilation cycle and medium range forecasting, the regional data assimilation spin-up cycle and short-range forecasting. Furthermore mesoscale forecasts are produced overnight and are available to the operational forecasters. A growing number of meteorological applications are now either based on or use the GEM model. Output from the GEM goes out to 10 days, on par with the IFS and the effective range of the GFS, the GEM's primary rivals from Europe and the United States respectively. An ensemble variant of the GEM runs alongside the GFS ensemble to form the North American Ensemble Forecast System (NAEFS).

The GEM model has been developed to meet the operational weather forecasting needs of Canada for the coming years. These presently include short-range regional forecasting, medium-range global forecasting, and data assimilation. In the future they will include nowcasting at the meso-scales, and dynamic extended-range forecasting on monthly to seasonal timescales. The essence of the approach is to develop a single highly efficient model that can be reconfigured at run time to either run globally at uniform-resolution (with possibly degraded resolution in the "other" hemisphere), or to run with variable resolution over a global domain such that higher resolution is focused over an area of interest.

The operational GEM model dynamics is formulated in terms of the hydrostatic primitive equations with a terrain following pressure vertical coordinate. The time discretization is an implicit two-time-level semi-Lagrangian scheme. The spatial discretization is a Galerkin grid point formulation on an Arakawa C-grid in the horizontal (lat-lon) and an unstaggered vertical discretization. The horizontal mesh can be of uniform or variable resolution, and furthermore can be arbitrarily rotated. The vertical mesh is also variable.

The operational GEM model is interfaced with a full complement of physical parameterizations, these currently include:

- Solar and infrared radiation interactive with water vapor,carbon dioxide, ozone, and clouds;
- Prediction of surface temperature over land with the force-restore method;
- Turbulence in the PBL through vertical diffusion, diffusion coefficients based on stability and turbulent kinetic energy;

- Surface layer based on Monin-Obukhov similarity theory;
- Shallow convection scheme (non precipitating);
- Kuo-type deep convection scheme (GFS);
- Fritsch-Chappell (1980) type deep convection scheme (regional forecast system);
- Sundqvist condensation scheme for stratiform precipitation; and
- Gravity wave drag.

The next stage of development of the GEM model is to evaluate the non-hydrostatic version for mesoscale applications where the hydrostatic assumption breaks down. The limited-area (open boundary) version is scheduled to follow. The distributed memory version of GEM is almost completed; it is a major recoding effort that is based upon a locally developed communication interface currently using Message Passing Interface. Research on the performance of different land surface schemes such as ISBA (Interaction Soil-Biosphere-Atmosphere) and CLASS (Canadian Land Surface Scheme) is making progress. The strategy is progressing towards a unified data assimilation and forecast system, at the heart of which lies a single multipurpose and multiscale numerical model.

### 8.1 The Latest GEM Global Upgrade

The latest major upgrade to the GEM - GDPS version 3.0.0 at the CMC occurred on 13 February 2013, starting with the 1200 UTC run. This major upgrade includes a new version to the GEM model, important changes to its 4D-Var data assimilation scheme and to some of the model's physics schemes. The grid size of the model was also reduced to a resolution of 25 km. Also, this version now uses staggered hybrid vertical coordinates. Objective scores show improvements in the forecasts with most metrics throughout most of the atmosphere, in particular over North America in winter. A subjective evaluation by operational meteorologists confirmed those improvements.

A list of the most recent changes to the GEM Global is:

- 13 February 2013 Version 3.0.0 - Increase in resolution to 25 km, improvements to assimilation, introduction of staggered hybrid coordinate levels.
- 19 December 2011 Version 2.2.2 - Addition of satellite data and a higher quality analysis of the sea surface temperature.
- 7 December 2011 Version 2.2.1 - Addition of satellite data and a higher quality analysis of the sea surface temperature.
- 16 November 2011 Version 2.2.2 - Addition of satellite data and a higher quality analysis of the sea surface temperature.
- 12 July 2011 Version 2.1.0 - Improvements to reduce the tropical cyclone false alarm rate.

# 9.0 THE REGIONAL DETERMINISTIC PREDICTION SYSTEM

Under the RDPS, the GEM model is run on a variable-step grid with a 10 km central core resolution. The fields in the 10 km resolution regional dataset are made available on a 935 × 824 polar-stereographic grid covering North America and adjacent waters with a 10 km resolution at 60°N.

## 9.1 The Latest Global Environmental Multi-scale Model Regional Upgrade

The last major upgrade to the RDPS at the CMC occurred on February 13, 2013. Changes were made to the RDPS to harmonize it with GDPS-3.0.0, and the RDPS forecasts are also improved. As a result of these RDPS adjustments, the version of RDPS is now 3.1.0.

On 3 October 2012, starting with the 1200 UTC run, the CMC implemented version 3.0.0 of its RDPS. The upgrade included an increase in resolution to 10 km from the previous 15 km, a 4D-Var data assimilation system replacing the previous 3D-Var, as well as important changes in the GEM model physics. This resulted in significant forecast improvements especially for the winter season.

Objective scores show improvements in the forecasts with most metrics throughout most of the atmosphere, in particular for the lower portion of the atmosphere and at the surface. A subjective evaluation by operational meteorologists confirmed those improvements. Other forecast systems which depend on RDPS output include similar changes and as a result they also benefit from this version of the RDPS.

The most recent changes to the GEM Regional is:

- 2013-02-13: RDPS version 3.1.0 - in conjunction with GDPS 3.0.0.
- 2012-10-19: RDPS observation cut-off extended to +2:00.
- 2012-10-03: RDPS version 3.0.0 (10 km grid, 4DVar), observation cutoff +1:55.
- 2011-11-16: RDPS version 2.0.0 (Add satellite data, higher quality analysis of sea surface temperature, observation cut-off +2:05.
- 2010-10-20: Regional system modified to incorporate limited area version of GEM model, regional system now referred to as REG-LAM3D.

The main motivations for changes in the physics configuration of the RDPS-300 were the following.

- Early in the project the very first series of forecasts obtained at the increased resolution of 10 km showed significant increases in precipitation over land and water for both summer and winter seasons at all lead times. This precipitation increase was a concern given that the RDPS-200 already tended to over-estimate precipitation quantities. Furthermore, precipitation scores showed an increase in the occurrence of higher rates of precipitation (i.e. >15 mm/day).

- Comparison of surface fluxes with detailed observations from a station at Lake Superior (Deacu et al., 2012) as well as comparisons with daily global analysis of surface fluxes from the Woods Hole Oceanographic Institution's "OAflux" project (Yu et al., 2008) showed that the RDPS-200 significantly over-estimates the latent heat fluxes from water bodies. Latent heat fluxes (water vapor fluxes) are important for all elements of the hydrological cycle (humidity, clouds, precipitation, etc.). As demonstrated in Deacu et al. (2012), they are critical for obtaining a realistic budget of evaporation-precipitation over water bodies. Furthermore, these fluxes provide fuel for the development of tropical storms as well as extra-tropical systems. Over-intensification of extra-tropical systems over the Gulf Stream region, often noted by operational meteorologists at A&P and regional EC forecast centres, could be related to the over-estimation of the latent heat fluxes in this region.
- A long-standing problem of the RDPS has been significant warm errors in surface air temperature associated with warm air advection in winter and spring (so-called warm episodes). Obviously, such errors in the temperature profiles lead to errors in forecasting of precipitation type, namely a well-known under-estimation of freezing rain.

## 9.2 Summary of Impacts of Model Changes

As a result of the increased resolution and the modifications to the physics incorporated in the new RDPS-300, the following changes with respect to RDPS-200 have been obtained:

- Decreased precipitation in winter over land and water surfaces, decreased precipitation in summer over water surfaces, increased precipitation in summer over land at the time of the diurnal peak.
- Increased occurrence of high precipitation rates in summer.
- More realistic precipitation rates in the first 6 hours of integration.
- Significantly reduced evaporation (latent heat fluxes) from water bodies, in particular in winter and over the gulf stream.
- Improved surface temperature and temperature profile in warm air advection situations in winter and spring.
- Improved forecast of precipitation types in warm air advection situations in winter and spring.
- On several occasions during the winter, meteorologists have noted improvements in surface temperature due to the better resolved topography (cold air channeling in valleys).

## 10.0 HIGH RESOLUTION DETERMINISTIC PREDICTION SYSTEM

In 1997, EC's CMC began investigating high resolution NWP. Two 10 km experimental domains were run. In 1999, the grid spacing was reduced to 4 km. In 2001, a 2.5 km window was run over the Great Lakes regions in support of the Elbow project. In 2004, two GEM-LAM 2.5 km domains were set up in the west (BC) and in the east (ON-QC) and run by CMC operations in an experimental mode during 2005. In 2007, two new 2.5 km grids were added in the Arctic and Maritimes. In 2009, a second Arctic grid was added, and subsequently, various upgrades were made for a special configuration to support the Vancouver 2010 winter Olympics.

Currently, the HRDPS consists of several nested limited-area domains across Canada, having either operational or experimental status, all run under operational supervision and support. The primary roles of the HRDPS are to improve the short-term NWP model guidance for high impact weather in Canada over that from the RDPS, and to serve as a temporary, transitional operational system before a change of status to operational. Currently, the planned start for an experimental pan-Canadian domain, operational 2.5 km resolution HRDPS is for the summer of 2014 (J. Milbrandt, private communication).

The HRDPS promises to be the best NWP model to meet the future needs of the ESRD RFC. The 2.5 km resolution will provide an improved grid to handle the complex terrain features of the mountains and head waters of the primary river basins in Alberta. Secondly, the improved, detailed physics should be able to include many of the complicated physical feedback processes involved in convective, upslope, rain on snow events that are common to the extreme flood events in Alberta. One challenge will be to supply and assimilate data to provide the necessary initial and boundary conditions required by the model. Satellite data, weather radar data, and microphysical particle recycling between model runs will likely play important roles in improving model performance. Certainly there will be some time required to adjust some of the model parameters to maximize its performance, especially with respect to QPFs.

## 11.0 NATIONAL O CEANIC AN D ATMOSPHERIC AD MINISTRATION O F THE US A ENVIRONMENTAL MODELING SYSTEM

For the past several years in the USA, a common modeling framework called the NOAA Environmental Modeling System (NEMS) has been in development to streamline the interaction of analysis, forecast, and post-processing systems within the NCEP. The NEMS architecture is based on the Earth System Modeling Framework (ESMF). NEMS is a shared, portable, high performance software superstructure and infrastructure for use in operational prediction models at NCEP. It is also part of the National Unified Operational Predication Capability (NUOPC) with Navy and the Air Force, and will eventually provide support to the community through the Developmental Test Center (DTC). Currently, the GFS, the Global Ensemble Forecast System (GEFS), the B-grid version of the non-hydrostatic multiscale model (NMM-B), and the flow-following finite-volume Icosahedral Model (FIM) are placed together within NEMS.

## 12.0 GLOBAL FORECAST SYSTEM MODEL DESCRIPTION

The GFS is a weather forecast model produced by the NCEP. Dozens of atmospheric and land-soil variables are available through this dataset, from temperatures, winds, and precipitation to soil moisture and atmospheric ozone concentration. The entire globe is covered by the GFS at a base horizontal resolution of 18 miles (28 km) between grid points, which is used by the operational forecasters who predict weather out to 16 days in the future. Horizontal resolution drops to 44 miles (70 km) between grid point for forecasts between 1 and 2 weeks. The GFS model is a coupled model, composed of four separate models (an atmosphere model, an ocean model, a land/soil model, and a sea ice model), which work together to provide an accurate picture of weather conditions. Changes are regularly made to the GFS model to improve its performance and forecast accuracy. It is a constantly evolving and improving weather model. The GFS model was originally called the AVN model, and the name was changed to GFS in September 2002.

### 12.1 Recent Changes to the Global Forecast System Model

May 22, 2012: The data assimilation system for the GFS had a major upgrade. There were minor output product changes to the GFS model output. A hybrid variational ensemble assimilation system is now employed. In this system, the background error used to project the information in the observations into the analysis is created by a combination of a static background error (as in the prior system) and a new background error produced from a lower resolution (T254) Ensemble Kalman Filter. Other analysis changes included:

- Use GPS RO bending angle rather than refractivity;
- Include compressibility factors for atmosphere;
- Retune SBUV observation errors, fix bug at top;
- Update radiance usage flags;
- Prepare for monitoring NPP and Metop-B satellite data;
- Add NPP ATMS satellite data, GOES-13/15 radiance data, and SEVERI CSBT radiance product;
- Include satellite monitoring statistics code in operations; and
- Add new satellite wind data and quality control.

July 28, 2010: Changes included:

- Change in resolution from ~35 to ~27 km;
- 3-hourly output available to 192 hours; and
- Model physics changes.

## 13.0 NORTH AMERICAN MESO-SCALE FORECAST SYSTEM

The NAM is one of the primary vehicles by which NCEP's Environmental Modeling Center provides mesoscale guidance to public and private sector meteorologists. It runs four times daily at 00 UTC, 06 UTC, 12 UTC, and 18 UTC and consists of:

- The NOAA NEMS version of the NMMB; and
- The NCEP regional Grid-Point Statistical Interpolation (GSI) analysis.

The NAM is initialized with a 12-hour run of the NAM Data Assimilation System, which runs a sequence of four GSI analyses and 3-hour NEMS-NMMB forecasts using all available observations to provide a first guess to the NAM "on-time" analysis.

The NCEP High-Resolution Window Forecast System (HIRESW) consists of daily runs of the WRF versions of the NMM and the NCAR Advanced Research WRF (ARW) at ~5 km resolution. All runs except the Alaska domain use the NAM for initial and boundary conditions. The Alaska run uses the NCEP GFS for initial/boundary conditions. Currently, six nested domains are being run, three large domains (East/Central U.S., West/Central U.S., Alaska) and three small domains (Hawaii, Puerto Rico, Guam).

The last major upgrade to the NAM model occurred on 18 October 2011. Those changes to the NAM included a major change to the modeling system and many additional products, including new 4 km NAM nests.

## 14.0 THE WEATHER RESEARCH FORECASTING MODEL

The Weather Research and Forecasting Environmental Modeling System (WRFEMS, henceforth referred to as WRF) is a state of the art, full physics NWP model (Michalakes et al., 1999, 2001; Skamarock et al. 2008) available publicly through the National Center for Atmospheric Research (NCAR). To test how well a private group (as opposed to a national meteorological organization) can model precipitation for heavy rainfall events in Alberta, we ran the WRF model in-house. WRF features non-hydrostatic dynamics, multi-nest capability, and several physics options for boundary layer processes, radiation schemes, cloud microphysics, and cumulus parameterization schemes. WRF version 3.3.1 was used for this project.

WRF daily forecasts for this study were initialized using archived GFS model output, and boundary conditions were updated every 3 hours. WRF forecasts and simulations were initialized 48 hours prior to the 72-hour extreme rainfall event, and included 120 hours of simulation length. This was done to allow for model spin-up and to complete the simulation of the atmosphere for the following three entire days. WRF processes simulations using 45 pressure levels, using sigma vertical coordinates (Skamarock et al., 2008), with the pressure top at 50 mb. The Thompson et al. (2008) microphysics scheme was used. It uses six categories of water substance - water vapor, cloud water, rain, cloud ice, snow, and graupel. The Thompson et al. (2008) microphysics scheme has been shown to be superior to other schemes in the simulation of precipitation over complex terrain (Liu et al., 2011).

There have been many verification studies performed using the WRF model. Davis et al. (2006) verified precipitation forecasts over the continental United States. WRF was used by Flesch and Reuter (2012) to simulate major flooding events in Alberta as well as understanding how WRF performs when the topography of the nearby Rocky Mountains was altered. Cheng and Steenburgh (2005) performed temperature, dew point, and wind speed verification during summer in the western United States, as well as sensitivity studies regarding WRF's slab-soil model. Done et al. (2004) performed high resolution forecasts for summer days with MCSs using 10 km grid resolution simulations with a cumulus parameterization scheme, as well as 4 km resolution simulations without one. Even if WRF is found to be less accurate than EC's temperature forecast, which is anticipated due to their massive infrastructure in predicting the weather, WRF still can be used in important ways. While EC's forecasts might be more accurate, their daily forecasts may not align with the information required by many users. An example would be that EC releases a forecast for heavy precipitation amounts at certain locations during an intense rain period, but does not publically release the precipitation information regarding the entire river basin. This information would be very valuable to a hydrologist, or a flood forecaster, and would be easy to produce using the WRF model. The ability to create powerful scripts to be used on model output from WRF can be very useful, from research applications to those who require detailed specifics about the weather for their own operational use.

Hydrological models of estimating water flow for rivers in Alberta need a high spatial and temporal resolution of precipitation data. Rain gauge measurements alone do not have adequate resolution, particularly in the orographic regions of southwestern Alberta. Weather

radar imagery can estimate rainfall rate, but not for mountainous terrain because of ground clutter producing spurious radar echoes. Furthermore, relying on precipitation estimated using radar has little predictive skills in terms of forecasting precipitation runoff beyond a few hours into the future, because radar images cannot be predicted ahead of time. In recent years there have been efforts to use precipitation estimates from NWP models as input for hydrological models. With the advance of computing power and data assimilation it is now possible to run custom stand-alone NWP models such as WRF as a tool for flood forecasters.

An important issue is to assess the skillfulness of these models in predicting the spatial distribution of rainfall to obtain reliable estimates of the total water mass falling over the catchment areas of the river systems. Flesch and Reuter (2012) used WRF to simulate heavy precipitation events over Alberta and examined the role of the topography in simulating and organizing the precipitation. Specifically, they performed simulations using the actual topographic grid and other simulations with reduced mountain elevations. They concluded that a reduction of mountain elevation decreases maximum precipitation by about 50% over the mountains and foothills. Due to the difference between the resolution of NWP models, typically between 15 and 30 km, and the scale of the cumulus cells (1 to 10 km), NWP models use CP schemes to mimic the effects of cumulus clouds which are not resolved as they are smaller than individual model grid points. These schemes, discussed earlier in this report, attempt to trigger the convection and modify the temperature and moisture profiles within a model column based on the grid-scale meteorological information. How cumulus parameterization schemes operate in NWP models is particularly important for hydrological applications because the total volume of rainwater is sensitive to the cumulus parameterization scheme (Wang and Seaman, 1997).

The results of a NWP model can be quite dependent on the spatial resolution of the numerical grid. Intuitively, one would expect that simulations using the highest spatial resolution would provide the most accurate model simulation. Wang and Seaman (1997) and Done et al. (2004) found that the finest grid resolution yielded the most accurate results, but Grubisic et al. (2005) and Roberts and Lean (2008) showed cases for which the finer grid spacing did not improve the simulation accuracy.

### 14.1 Weather Research Forecast Model Options Used In This Study

The following options and settings were used for the WRF model runs on this project, based on previous studies of extreme rainfall events in the Colorado Mountains (private communication courtesy of Roy Rasmussen - NCAR):

- Model version: WRF V3.3.1 Non-hydrostatic.
- Nested domain:
  - 1,500 km × 1,500 km at 20 km resolution outer domain.
  - 744 km × 624 km at 4 km horizontal resolution inner domain.
  - 51 vertical levels.
- Boundary layer: Mellor-Yamada-Janjic.
- Radiation: The rapid radiative transfer model (RRTMG) scheme.

- Land Surface Physics: Noah land-surface model with snow physics improvements based on Barlage et al. (2010).
- Microphysics: Thompson et al. (2008) mixed-phase microphysics.
- No Cumulus parameterization used (assumed explicit).
- Forcing Boundary and Initial Conditions: GFS initial and 3-hourly GFS.
- Simulation Length: 120 hours.

## 15.0 NUMERICAL WEATHER PREDICTION IN COMPLEX TERRAIN

Essentially all NWP models have an unavoidable consequence that the model topography and the surface description are very different from the real one. Dependent on the horizontal grid resolution, height differences of several hundred metres are usual (even at 2.5 km horizontal grid resolution). In addition, nearly all the main mountain valleys are not fully resolved. All the unresolved processes have to be parameterized and simplifications are unavoidable. For example, the observed sub-grid scale surface heterogeneity over an area covered by a model grid box can be large. Nevertheless, the majority of NWP models employ an averaged land use for the entire grid cell. This strongly influences the ability of the NWP model to reproduce the correct surface turbulent fluxes (Molders and Raabe, 1996), having consequences also in the vertical characteristics of the PBL (Molod et al., 2003). Ament and Simmer (2006) have shown that an improved representation of the land-surface heterogeneity with a subgrid scale mosaic approach better reproduces the observed turbulent fluxes at the surface.

Furthermore, the boundary layer parameterizations, which should represent all the unresolvable or sub-grid scale processes, are generally inappropriate for highly complex terrain, because they have originally been developed for flat environments (Rotach and Zardi, 2007). Further topographical effects and special local conditions (e.g., snow coverage), have to be accurately reproduced. All these aspects strongly limit the range of potential use of direct model output.

Experience gained in the last 10 years in the United States with the non-hydrostatic modelling approach is currently being used in the further development of new non-hydrostatic mesoscale models for use in complex terrain. The WRF model is one such example. The Swiss version, now called COSMO, recently became operational with a 7 km horizontal resolution. COSMO was one of the first non-hydrostatic models used operationally by a European weather forecast service.

The new generation of NWP non-hydrostatic models is or will be soon operated at horizontal resolution near 1 km. At this grid spacing additional physical aspects have to be considered. For example, coarse resolution models compute the radiation fluxes on horizontal surfaces. At very high resolution, topographic effects become important because the impact of slope aspect, slope angle or slope inclination, sky view factor as well as shadowing effects significantly modify radiation fluxes at the Earth's surface.

Another perspective for high resolution simulations is given by the concept of large eddy simulation (LES). Here, in contrast to the commonly used Reynolds averaging approach, the Navier-Stokes equations are spatially filtered on a well defined length scale (i.e. the larger scale of the turbulence spectrum is explicitly resolved). For the smaller scales a subgrid-scale turbulence model is used (e.g., Smagorinsky, 1963; Deardoff, 1980; Moeng, 1984). The method of LES was applied with the Advanced Regional Prediction System (ARPS) model in the Riviera Valley in the Swiss Alps (Weigel et al., 2007a, 2207b; Chow et al., 2006). Weigel et al. (2007a) initialised ARPS (Xue et al., 2000, 2001) with initial and boundary conditions from the ECMWF model with a resolution of 60 km, for simulations of the boundary layer structure in the Riviera Valley. The model setup was based on iteratively nesting from 9 km down to 150 m with three

intermediary steps. ARPS was adapted to the Riviera Valley conditions and specially initialised using additional information provided by a hydrological model to properly describe the distribution of soil moisture. The simulation results showed that the model could accurately reproduce the wind patterns observed under convective conditions in this highly complex terrain.

## 16.0 ENSEMBLE-BASED METHODS

Uncertainty is inherent in the forecasting process. Quantifying this uncertainty can provide important information to the decision making processes associated with extreme weather and flood forecasting. Ensemble-based approaches are popular because they allow effects of a wide range of uncertainties to be incorporated. There are a number of sources of uncertainty that contribute to forecast uncertainty. The main sources of modelling uncertainty are associated with the following main groups:

- Random or systematic errors in the model input boundary and initial conditions;
- Uncertainties due to less than optimal model parameter values;
- Uncertainties due to incomplete or biased model processes.

Small differences in the initial state of the atmosphere can result in large differences in the forecast. This is often referred to as the chaos effect. The degree of numerical precision in the initial conditions that are provided to a NWP model may affect the forecast significantly even at the short range projection times. The predictability of the weather is flow dependent and depends on the initial conditions. Several model runs (with different initial conditions and/or model error characteristics and/or boundary conditions) are able to explore different realistic realizations of the atmosphere, and thereby generate quantitative estimates of probabilities of occurrence.

The NAEFS is a joint project involving the Meteorological Service of Canada (MSC), the NWS and the National Meteorological Service of Mexico (NMSM). NAEFS was officially launched in November 2004 in the presence of representatives of the three countries.

NAEFS combines state of the art ensemble forecasts, developed at the MSC and the NWS. When combined, the grand ensemble can provide weather forecast guidance for the 1 to 14-day period that is of higher quality than the currently available operational guidance based on either set of ensembles alone. It allows the generation of a set of forecast products that are seamless across the national boundaries between Canada, the United States and Mexico. The research/development and operational costs of the NAEFS system are shared by the three organizations (MSC, NWS, and NMSM), which make it more cost effective and result in higher quality and more extensive weather forecast products.

Global ensemble forecasts are made twice a day using the Canadian GEM model to generate potential weather scenarios up to 14 days. Twenty "perturbed" weather forecasts are performed as well as an unperturbed 16-day control forecast. The 20 models have different physics parameterizations, data assimilation cycles and sets of perturbed observations.

Every 6 hours, the standard deviations of temperature from the trial fields used in the assimilation cycles of the temperature at a level at approximately 5 km of altitude are computed. Where the standard deviations of the trial fields is large, the degree of uncertainty is large. It is important to have good observations for these uncertain areas. One might target additional observations to such areas to try to diminish the uncertainty.

The daily ensemble forecasts have been available on an operational basis since 24 January 1996. They were originally performed with eight members. On 24 August 1999, 8 more members were added creating a 16-member ensemble forecast system. On 12 January 2005, the Optimal Interpolation Technique for the analysis cycle was replaced with the Ensemble Kalman Filter Technique. Starting in July 2007, four more members were added to produce a 20-member ensemble. Since that time, the system is regularly upgraded (higher resolution, better initial conditions, better parameterizations, etc.).

The ensemble mean may not always be a good forecast. The value of ensemble predictions is in their probabilistic forecasts, and resides in the spread amongst the members. This has important implications for flood forecasting where the decision support information involves a lot more than simply forecasting specific parameters. For example, from an ensemble forecast we are able to construct a forecast probability distribution function (PDF) for a given variable P. The user ought to define a critical value of P such that if it is exceeded, action will be required. From the forecast PDF, one can calculate the probability that the critical P will be exceeded. According to the level of risk, the user may choose to define different critical probability values, on a case by case basis. If the probability exceeds a critical value, then action is required.

In summary; when assessing forecast uncertainty, the departure of the deterministic model from the ensemble mean is an indication of higher uncertainty. Ensemble spread is an indication of uncertainty and confidence:

- Small ensemble spread indicates higher confidence and higher predictability; and
- Large ensemble spread indicates lower confidence and lower predictability.

The ensemble distribution ought to be looked at when assessing possible scenarios. Statistical post-processing of ensembles can provide insights on probability of occurrences of events. The goal of providing detailed deterministic forecasts at all projection times should likely be abandoned. For all intents and purposes, forecasting precipitation should be thought in terms of probabilities. Ensemble statistics can be used to provide a better estimate of the likelihood of future events. The best recommendation is that QPF should be probabilistic, especially at longer projection times.

Ensemble approaches hold great potential for operational hydrologic forecasting. As demonstrated with atmospheric ensemble forecasts, the estimates of predictive uncertainty provide forecasters and users with objective guidance on the level of confidence that they may place in the forecasts. The end users can decide to take action based on their risk tolerance.

### 16.1 Canadian Regional Ensemble Prediction System

Mesoscale Ensemble Prediction System (EPS) can provide more valuable information for short-range forecasts compared to global EPS (more resolution) and deterministic forecasts (PDF), especially for high impact weather events. The Regional Ensemble Prediction System (REPS) as of December 2013 has the following setup:

- Region: North America.

- Model: GEM-Meso with 15 km resolution and 48 vertical levels.
- Forecast range: 3 days.
- Number of members: 20.
- Initial and boundary conditions uncertainty simulation downscaling of Global EPS system forecast.
- Model uncertainty simulation using stochastic physics: Perturbations of physics tendencies (PTP)

**Figure 17** shows the mean (contoured) and standard deviation (colored background) for 24-hour precipitation amounts. This is a 72-hour forecast, valid at 0 UTC 21 June 2013. In the example, the maximum mean 24-hour precipitation ensemble forecast in the Calgary region is 82 mm, with a standard deviation of approximately 40 mm. The mean and standard-deviation can be used as input to an extreme value probability function (shown in **Figure 18**) to compute corresponding precipitation amounts for a range of probabilities. For the 21 June 2013 example, the corresponding 1/100-year (1%) rainfall amount is 207 mm. Burns Creek, a mountain station west of Calgary, received 348.1 mm of precipitation over the 72-hour period 19 to 22 June 2013, and approximately 240 mm in the 24-hour period from 0 UTC 20 June 2013 to 0 UTC 21 June 2013. The 240 mm corresponds to the 1/300-year (0.3%) probability value for 24-hour rainfall.

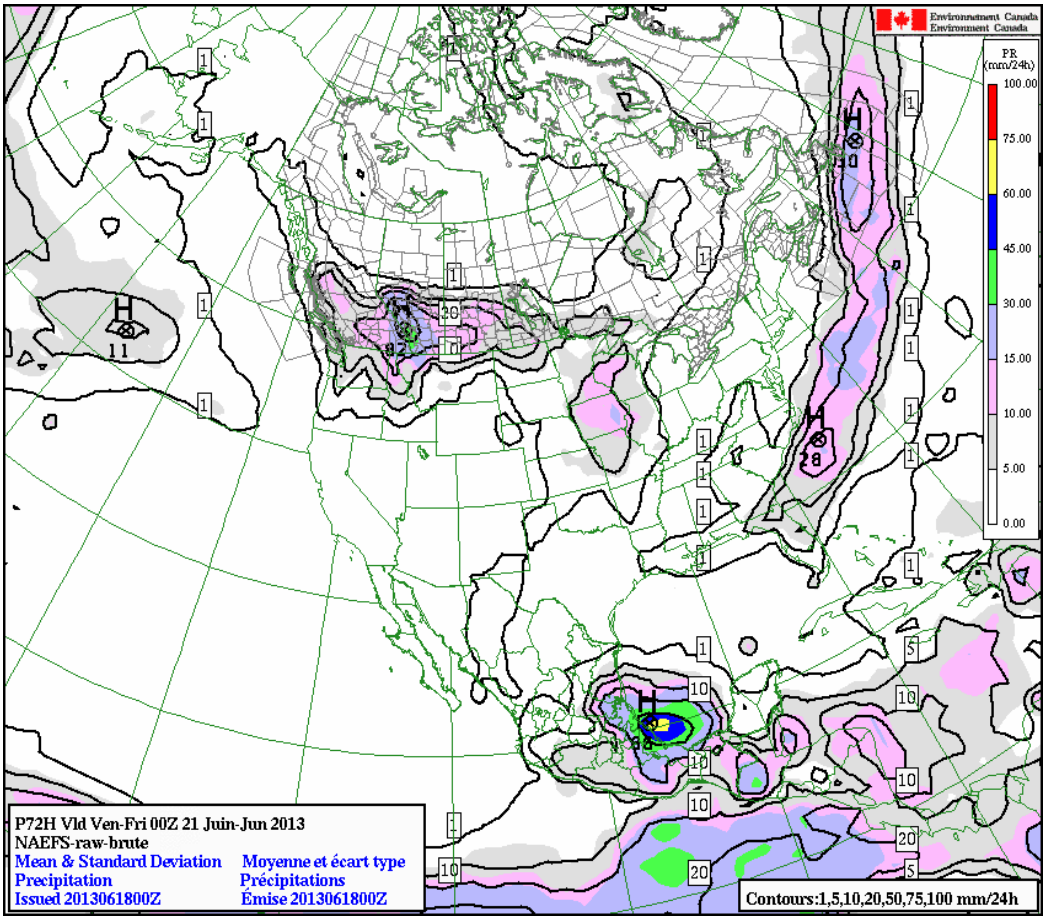


**Figure 17: Mean (Contoured) and Standard Deviation (Colored Background) for 24-hour Precipitation Amounts**

*This is a 72-h forecast, valid at 0 UTC June 21, 2013.

Currently a number of probability of exceedance products are produced by the REPS. They are all produced by counting the number of members exceeding the threshold values of interest and are not calibrated. The first series of such products give the probability that a given variable will exceed a specified threshold value over a 24-hour period at least once during the specified forecast time period. One product gives the probability that precipitation amounts will exceed 5 mm over a 24-hour period at least once during the forecast, 5-day period. This is currently available for the following precipitation amount threshold values: less than 0.2 and more than 2, 5, 10, and 25 mm per 24-hour periods. These probability products are the real strength of the REPS, since they help to quantify the probability or chance of a specific outcome. This may be very useful for flood forecasting, since the ensemble system can produce and display probabilities of exceeding critical values of precipitation over the full domain or a specific area of interest.

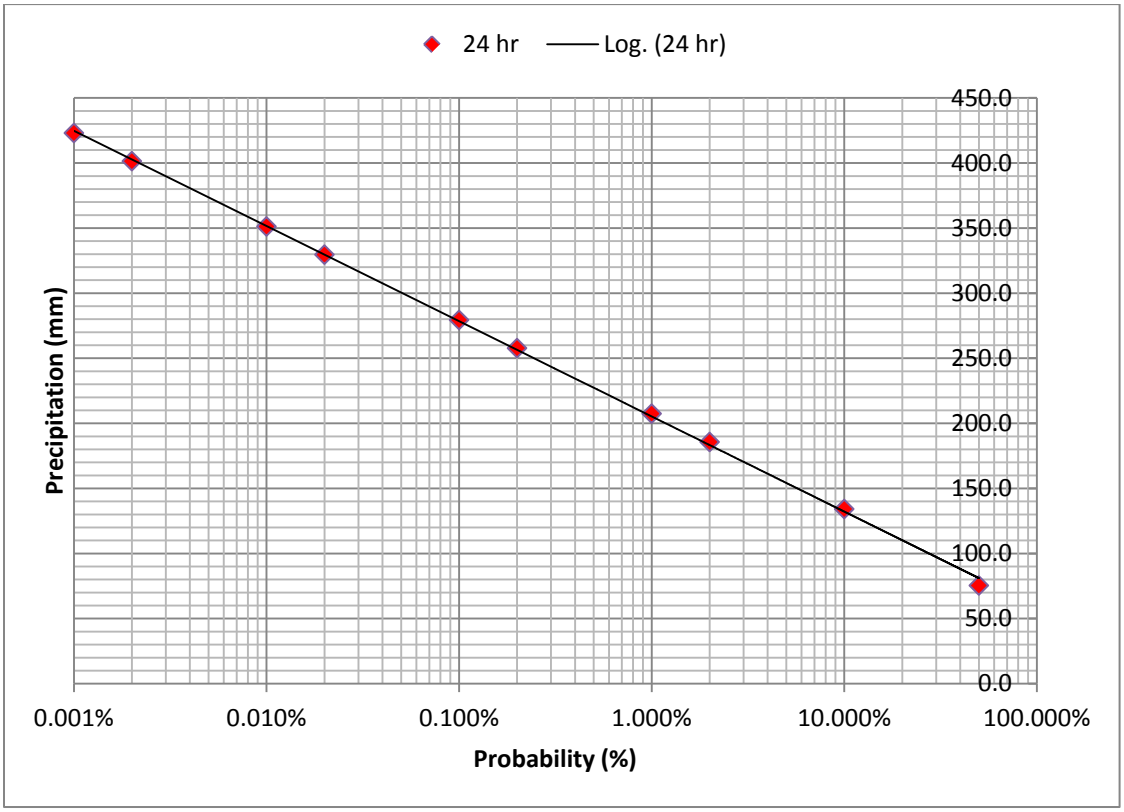


**Figure 18: Method-of-Moments Extreme Value Probability Distribution of 24-hour Rainfall Using a Mean Value of 82 mm and a Standard-Deviation Value of 40 mm, Taken From the 72-hour Forecast at 0 UTC on June 21, 2013.**

## 17.0 QUANTITATIVE PRECIPITATION FORECAST VERIFICATION

Assessing the quality of QPFs from NWP models is generally accomplished by either comparing a precipitation forecast grid to observation stations or to an analysed gridded field of precipitation. The intercomparison between model precipitation and rain gauge observations was performed on the model grid and also averaged across the key precipitation zones of the river basins.

The important headwater (source) precipitation zones of the major river basins in Alberta are shown on **Figure 19**. The names of the precipitation zones (sub-basins) corresponding to the numbers on **Figure 19** are as follows:

A. Bow-Oldman
    1. Bow Banff
    2. Bow Spray Cascade
    3. Bow Kananaskis Ghost
    4. Upper Sheep Upper Elbow
    5. Upper Highwood
    6. Lower Elbow
    7. Lower Sheep Lower Highwood
    8. Upper Oldman Lower Castle
    9. Upper Castle Upper Crowsnest
    10. Upper Belly Upper Waterton
    11. Upper St Mary Lee Creek
    12. Lower Belly Lower Waterton
    13. Willow Creek
    14. Lower St Mary Mid-Oldman
    15. Little Bow River
B. Cypress
    1. South Cypress
    2. North Cypress
C. Hanging Christina
    1. Christina/Hangingstone
D. Milk
    1. Milk
E. North Saskatchewan
    1. Bighorn Reservoir
    2. Brazeau Nordegg
    3. Drayton Valley to Telfordville
    4. Ram/Baptist
F. Red Deer
    1. James/Fallentimber/Burntimber
    2. Little Red Deer/Raven
    3. Medicine/Blindman
G. Smoky
    1. Upper Wapati Beaverlodge

2. Lower Wapati Bear
3. UpperSmoky
4. Kakwa Cutbank
5. Simonette River
6. Little Smoky River

H. Swan Hills
    1. Swan Hills

I. Upper Athabasca
    1. Windfall
    2. Pembina upper
    3. Pembina Paddle Conf
    4. Mcleod River
    5. Wildhay Berland
    6. Upper Athabasca

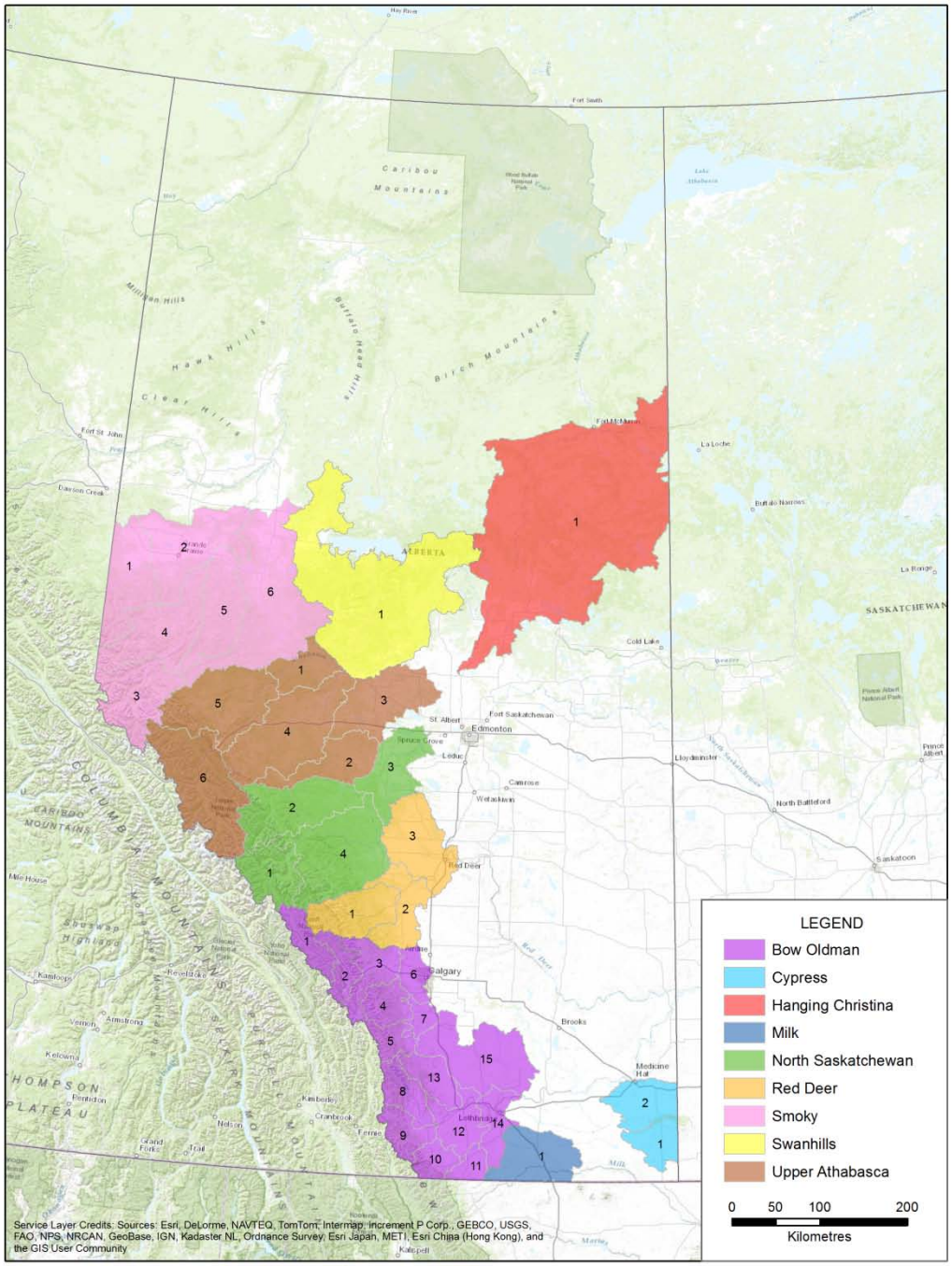


**Figure 19: The Headwater (Source) Precipitation Zones for the Major River Basins in Alberta**

One limitation to NWP precipitation forecasts is the period covered by their forecasts. The total forecast period for each model is as follows:

- GFS 180 hours 7.5 days
- GDPS 144 hours 6 days
- NAM 84 hours 3.5 days
- RDPS 48 hours 2 days

Therefore, if the parameter to be forecast is 72-hour accumulated precipitation, this means that the RDPS is unable to predict this quantity in advance of the event, only 48-hour accumulated precipitation is available. However, we can compare the 2-day forecast of total precipitation for each run, to investigate its capability to capture portions of the period of interest. For similar reasons, none of the models are able to predict 72-hour accumulated precipitation a full 5 days in advance of the start of the event. However, the GFS is able to provide a forecast 7.5 days in advance, which includes 2.5 days of the extreme event at the tail end of its forecast period. Therefore, the reader must keep in mind the limitations of the model forecast periods when interpreting some of the QPF verification results.

### 17.1 19 to 22 June 2013 Southern Alberta Numerical Weather Prediction Assessment

For the 19 to 22 June 2013 event, the greatest precipitation was reported at Burns Creek station in the foothills region southwest of Calgary. Burns Creek received 348.1 mm of precipitation over the 72-hour period 19 to 22 June 2013. Burns Creek is located very near the boundary of basin precipitation zones Bow-Oldman (BO) #4 and BO #5. A map of the important headwater (source) precipitation zones for the River Basins of Alberta is shown on **Figure 17**. The mean precipitation depth per 6-hour interval for each NWP model for each zone was computed. For this analysis, time-zero was chosen to be 12:00 UTC (5 am MST) on 19 June 2013, as the official start of the 72-hour extreme rain event.

The map of the observed 72-hour accumulated precipitation for the 19 to 22 June 2013 event, is shown in **Figure 20**.

The precipitation forecast maps by the GFS model 5, 4, 3, 2, and 1-day in advance of the precipitation for the 72-hour period 19 June (5 am MST) to 22 June (5 am MST), 2013 are shown in **Figures 21, 23, 25, 2 7, and 29** respectively. The corresponding maps of the difference between the observed precipitation and model forecast precipitation for each forecast lead time are shown in **Figures 22, 24, 26, 28, and 30** . The 5-day advance forecast looked reasonable in the predicted area and maximum amounts >300 mm. The difference map for 5 days in advance, shows that the model forecast area of maximum precipitation was further north than observed and more extensive. The GFS forecast generated on 15 June 2013 (4 days in advance), shown in **Figure 23**, was poorer, shifting the area of maximum precipitation further north and greatly underestimating the precipitation within the Bow-Oldman basin. The GFS model forecasts 3, 2, and 1-day in advance show the various displacements of the maximum forecast precipitation generally to the north, and the greater area forecast of the heavy

precipitation. However, the magnitude of the maximum 72-hour precipitation was reasonable; therefore, the GFS model indicated the potential danger of extreme rainfall and the potential danger of significant flooding.

The NAM forecast 72-hr precipitation generated 1 day before the start of the significant rainfall event, is shown in **Figure 31**. Extreme rainfall amounts >300 mm were predicted and the area was generally shifted north of where the greatest precipitation was observed. Similar to the GFS, the NAM forecast of extreme rainfall >300 mm was larger than observed. The NWP precipitation forecasts certainly indicated flood dangers several days in advance based on the guidance of the GFS and NAM; however, the forecast area was much larger than what transpired in reality.

The GDPS model forecasts are shown in **Figures 33, 35, and 37** for 3, 2, and 1 day in advance of the start of the event. In general, the area of maximum precipitation looks to be more in agreement with the area observed; however, the predicted amount of rainfall was significantly less (typically 100 to 200 mm less than observed).

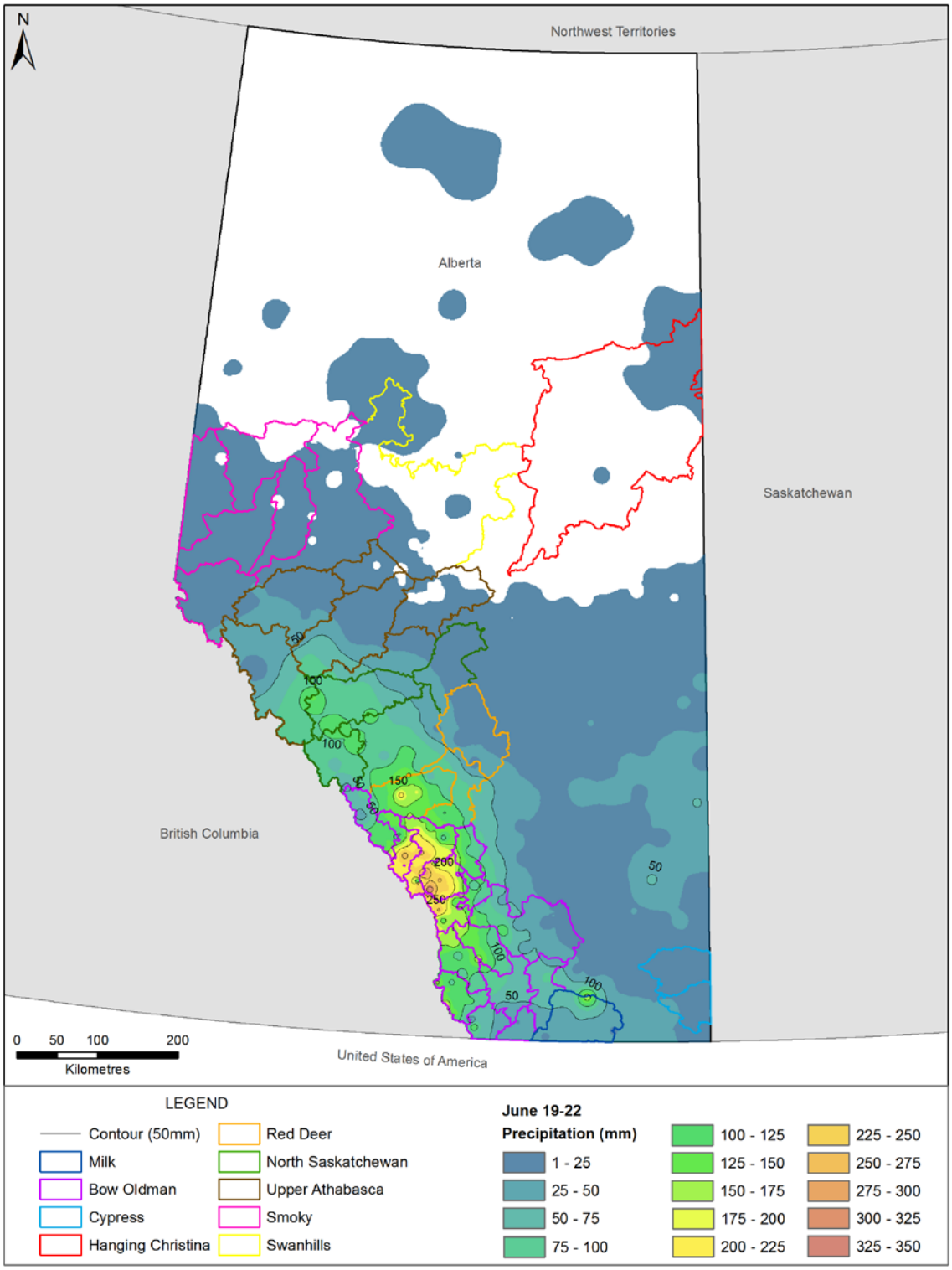


**Figure 20: Observed 72-hour Accumulated Precipitation for the 19 to 22 June 2013**

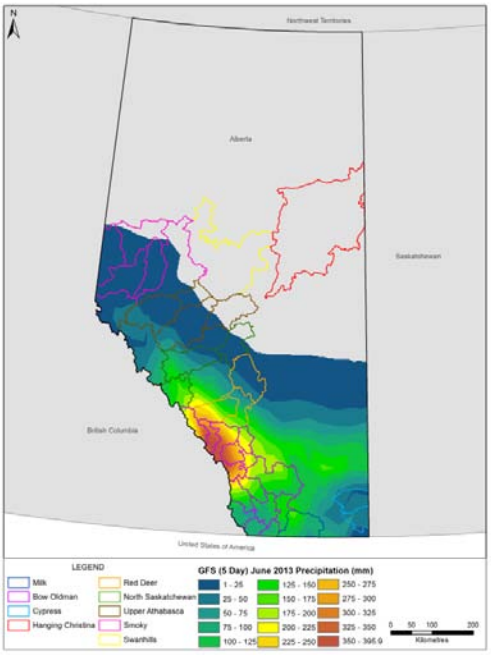


**Figure 21: GFS 5-day in Advance Forecast of 72-hour Precipitation Generated on 20130614 (5 am MST)**

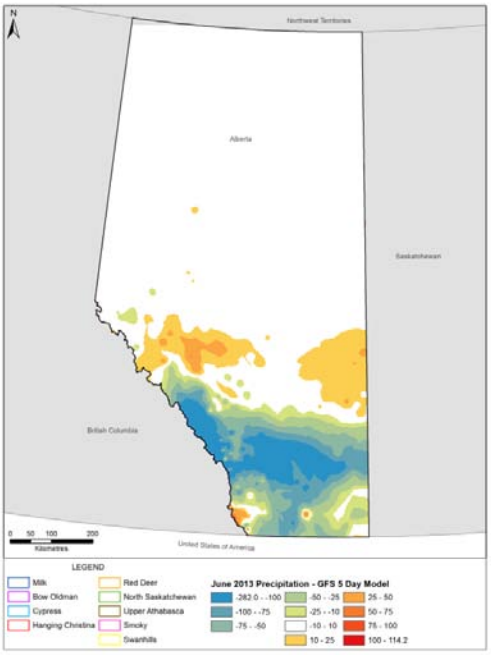


**Figure 22: Observed 72-hour Precipitation Minus GFS 5-day in Advance Forecast of the 72-hour Precipitation**

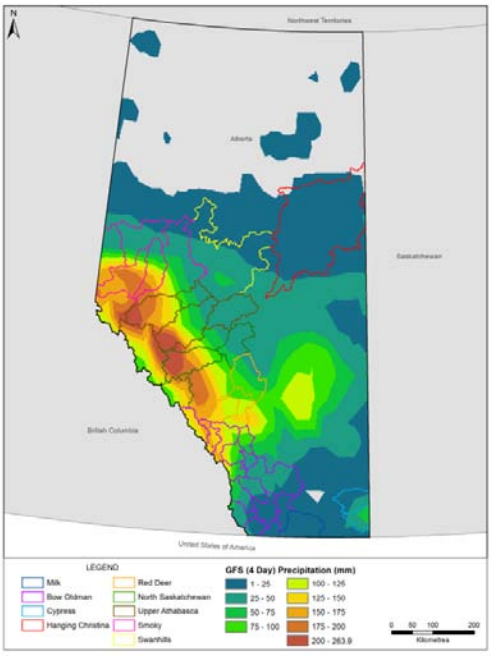


**Figure 23: GFS 4-day in Advance Forecast of 72-hour Precipitation Generated on 20130615 (5 am MST)**

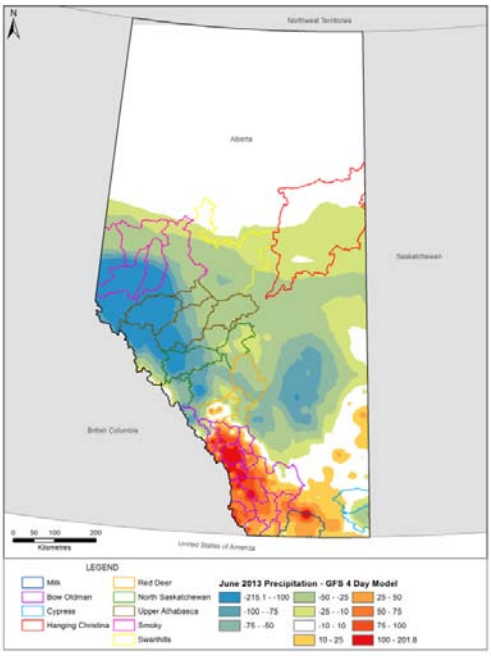


**Figure 24: Observed 72-hour Precipitation Minus GFS 4-day in Advance Forecast of the 72-hour Precipitation**

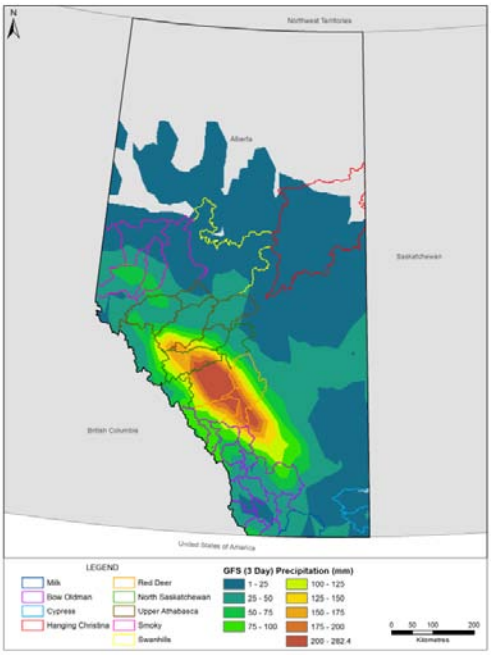


**Figure 25: GFS 3-day in Advance Forecast of 72-hour Precipitation Generated on 20130616 (5 am MST)**

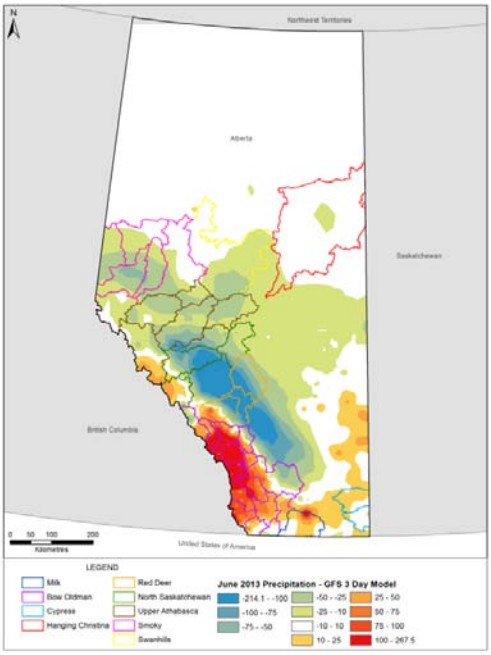


**Figure 26: Observed 72-hour Precipitation Minus GFS 3-day in Advance Forecast of the 72-hour Precipitation**

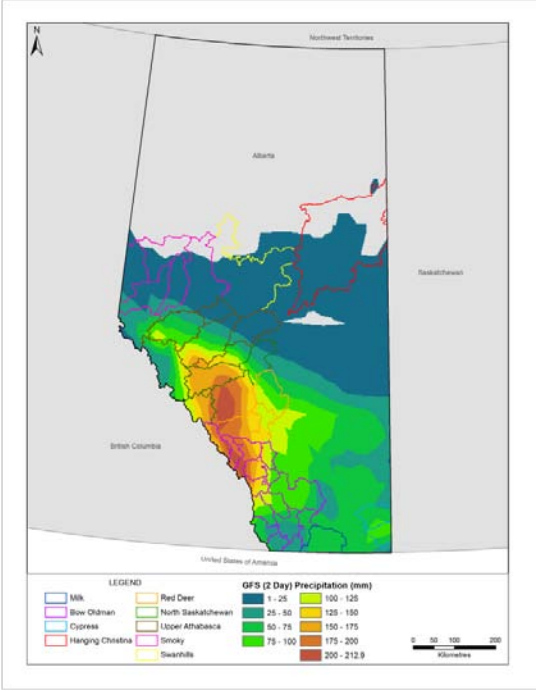


**Figure 27: GFS 2-day in Advance Forecast of 72-hour Precipitation Generated on 20130617 (5 am MST)**

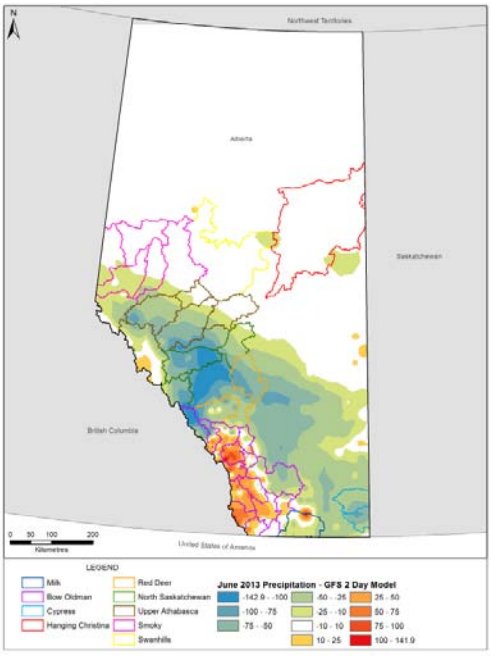


**Figure 28: Observed 72-hour precipitation Minus GFS 2-day in Advance Forecast of the 72-hour Precipitation**

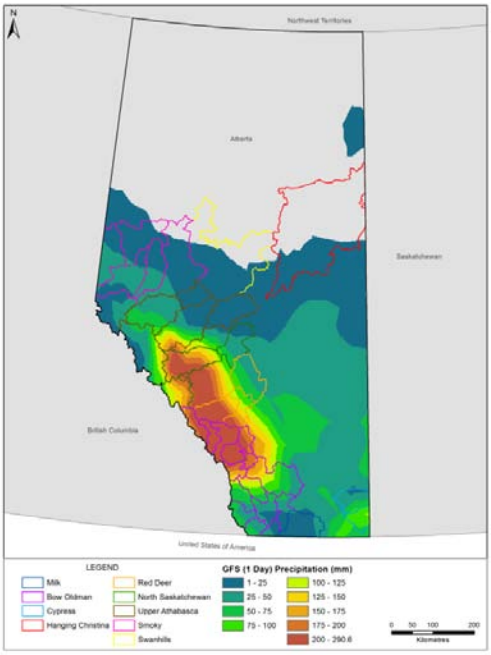


**Figure 29: GFS 1-day in Advance Forecast of 72-hour Precipitation Generated on 20130618 (5 am MST)**

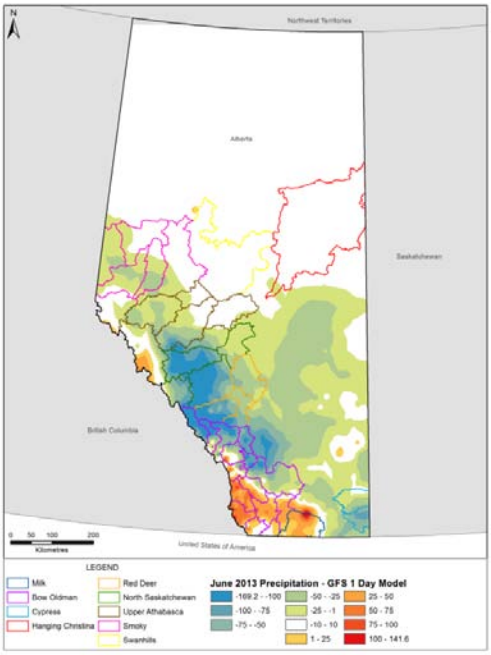


**Figure 30: Observed 72-hour Precipitation Minus GFS 1-day in Advance Forecast of the 72-hour Precipitation**

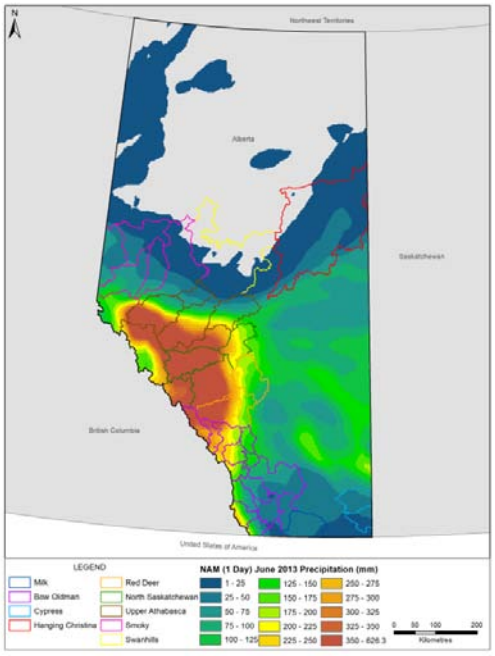


**Figure 31: NAM 1-day in Advance Forecast of 72-hour Precipitation Generated on 20130614 (5 am MST).**

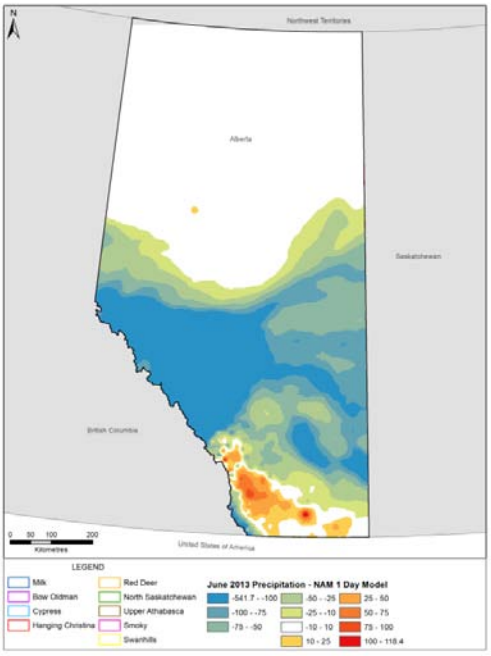


**Figure 32: Observed 72-hour Precipitation Minus NAM 1-day in Advance Forecast of the 72-hour Precipitation**

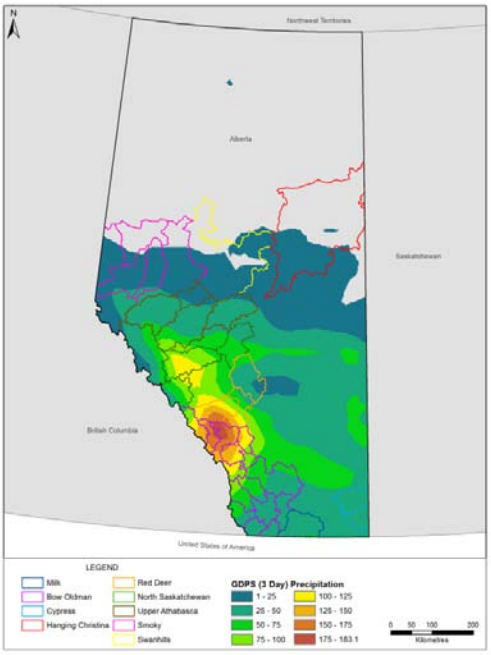


**Figure 33: GDPS 3-day in Advance Forecast of 72-hour Precipitation Generated on 20130616 (5 am MST)**

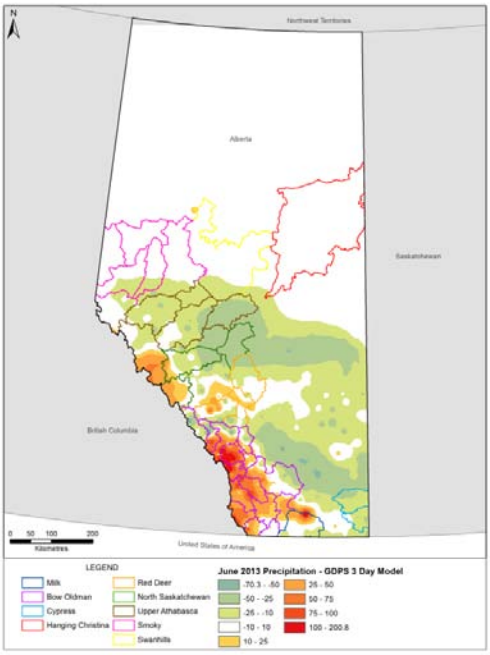


**Figure 34: Observed 72-hour Precipitation Minus GDS 3-day in Advance Forecast of the 72-hour Precipitation**

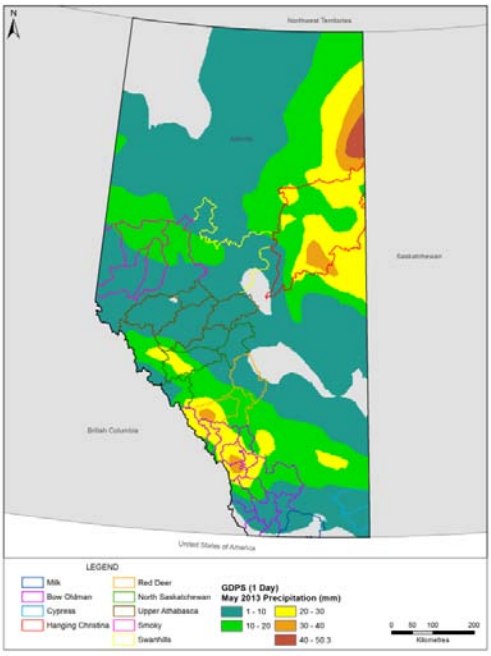


**Figure 35: GDPS 1-day in Advance Forecast of 72-hour Precipitation Generated on 20130618 (5 am MST)**

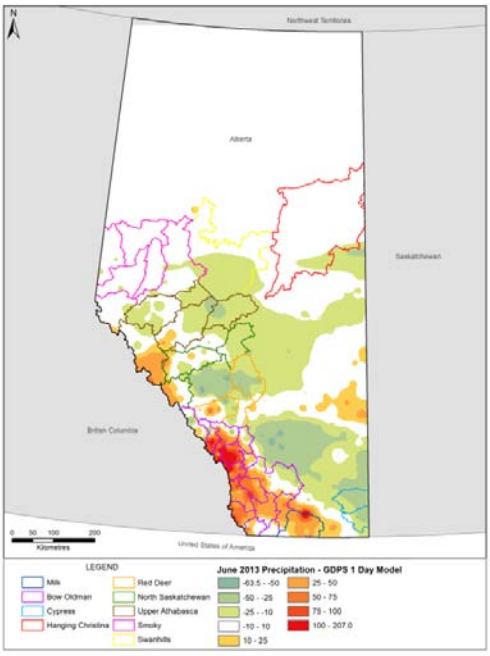


**Figure 36: Observed 72-hour Precipitation Minus GDPS 1-day in Advance Forecast of the 72-hour Precipitation**

Scatter plots of the predicted 72-hour precipitation (sub-basin area-averaged depth) versus forecast lead time for the zones BO #4 and #5 are shown in **Figures 37 and 38,** respectively. These plots show the forecast 72-hour precipitation >0 mm every 6 hours, for each model. Burns Creek reported 348.1 mm for this event, for comparison purposes. The NAM model produced the most rain; >150 mm, 48 hours before the start of the flood event. However, an interesting observation is that the forecasts at 6 and 18 UTC each day fluctuate considerably, with significantly lower values, which lowers the confidence. The reader is reminded that some models do not completely cover the 72-hour period at the longer lead times; therefore, it is natural that some models under predict at the longer lead times, due to incomplete coverage of the entire 72-hour period. However, all of the models under predicted the precipitation at Burns Creek for all periods to varying degrees.

It is interesting to note that the NAM model predicted the most precipitation 48 hours in advance, even though the total forecast period is 3.5 days, indicating that the NAM was forecasting very high precipitation amounts in the first 36 hours of the 3 day period.

The GFS model produced the most consistent high values of precipitation for these zones, extending out to 120 hours. Zone precipitation >100 mm was consistently forecast 72 hours in advance; however, there were also significant deviations at the 6-hour intervals. It is quite evident that the model forecasts at 06 UTC (11 pm MST) and 18 UTC (11 am MST) have greater variability, most likely associated with the lack of updated radiosonde data at 06 and 18 UTC for their initialization. One must conclude that the 06 UTC (11 pm MST) and 18 UTC (11 am MST) forecasts for all models are less reliable than the 00 UTC (5 pm MST) and 12 UTC (5 am MST) forecasts for QPF.

The GDPS model had one high forecast value 3 days in advance, and then consistently forecast about 80 to 100 mm (approximately 25% to 30% of the maximum observed) in the period 2 to 4 days before the event.

The RDPS model forecast the least precipitation, predicting 50 to 80 mm the day before the event started; however, this is partly due to the fact that the RDPS has the shortest total forecast period (48 hours maximum).

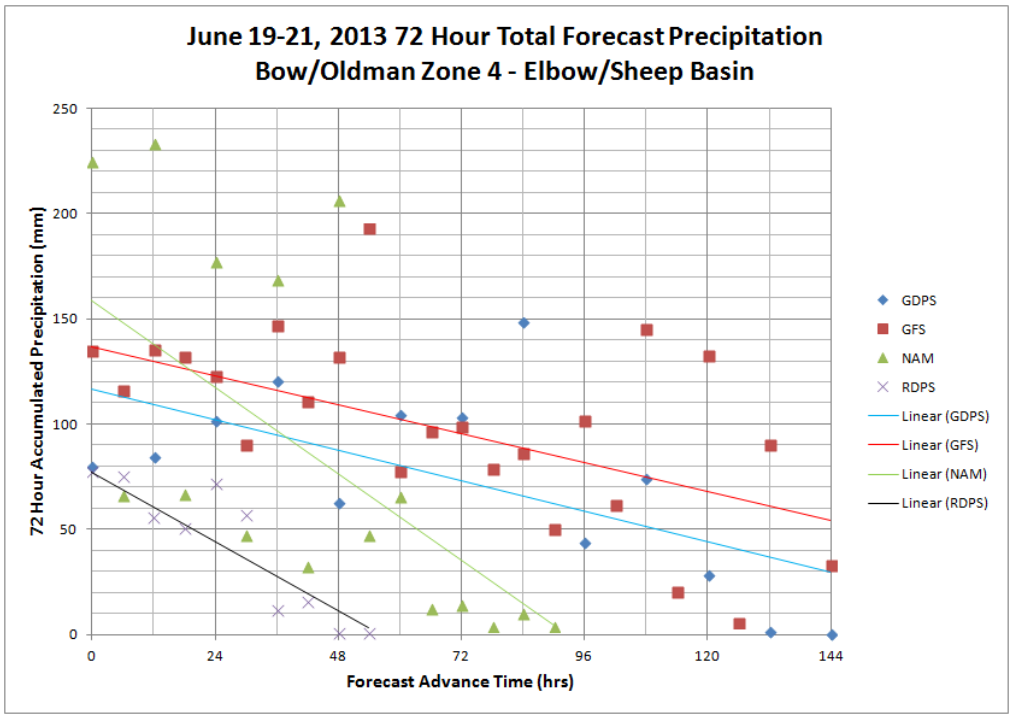


**Figure 37: Forecast 72-hour Area-Averaged Total Precipitation Versus Forecast Lead Time for the Bow-Oldman Zone #4 Elbow-Sheep Basin**

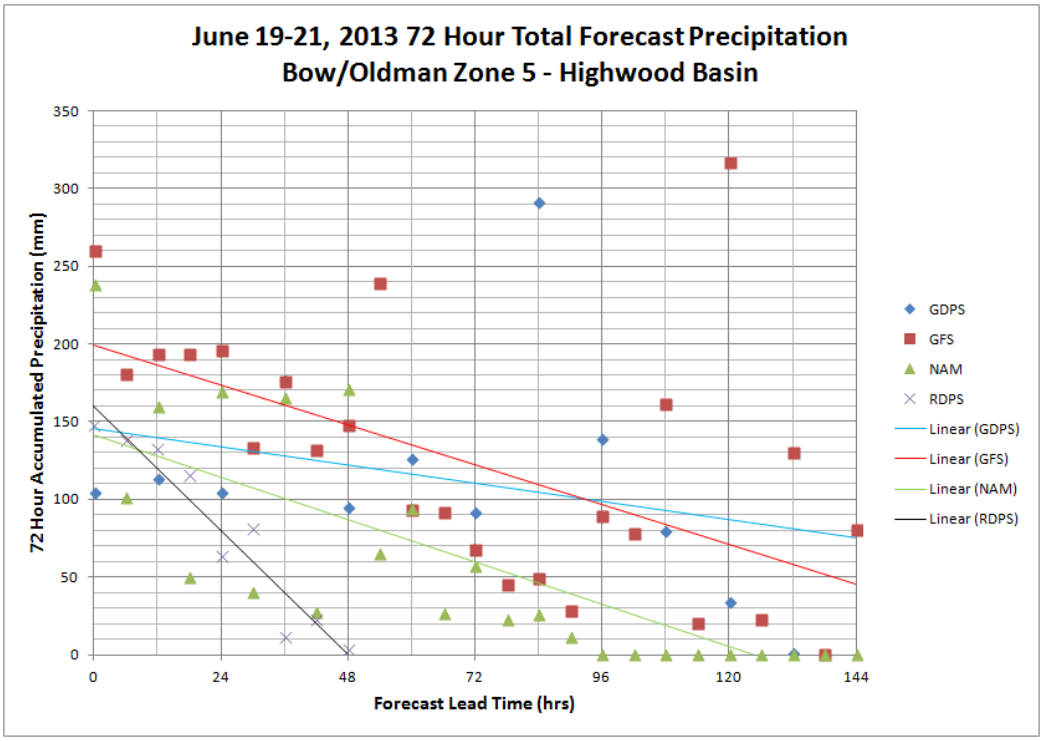


**Figure 38: Forecast 72-hour Area-Averaged Total Precipitation Versus Forecast Lead Time for the Bow-Oldman Zone #5 Highwood Basin**

The WRF model forecasts of 72-hour precipitation, 2 days in advance and 1-day in advance are shown in **Figures 39 a nd 41** respectively. The differences between the observed precipitation and the model forecast precipitation are shown in **Figures 40 and 42** respectively. The results are rather disappointing since there is no obvious difference or advantage to using the WRF, in spite of its very high spatial resolution (4 km) and advanced physics parameterization schemes and explicit convection. However, the simulation was conducted in the same manner in which it would have been run in real-time, with initialization using the current GFS model values as initial and boundary conditions. Therefore, the initial conditions are only as good as the GFS simulation, and therein lies the problem. Recent publications using WRF to simulate Alberta flood events have reported very good results (Pennelly et al., 2014; Flesch and Reuter, 2012); however, those research simulations were initialized the day before the first day for which the precipitation was to be evaluated to allow for model spin-up, and the boundary conditions were obtained from the North American regional reanalysis dataset (Messinger et al., 2006). Initializing using a reanalysis hind-cast makes a significant difference. The WRF model results in this study in essence display the forward propagation of the errors introduced by the real-time, erroneous GFS initialization.

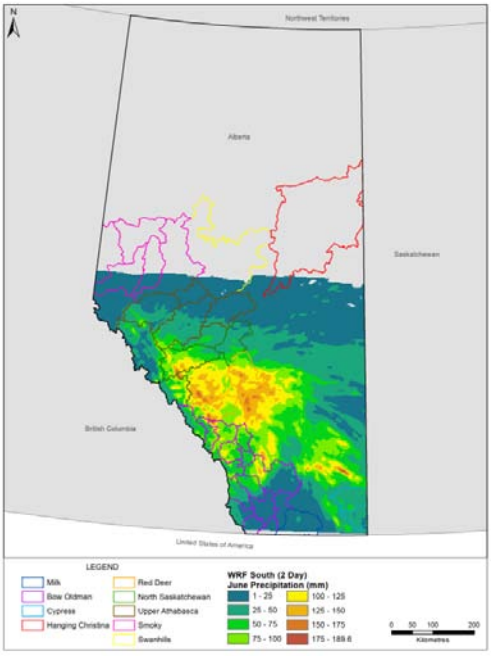


**Figure 39: WRF 2-day in Advance Forecast of 72-hour Precipitation Generated on 20130617 (5 am MST)**

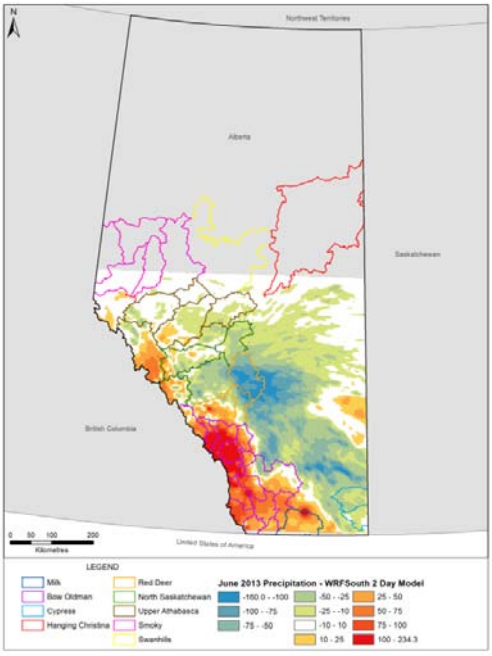


**Figure 40: Observed 72-hour Precipitation Minus WRF 2-day in Advance Forecast of the 72-hour Precipitation**

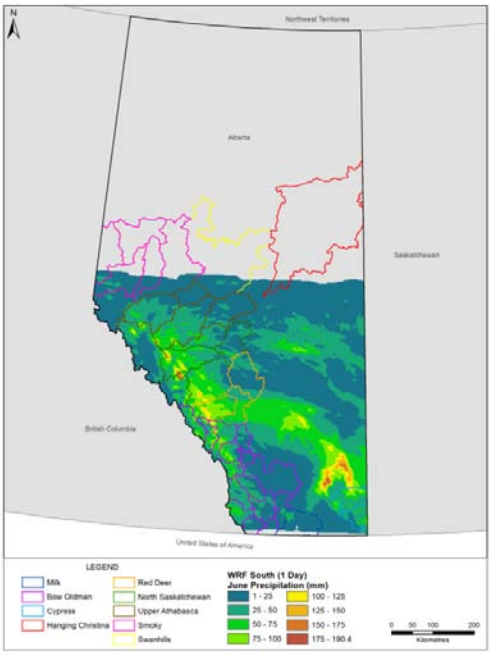


**Figure 41: WRF 1-day in Advance Forecast of 72-hour Precipitation Generated on 20130618 (5 am MST)**

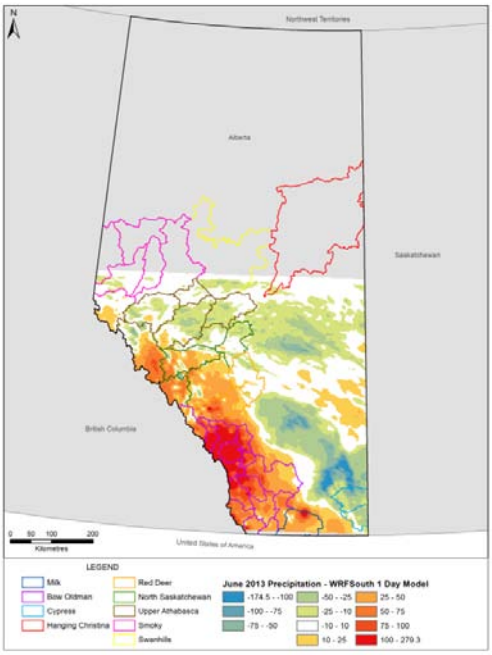


**Figure 42: Observed 72-hour Precipitation Minus WRF 1-day in Advance Forecast of the 72-hour Precipitation**

### 17.1.1 Forecast Precipitation Intensity 24 Hours before the 19 to 22 June 2013 Event

The various model QPFs at 3-hour intervals for the Bow-Oldman basin Zone #4, produced 24 hours before the start of the June 2013 extreme rainfall event, are shown on **Figure 43**. The rainfall recorded at Burns Creek (maximum reported rainfall) and Elbow Ranger Station (minimum reported rainfall) and the average rainfall calculated from all stations within Zone #4 are shown for comparison purposes. The model precipitation rates have been averaged for the entire Zone #4.

The NAM model predicted the start of the rain 6 hours before the actual start of the heaviest rainfall and 6 hours before the other models. The GFS model QPF agrees quite well with the average station rainfall with respect to the timing and amount.

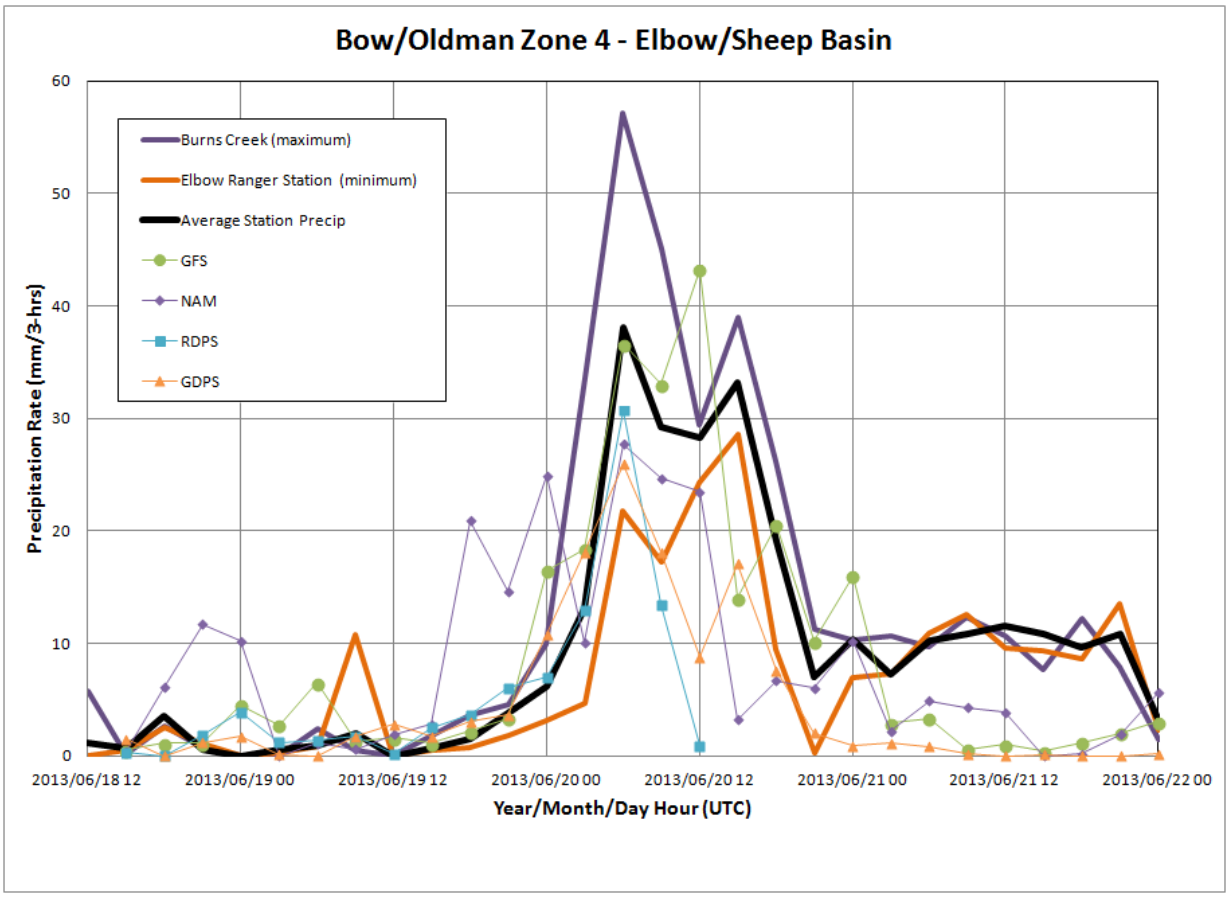


**Figure 43: Model and Gauge Precipitation Rate (mm per 3 hours) versus Time (18 June 2013 12 UTC to 22 June 2013 0 UTC) for the Bow/Oldman Zone #4**

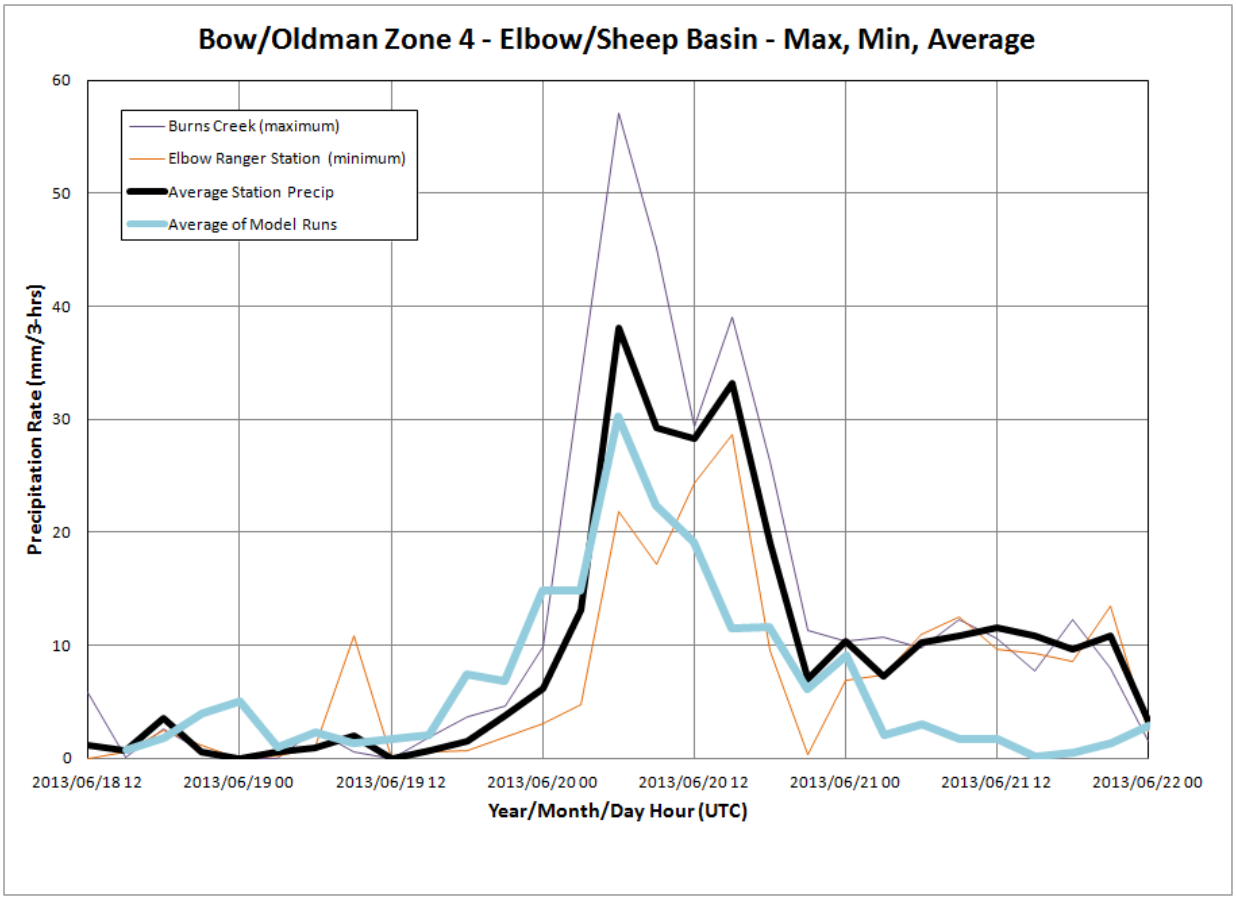


**Figure 44: Average Model and Average Gauge Precipitation Rate (mm per 3 hours) versus Time (18 June 2013 12 UTC to 22 June 2013 0 UTC) for the Bow/Oldman Zone #4**

The average model QPFs at 3-hour intervals for the Bow-Oldman basin Zone #4, produced 24 hours before the start of the June 2013 extreme rainfall event, are shown on **Figure 44**. The rainfall recorded at Burns Creek (maximum reported rainfall) and Elbow Ranger Station (minimum reported rainfall) and the average rainfall calculated from all stations within Zone #4 are shown for comparison purposes. The model average rainfall intensities started at the right time and exceeded the observed average rainfall rates for the first 6 hours and peaked at approximately the same time as the observed maximum. The model averaged rainfall maximum was within 10 mm for the station averaged rainfall maximum for Zone #4. The model QPFs dropped sooner than observed although the duration of the event was in general agreement.

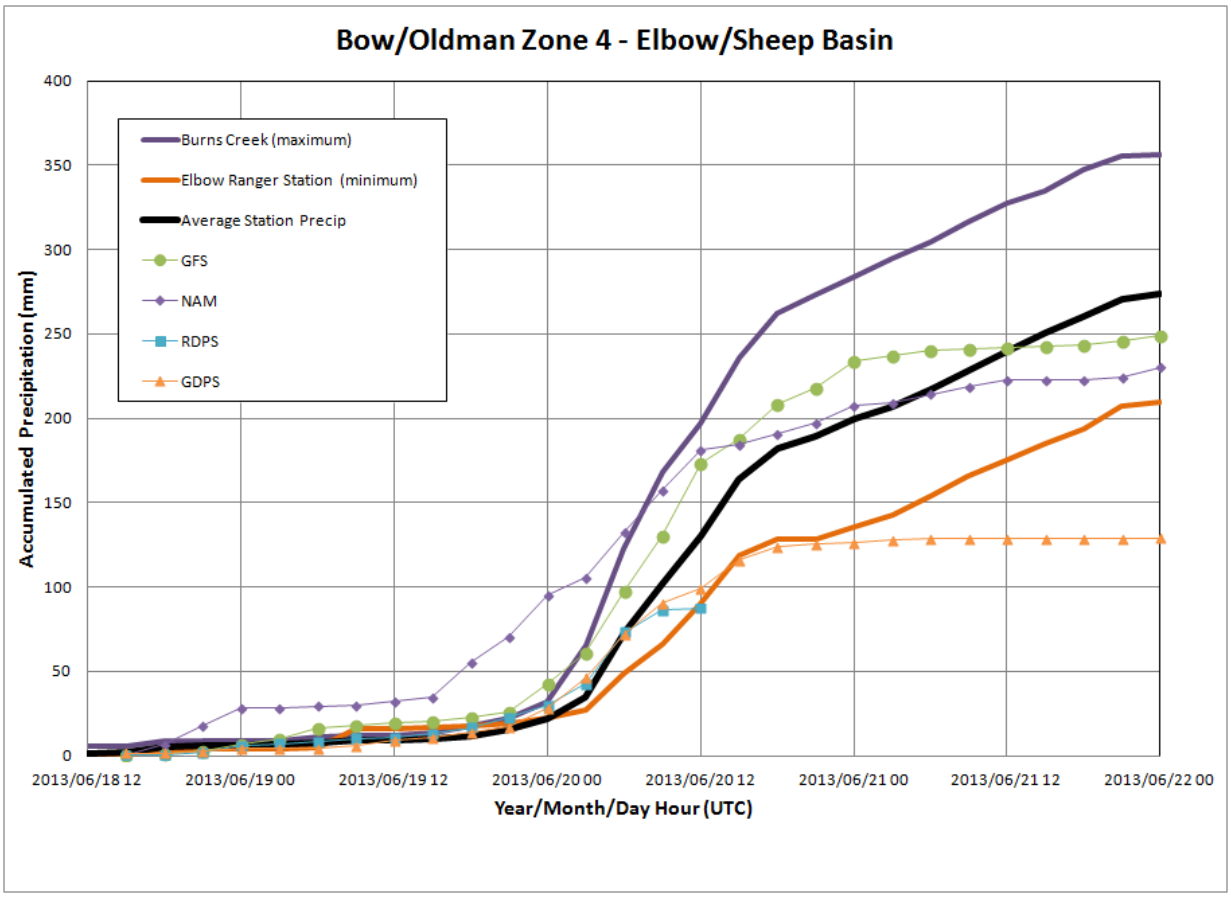


**Figure 45: Model and Gauge Accumulated Precipitation (mm) versus Time (18 June 2013 12 UTC to 22 June 2013 0 UTC) for the Bow/Oldman Zone #4**

The various model QPF accumulations at 3-hour intervals for the Bow-Oldman basin Zone #4, produced 24 hours before the start of the June 2013 extreme rainfall event, are shown on **Figure 45**. The accumulated rainfall recorded at Burns Creek (maximum reported rainfall) and Elbow Ranger Station (minimum reported rainfall) and the average accumulated rainfall calculated from all stations within Zone #4 are shown for comparison purposes.

The NAM model predicted significant accumulation (>100 mm) approximately 6 hours before it was observed and before the other models. The GFS and NAM models predicted the total accumulation for Zone #4 within 25 and 50 mm, respectively, of the zone average accumulated rainfall. All of the models under predicted the total rainfall accumulation for Zone #4.

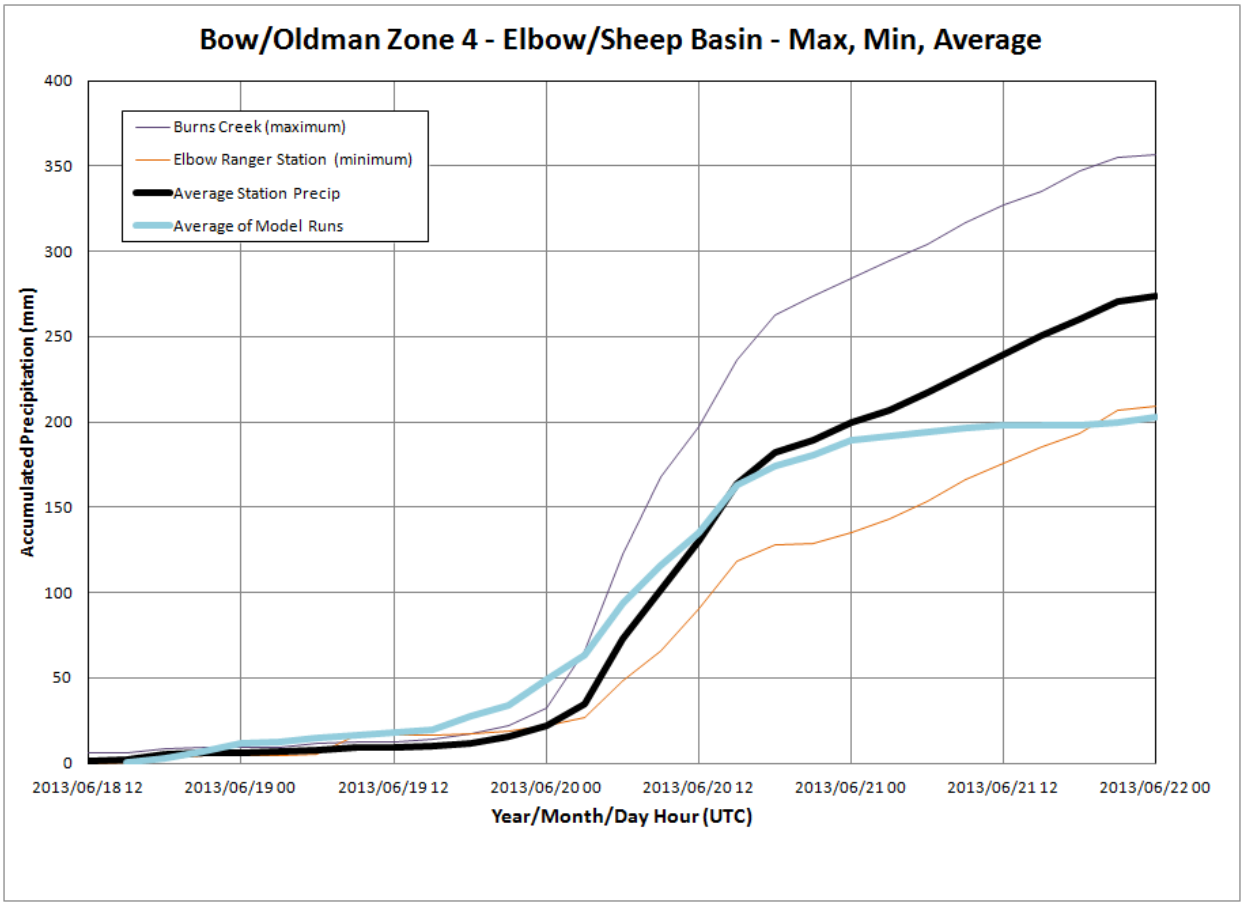


**Figure 46: Average Model and Average Gauge Accumulated Precipitation (mm) versus Time (18 June 2013 12 UTC to 22 June 2013 0 UTC) for the Bow/Oldman Zone #4**

The average model QPF accumulation at 3-hour intervals for the Bow-Oldman basin Zone #4, produced 24 hrs before the start of the June 2013 extreme rainfall event, is shown on **Figure 46**. The accumulated rainfall recorded at Burns Creek (maximum reported rainfall) and Elbow Ranger Station (minimum reported rainfall) and the average accumulated rainfall calculated from all stations within Zone #4 are shown for comparison purposes. The average model total rainfall was approximately 70 mm below the observed average accumulated rainfall. The timing of the model averaged extreme rainfall event was in general agreement with the recorded average rainfall accumulation.

The various model QPFs at 3-hour intervals for the Bow-Oldman basin Zone #5, produced 24 hours before the start of the June 2013 extreme rainfall event, are shown in **Figure 47** . The rainfall recorded at Highwood (maximum reported rainfall) and Sullivan Creek (minimum reported rainfall) and the average rainfall calculated from all stations within Zone #5 are shown for comparison purposes. The model precipitation rates have been averaged for the entire Zone #5.

The NAM model once again predicted the start of the rain 6 hours before the actual start of the heaviest rainfall and 6 hours before the other models. The GFS model QPF agreed quite well with the average station rainfall with respect to the timing and amount.

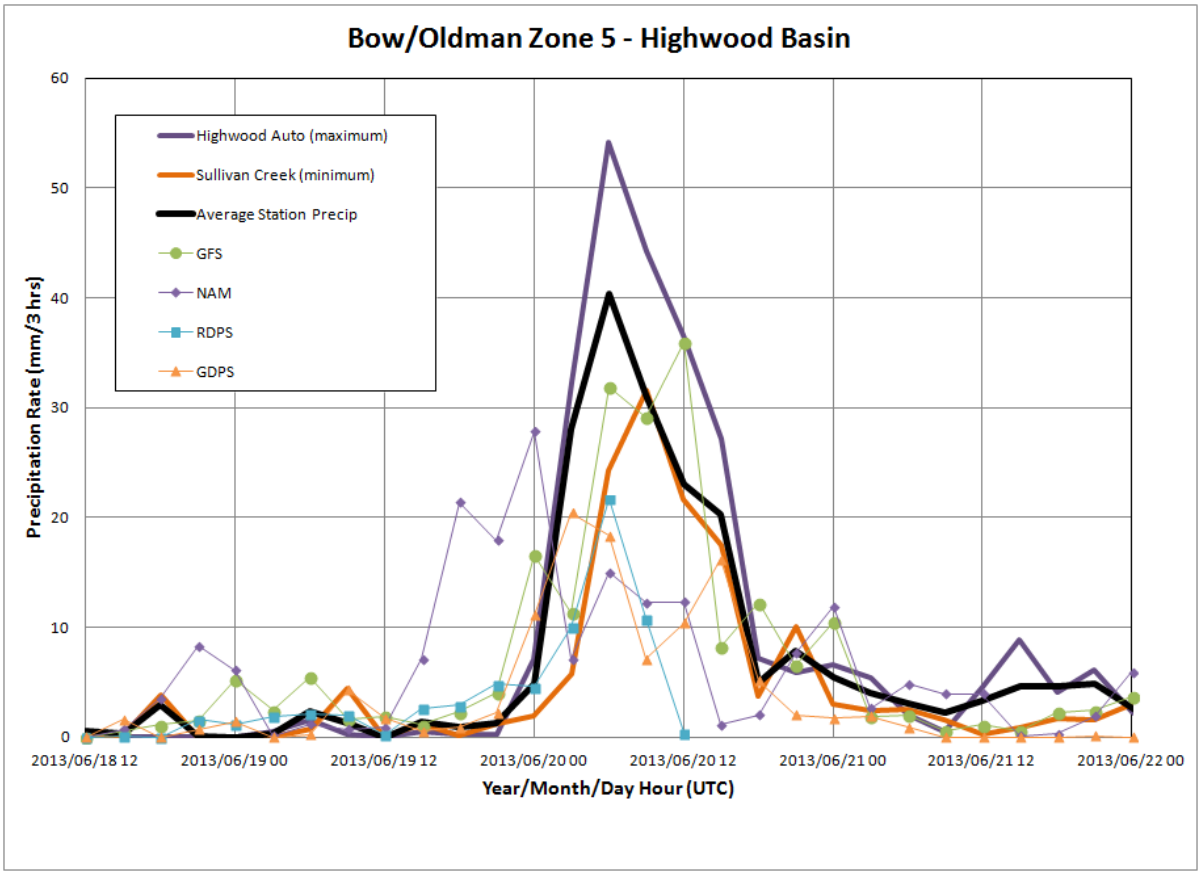


**Figure 47: Model and Gauge Precipitation Rate (mm per 3 hours) versus Time (18 June 2013 12 UTC to 22 June 2013 0 UTC) for the Bow/Oldman Zone #5**

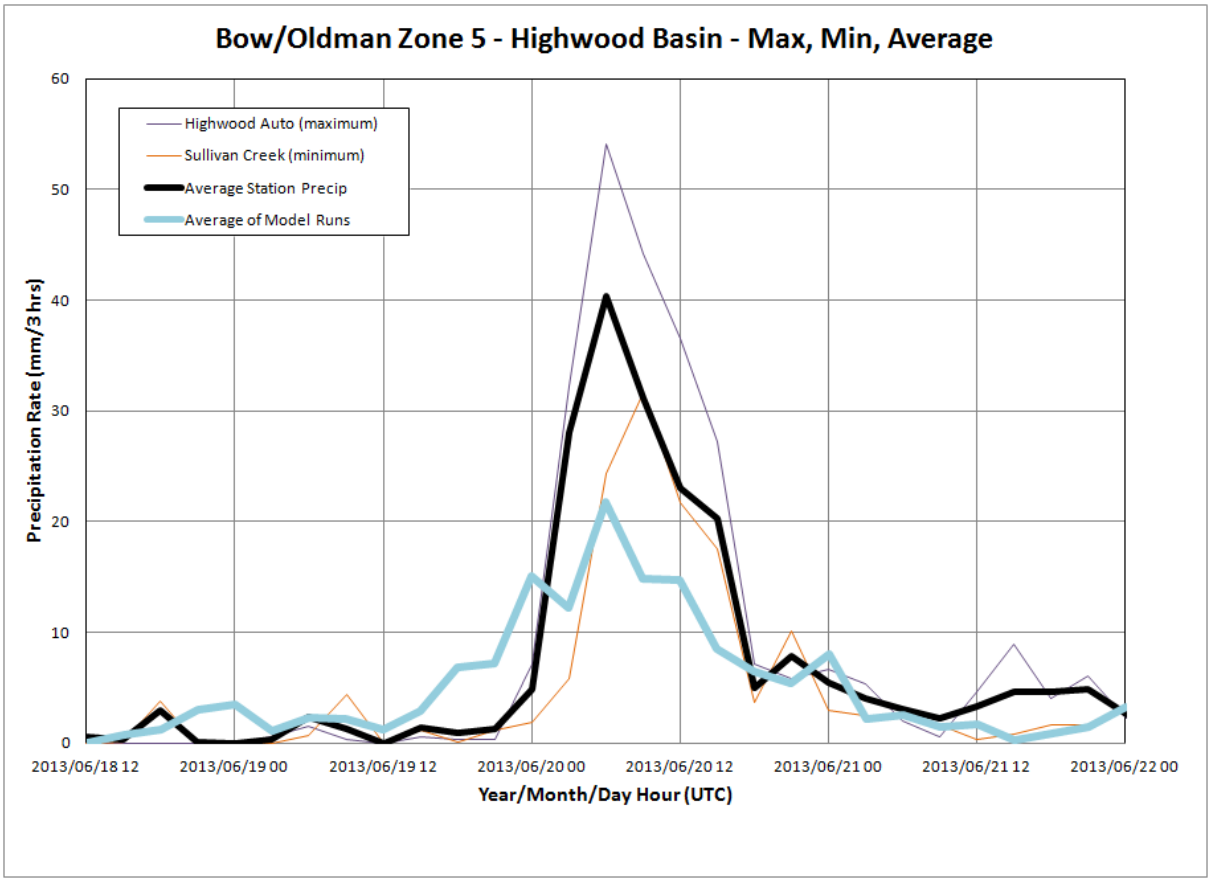


**Figure 48: Average Model and Average Gauge Precipitation Rate (mm per 3 hours) versus Time (18 June 2013 12 UTC to 22 June 2013 0 UTC) for the Bow/Oldman Zone #5**

The average model QPF at 3-hour intervals for the Bow-Oldman basin Zone #5, produced 24 hours before the start of the June 2013 extreme rainfall event, are shown in **Figure 48**. The rainfall recorded at Highwood (maximum reported rainfall) and Sullivan Creek Station (minimum reported rainfall) and the average rainfall calculated from all stations within Zone #5 are shown for comparison purposes. The model average rainfall intensities started approximately 6 hours early and exceeded the observed average rainfall rates for the first 6 hours and peaked at approximately the same time as the observed maximum. The model averaged rainfall maximum was approximately 20 mm less than the station averaged rainfall maximum for Zone #5. The model QPF duration of the event for Zone #5 was in general agreement.

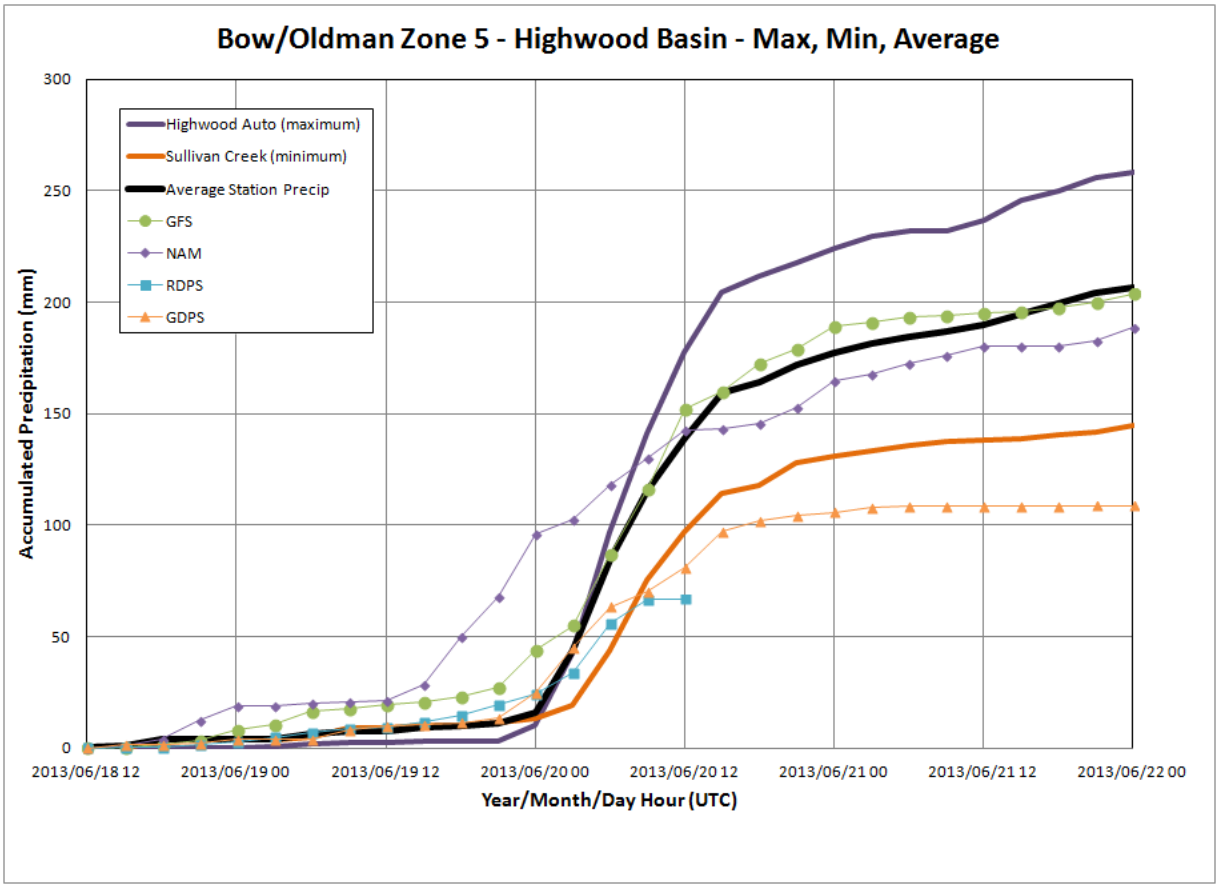


**Figure 49: Model and Gauge Accumulated Precipitation (mm) versus Time (18 June 2013 12 UTC to 22 June 2013 0 UTC) for the Bow/Oldman Zone #5**

The various model QPF accumulations at 3-hour intervals for the Bow-Oldman basin Zone #5, produced 24 hrs before the start of the June 2013 extreme rainfall event, are shown on **Figure 49**. The accumulated rainfall recorded at Highwood (maximum reported rainfall) and Sullivan Creek (minimum reported rainfall) and the average accumulated rainfall calculated from all stations within Zone #5 are shown for comparison purposes.

The NAM model predicted significant accumulation (>100 mm) approximately 6 hours before it was observed and before the other models. The GFS model predicted the total accumulation almost exactly and the NAM model predicted the total accumulation for Zone #5 within 20 mm of the zone average accumulated rainfall. The GDPS and RDPS models significantly under predicted the total rainfall accumulation for Zone #5 although the timing was generally good.

The average model QPF accumulation at 3-hour intervals for the Bow-Oldman basin Zone #5, produced 24 hours before the start of the June 2013 extreme rainfall event, is shown on **Figure 50**. The accumulated rainfall recorded at Highwood (maximum reported rainfall) and Sullivan Creek (minimum reported rainfall) and the average accumulated rainfall calculated from all stations within Zone #5 are shown for comparison purposes. The average model total rainfall was approximately 40 mm below the observed average accumulated rainfall. The timing of the

model averaged extreme rainfall event was in general agreement with the recorded average rainfall accumulation.

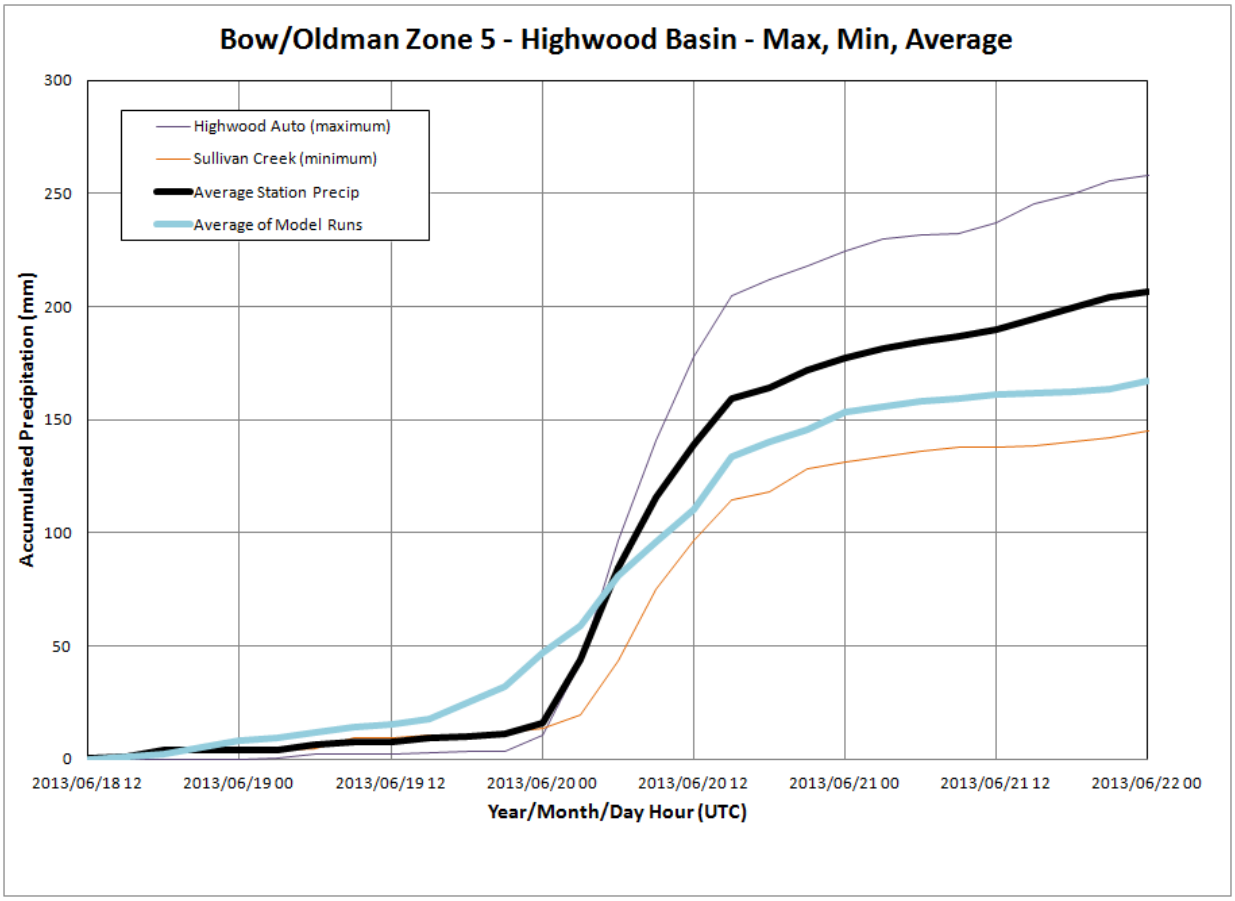


**Figure 50: Average Model and Average Gauge Accumulated Precipitation (mm) versus Time (18 June 2013 12 UTC to 22 June 2013 0 UTC) for the Bow/Oldman Zone #4**

### 17.1.2 Statistical Evaluation of 19 to 22 June 2013 Quantitative Precipitation Forecast Performance

A statistical evaluation of the QPF performance for the June 2013 event was conducted based on 119 stations within the river basin source precipitation zones of Alberta. The evaluation parameter was the observed precipitation recorded during the first day of the flood event (19 June [12 UTC] to 20 June [12 UTC] 2013). This gives the greatest lead time for the model forecasts and assesses the ability of the models to give warnings of potential extreme rainfall. Statistics were computed using surface station observations compared to the nearest grid point of each model. Of the 119 rainfall stations 86 are located within the Bow Oldman river basin; therefore, these statistics are most representative of the Bow-Oldman basin, which received the greatest precipitation.

The hit rate, also called the probability of detection (POD), is calculated from the contingency table shown below as:

| Event forecast | Event observed | | |
|---|---|---|---|
| | Yes | No | Marginal total |
| Yes | a | b | a + b |
| No | c | d | c + d |
| Marginal total | a + c | b + d | a + b + c + d =n |

$$H = POD = a / (a + c)$$

H = POD = (number of events correctly forecast) / (total number of events observed)

The range of H is 0 to 1 and the score is positively oriented. A perfect score is 1. Since the formula for H contains reference to "c" (misses) and not to "b" (false alarms), the hit rate is sensitive only to missed events rather than false alarms. This means that one can always improve the hit rate by forecasting the event more often, which usually results in higher false alarms and, especially for rare events, is likely to result in an over-forecasting bias. The false alarm ratio is the fraction of the forecasts of the event associated with non-occurrences, as the name implies and is defined by:

$$FAR = b / (a + b)$$

FAR = (false alarms) / (number of forecasts of the event)

The FAR can be controlled by deliberately under forecasting the event; such a strategy risks increasing the number of missed events, which is not considered in the FAR. For this reason, the POD and the FAR should both be considered for a better understanding of the performance of the forecast. The frequency bias, or just "bias" is computed from the contingency table shown above by:

$$B = FBI = (a + b) / (a + c)$$

B = (total forecast yes) / (total observed yes)

The bias has a range of possible values of 0 to ∞. When the number of observed occurrences of the event is small, the denominator becomes small and the bias correspondingly large and unstable. The desirable value for bias is 1, indicating an unbiased forecast where the event is forecast exactly as often as it is observed. The bias is often called "frequency bias" to distinguish it from the linear bias or mean error which is a verification measure for continuous

variables. When B is greater than 1, the event is over forecast. When B is less than 1, the event is under forecast.

The Critical Success Index, also called the Threat Score, is given by:

$$CSI = TS = a / (a + b + c)$$

CSI = (hits) / (hits + false alarms + misses)

Its range is 0 to 1, with a value of 1 indicating a perfect forecast. The CSI is frequently used, with good reason. Unlike the POD and the FAR, it takes into account both false alarms and missed events, and is therefore a more balanced score. The CSI is somewhat sensitive to the climatology of the event, tending to give poorer scores for rare events.

**Figures 51, 52, 53, and 54** show the POD, FAR, BIAS, and CSI of the QPF of each model, for a 25 mm threshold of precipitation as a function of forecast lead time for the first 24 hours of precipitation 19 to 20 June 2013 in southern Alberta. Only the 0 and 12 UTC model runs were evaluated. The previous analyses have already noted that the 06 and 18 UTC model runs have lower skill, due to their lack of updated initial and boundary conditions.

**Figure 51** shows that the POD of the fraction of stations receiving >25 mm was typically very good (80%) 5 days in advance. However, the FAR shown in **Figure 52** indicates that typically 30% or 40% of the number of forecasts >25 mm were actually false alarms. The BIAS on **Figure 45** >1 indicates that the forecast number of stations >25 mm was generally over forecast by 120% to as much as 180%.

The CSI shown in **Figure 54** indicates that the ratio of the number of stations correctly forecast to receive >25 mm of precipitation, divided by the number of stations correct plus false alarms plus missed forecast was typically 50% to 60% by all three models GDPS, GFS, and NAM.

The statistics suggest that in general the GFS is the first model to alert the user of potential extreme rainfall amounts, followed by the GDPS, and then the NAM.

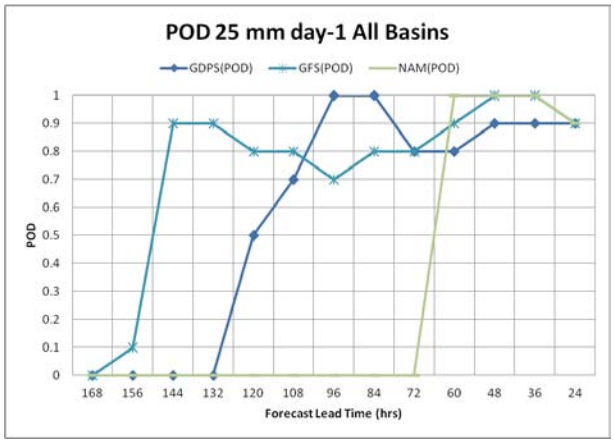


**Figure 51: Statistical Probability of Detection of QPF 25 mm Rainfall for all Basins as a Function of Lead Time**

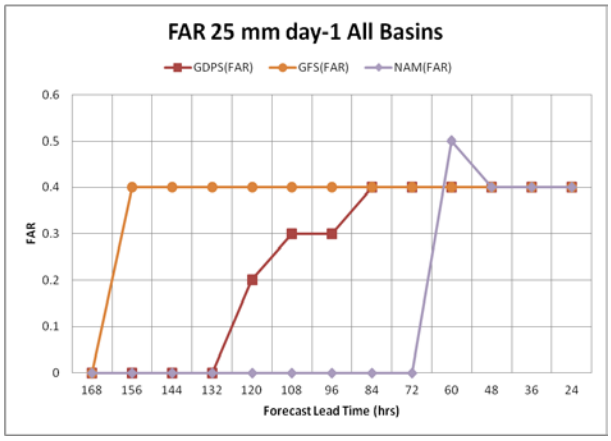


**Figure 52: Statistical False Alarm Ratio of QPF 25 mm Rainfall for all Basins as a Function of Lead Time**

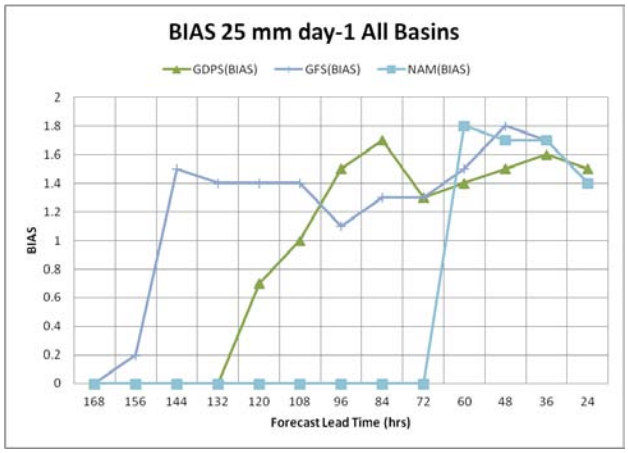


**Figure 53: Statistical Bias of QPF 25 mm Rainfall for all Basins as a Function of Lead Time**

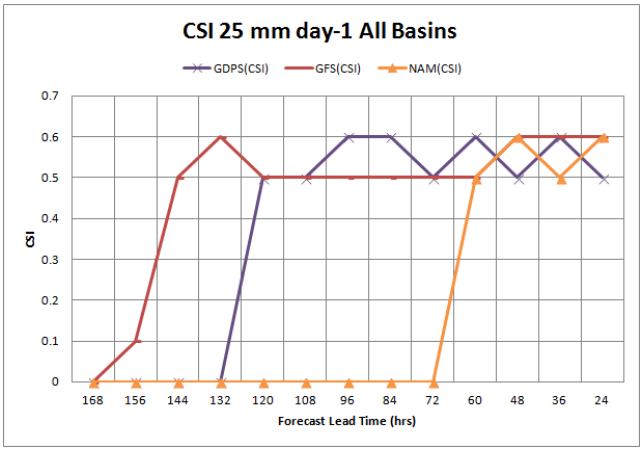


**Figure 54: Statistical Critical Success Index of QPF 25 mm Rainfall for all Basins as a Function of Lead Time**

**Figures 55, 56, 57, and 58** show the POD, FAR, BIAS, and CSI of the QPF for each model, for a 100 mm threshold of precipitation as a function of forecast lead time for the first 24 hours of precipitation 19 to 20 June 2013 in southern Alberta.

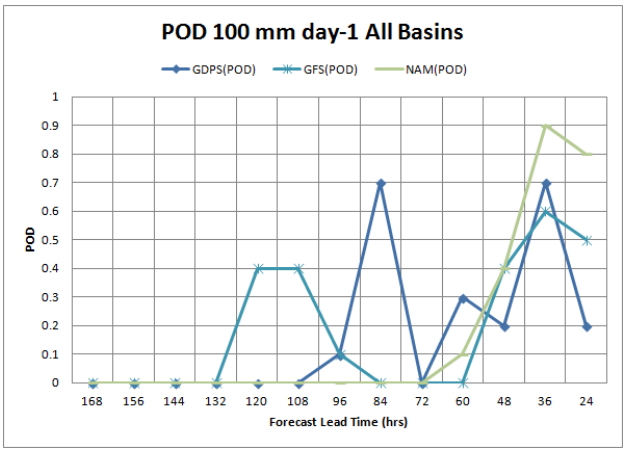


**Figure 55: Statistical Probability of Detection of QPF 100 mm Rainfall for all Basins as a Function of Lead Time**

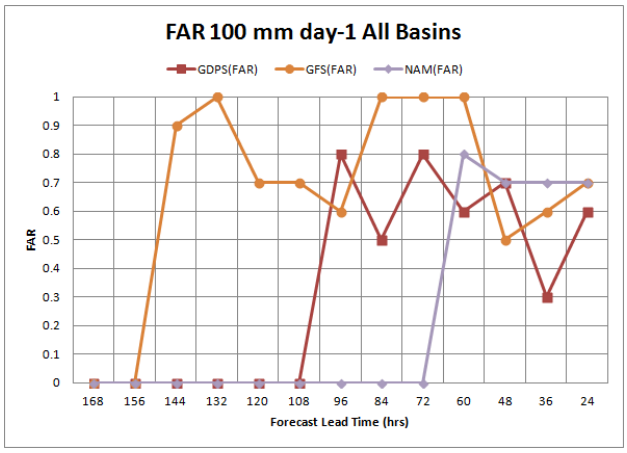


**Figure 56: Statistical False Alarm Ratio of QPF 100 mm Rainfall for all Basins as a Function of Lead Time**

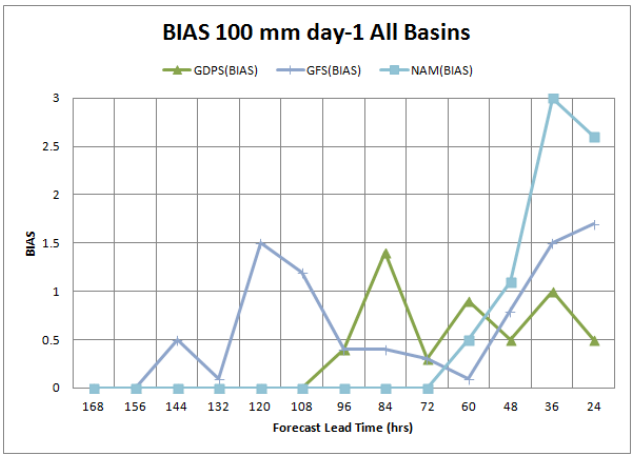


**Figure 57: Statistical Bias of QPF 100 mm Rainfall for all Basins as a Function of Lead Time**

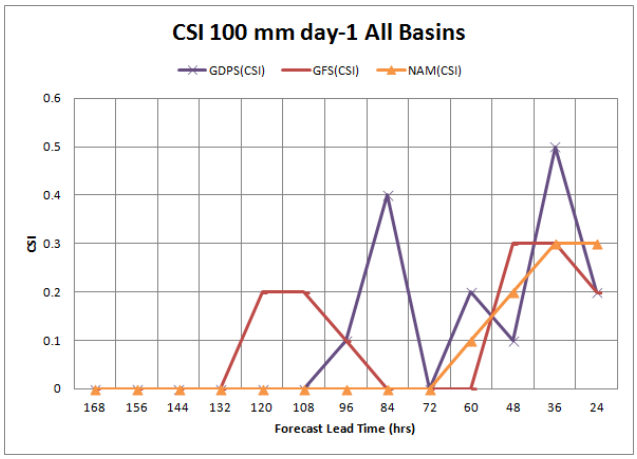


**Figure 58: Statistical Critical Success Index of QPF 100 mm Rainfall for all Basins as a Function of Lead Time**

The statistical evaluation for the 100 mm threshold shows that most of the models were able to forecast about 60% to 90% of the number of stations >100 mm, but there was a significant over forecast of the number of stations by the NAM and GFS 48 hours in advance, and generally an under forecast of the number by the GDPS although it was closer to reality. The CSI for the models was typically between 10% and 40%. The GDPS had the highest CSI 36 and 84 hours in advance, although it generally was the most modest in its predicted area of extreme precipitation, and it was also most modest and underestimated the greatest precipitation amounts. The NAM had the highest BIAS, over forecasting the number of stations exceeding 100 mm amounts and forecasting the greatest rainfall amounts 1 to 2 days in advance. Overall, the GFS and GDPS showed some skill in alerting to extreme precipitation amounts 3 to 5 days in advance. The NAM model tended to over forecast the rainfall amounts and area of high rainfall 48 hours in advance and less.

## 17.2 4 to 7 June 2013 Northern Alberta Numerical Weather Prediction Assessment

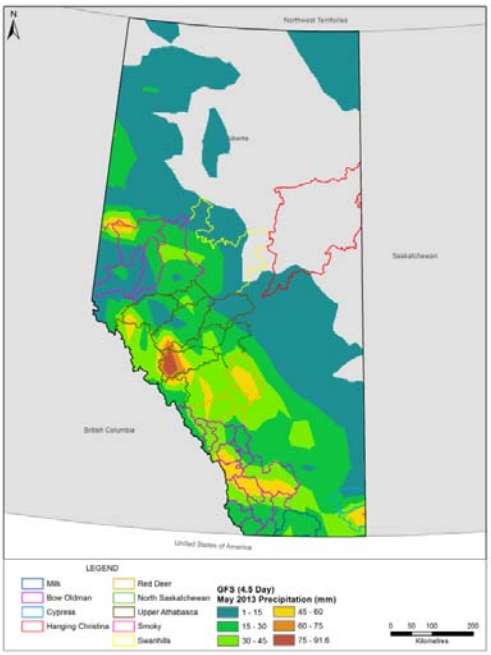


**Figure 59: GFS 4.5-day in Advance Forecast of 72-hour Precipitation Generated 20130603 (5pm MST)**

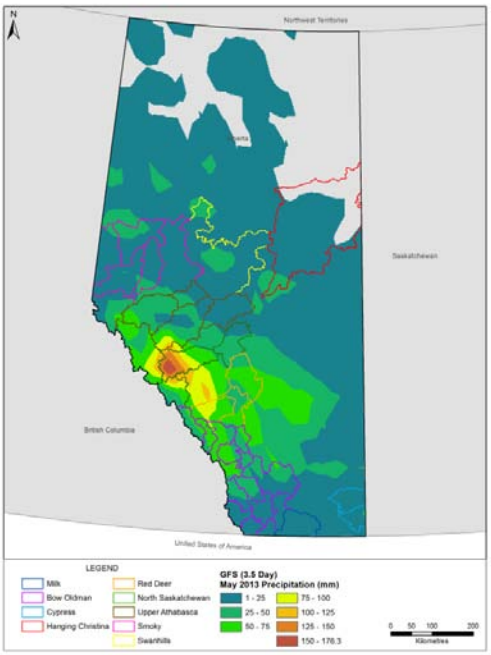


**Figure 60: GFS 3.5-day in Advance Forecast of 72-hour Precipitation Generated 20130604 (5pm MST)**

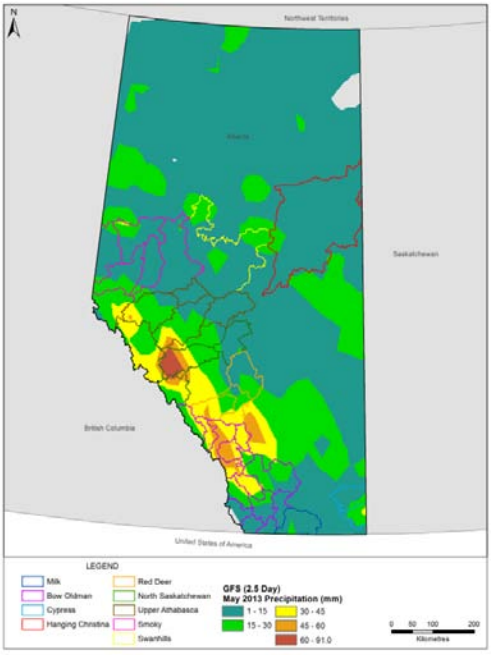


**Figure 61: GFS 2.5-day in Advance Forecast of 72-hour Precipitation Generated 20130605 (5pm MST)**

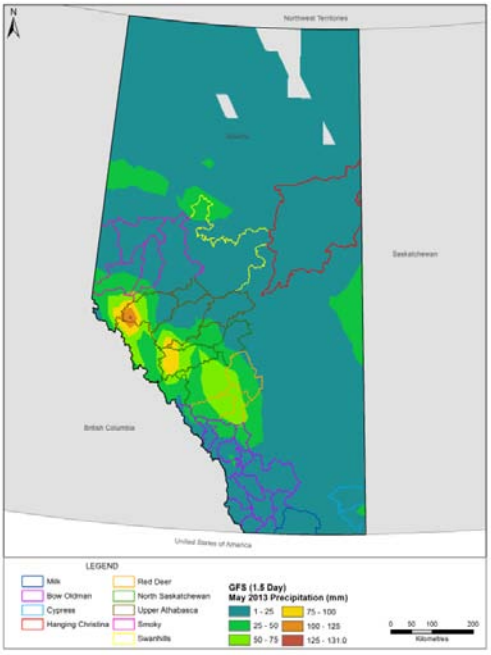


**Figure 62: GFS 1.5-day in Advance Forecast of 72-hour Precipitation Generated 20130606 (5pm MST)**

The map of the observed 72-hour accumulated precipitation for the 8 to 11 June 2013 event, is shown on **Figure 63**. This was the only data available at the time of this report. Maximum confirmed rainfall amount was reported at Conklin (129.4 mm) between 12 UTC 8 June 2013 and 12 UTC 11 June 2013. Conklin is located within the Hanging Christina sub-basin precipitation zone.

The maps of forecast 72-hour precipitation by the GFS model 4.5, 3.5, 2.5, and 1.5 days in advance of the precipitation for the 72-hour period 8 June (5 am MST) to 11 June (5 am MST), 2013 are shown on **Figures 59, 60, 61, an d 62** respectively. There was no precipitation predicted for the zone 5 days in advance of the event.

The GFS was not predicting significant rainfall in the Ft. McMurray area leading up to this event. The only significant precipitation forecast by the GFS was located in the foothills and mountains near Hinton and Jasper.

The GDPS model forecasts are shown on **Figures 64, 65, and 66** for 3, 2, and 1 day in advance of the start of the event. No significant precipitation was forecast in the zone near Ft. McMurray for the previous 2 days prior to the event. The GDPS originally was predicting most of its precipitation for the foothills and mountains; however, 2 days before the start of the event, the GDPS started to predict rainfall in the range of 75 to 90 mm in the northeast part of the Province, but not exactly within the basin affecting Ft. McMurray.

The WRF forecast 72-hour precipitation generated 2 days and 1 day before the start of the rainfall event, are shown on **Figures 67 and 68**. The greatest rainfall amounts >60 mm were predicted in an area south and southeast of the sub-basin. The WRF model was initialized using the GFS model 2 days before the event start. Once again, the poor GFS initial boundary conditions resulted in poor WRF forecasts for this event, in terms of the location and amounts of precipitation. The high resolution WRF produced greater precipitation amounts than the GFS, but not within the basin.

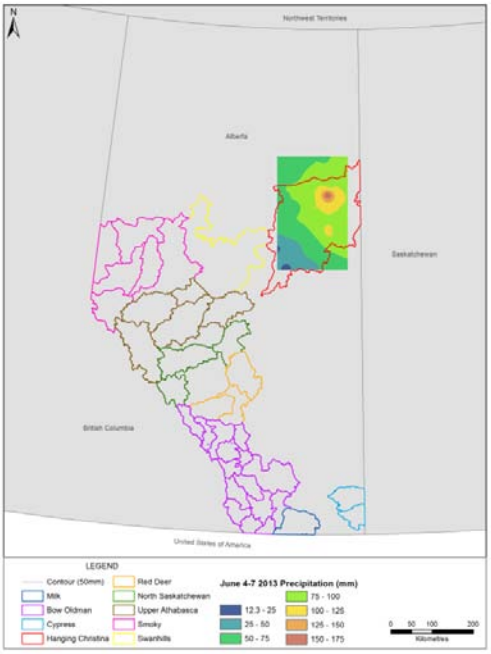


**Figure 63: Observed 72-hour Precipitation Observed 8 to 11 June 2013**

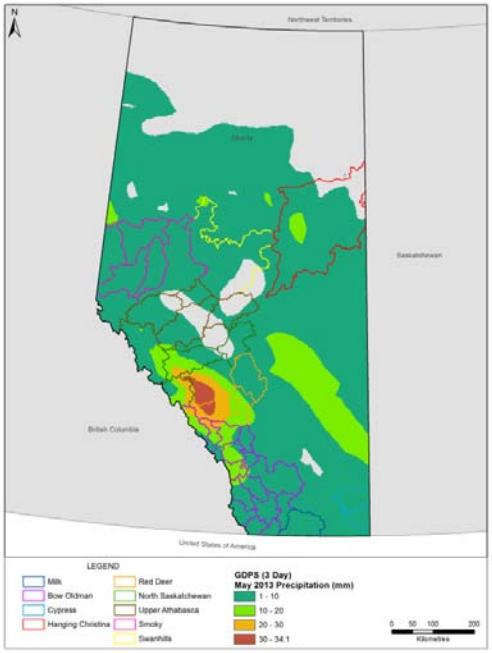


**Figure 64: GDPS 3-day in Advance Forecast of 72-hour Precipitation Generated 20130605 (5 am MST)**

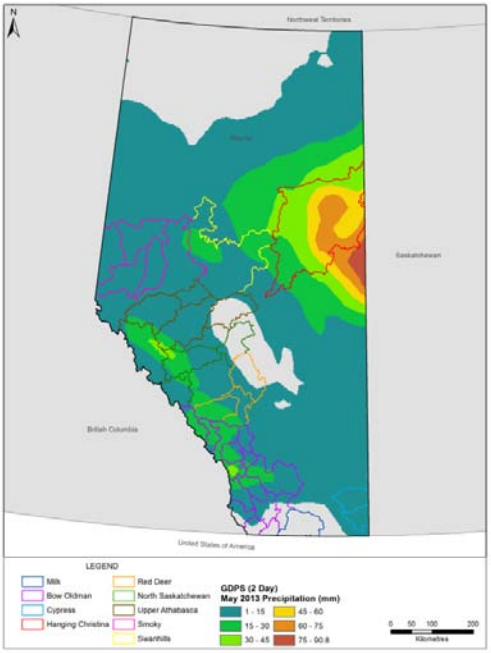


**Figure 65: GDPS 2-day in Advance Forecast of 72-hour Precipitation Generated 20130606 (5 am MST)**

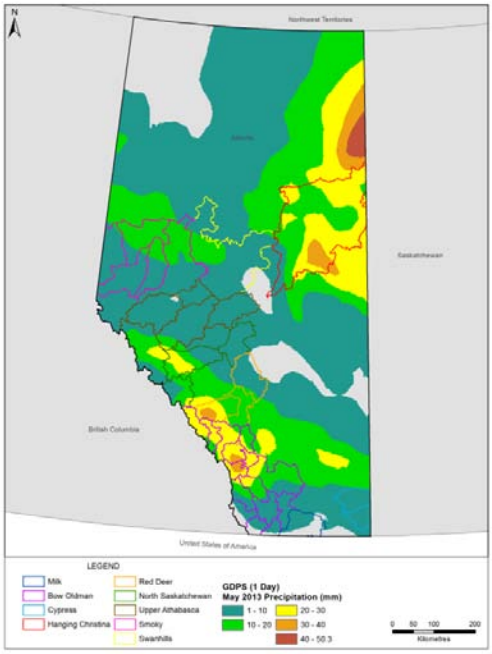


**Figure 66: GDPS 1-day in Advance Forecast of 72-hour Precipitation Generated 20130607 (5 am MST)**

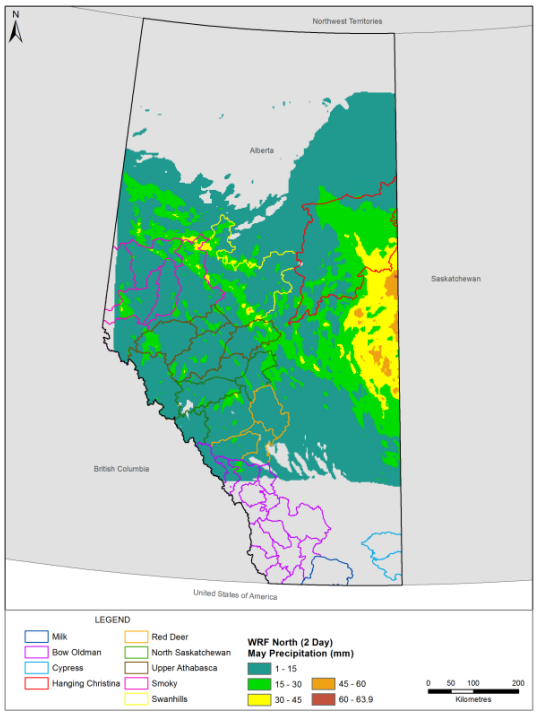


**Figure 67: WRF 2-day in Advance Forecast of 72-hour Precipitation Generated 20130606 (5 am MST)**

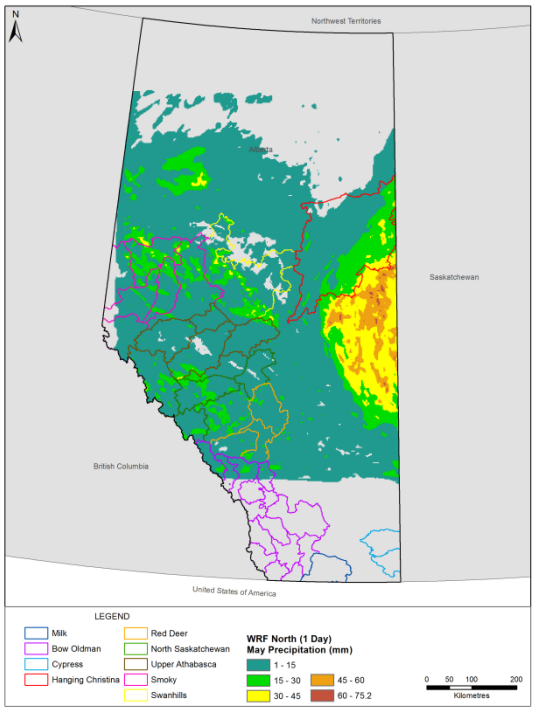


**Figure 68: WRF 1-day in Advance Forecast of 72-hour Precipitation Generated 20130607 (5 am MST)**

Scatter plots of the predicted 72-hour precipitation (sub-basin area-averaged depth) versus forecast lead time for the Hanging Christina (HC) zone #1 is shown on **Figure 69**.

As in the previous case, the NAM model predicted the most rain; >120 mm, 48 hours before the start of the extreme event. However, once again the daily forecasts at 6 and 18 UTC fluctuated considerably, with significantly lower values, which lowers ones confidence. All of the models under predicted the precipitation for all periods to varying degrees. The predicted rainfall is an average depth computed for the entire zone; therefore, the amounts >60 mm regularly forecast 48 hours in advance of the start of the event did indicate considerable volumes of water input to the basin.

The GFS and NAM models produced the most consistent high values of precipitation for the zone, extending out to 60 hours. The GDPS tended to forecast less rainfall than the GFS and NAM.

Note the particularly poor QPF performance of the GFS 48 hours lead time. The 48 hour lead time run was the run of the GFS that was used to initialize the WRF model simulations. In hindsight, this seems to have been a very unfortunate choice, and this indicates further that the poor initialization results in a poor simulation of the entire rain event, with respect to the precipitation zone and sub-basin of most interest. As before, there is considerable variability displayed by the intermediate (5 am MST and 5 pm MST) model runs. The lack of updated

radiosonde data and a sparse network of surface observations results in a poor initialization and boundary conditions, and this results in poorer precipitation forecasts.

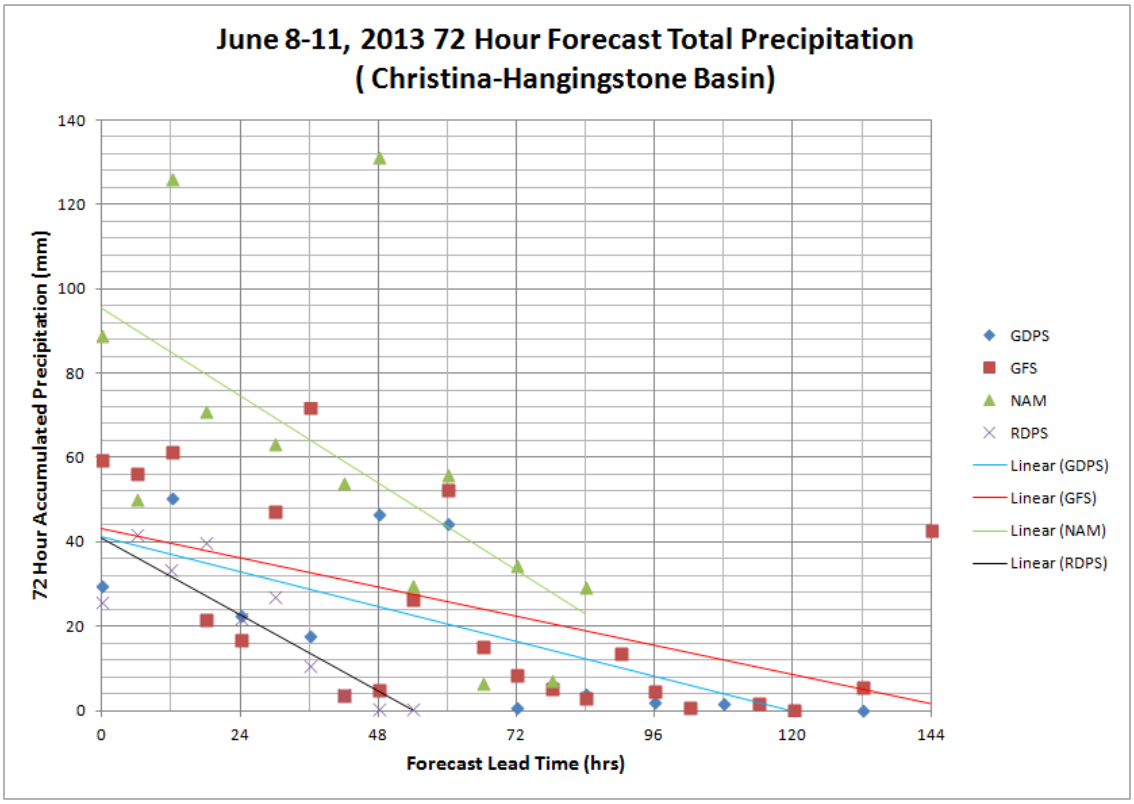


**Figure 69: 8 to 11 June 2013 72-hour Area-averaged Forecast Precipitation Versus Forecast Lead Time for the Christina-Hangingstone Zone**

## 17.3 June 2012 Bow Valley Numerical Weather Prediction Forecast Assessment

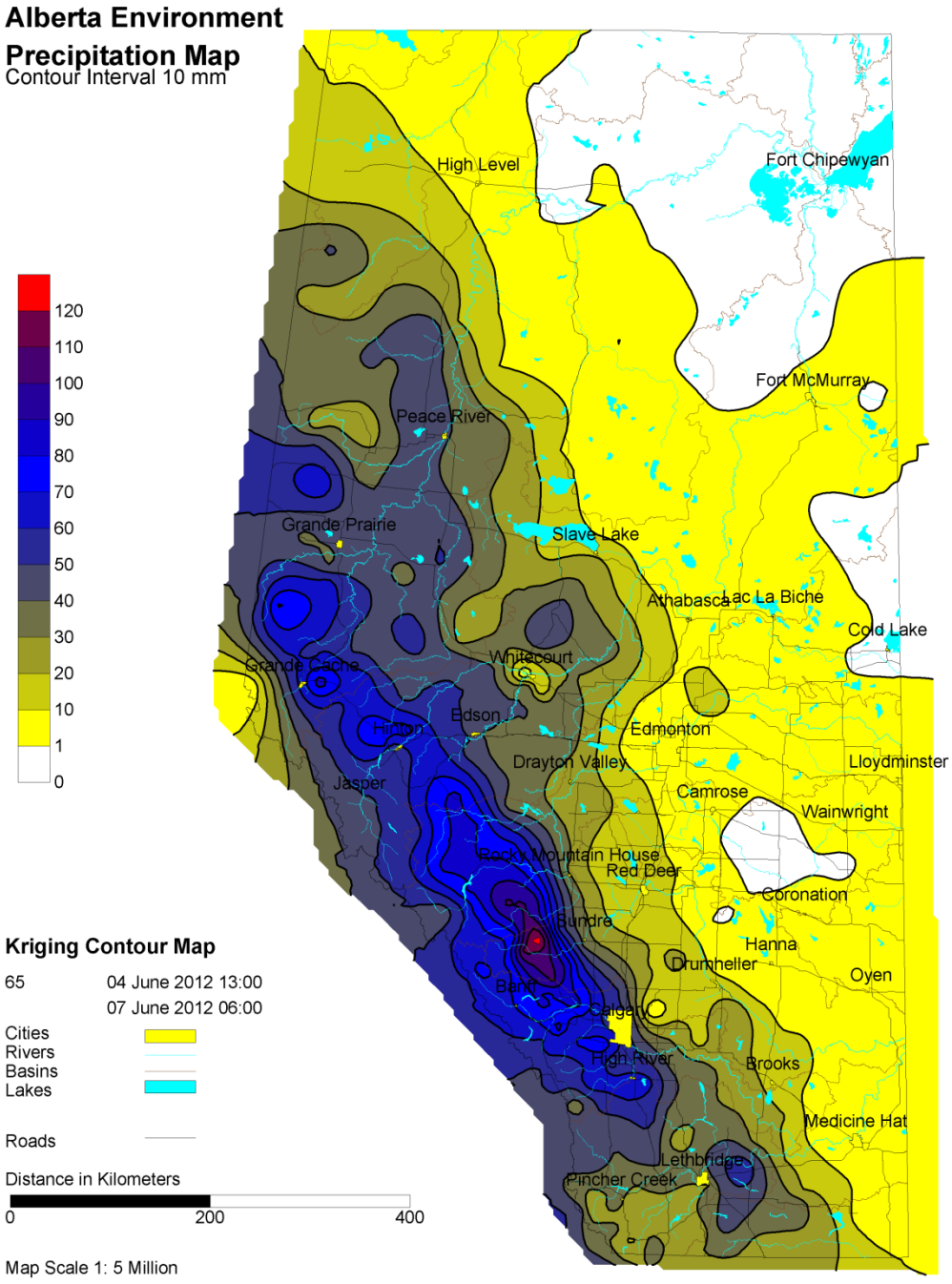


courtesy Alberta Environment

**Figure 70: Precipitation Map for 4 to 7 June 2012**

The total precipitation that fell in Alberta between 4 and 7 June 2012 is shown on **Figure 70**. The rain accumulations reported by rain gauge stations within the precipitation zone of interest to the RFC are shown in **Table 1**. The maximum rainfall reported from this event was 102.2 mm at Mockingbird Hill station. The average rainfall reported over the zone of interest was 71.4 mm.

**Table 1:**
**Total Rain Accumulation Reported at Rain Gauges for the 4 to 7 June 2012 Extreme Rainfall Event**

| Station<br>4 to 7 June 2012 Rainfall | Total<br>(mm) |
|---|---|
| Bow Valley Provincial Park - MSC PC | 65.3 |
| Bow Valley Provincial Park - MSC PR-01 | 65.6 |
| Spray Reservoir PR-01 | 65.81 |
| South Ghost Headwaters | 85.3 |
| Ghost Lake near Cochrane | 83.81 |
| Ghost Ranger Station (RS) | 83.5 |
| Ghost Diversion | 75.8 |
| Cascade Reservoir | 73.4 |
| Banff MSC | 71.9 |
| Sunshine Village | 64.2 |
| Cuthead Lake | 64.6 |
| Skoki Lodge | 68.8 |
| Pika Run | 79.8 |
| Lake Louise MSC | 63.48 |
| Bow Summit | 64.8 |
| Cop Upper | 52.2 |
| Compression Ridge | 64.9 |
| Jumpingpound Ranger Station | 60.6 |
| Cox Hill | 86.3 |
| Kananaskis Boundary | 59.66 |
| Mockingbird Hill | 102.2 |
| Barrier Lake | 78.53 |
| Moose Mountain | 61.22 |
| | |
| Maximum reported amount | 102.2 |
| Average | 71.4 |

The model QPF 72-hour accumulated precipitation for the 4 to 7June 2012 event, area-averaged for Red Deer Zone #1 (James/Fallentimber/Burntimber) according to forecast lead time is shown on **Figure 71**. A close examination of **Figure 71** reveals the following.

- The GFS consistently predicted the greatest rainfall amounts at the longest lead times (3 to 5 days in advance). For the June 2012 event, the GFS area-averaged precipitation was reasonably accurate (approximately 80 mm) 3 to 4 days in advance of the event.

- The GFS generally predicts less rainfall at the 6 UTC (11 pm MST) and 18 UTC (11 am MST) model runs, but the variability is less than the NAM model.
- The GDPS consistently predicted less rainfall than the GFS at all lead times for the 2012 case study precipitation zone of interest. The GDPS was only available at the 0 UTC (5 pm MST) and 12 UTC (5 am MST) time periods.
- The NAM model consistently predicted the most rainfall within 48 hours lead time.
- The NAM QPF predictions at 0 and 12 UTC generally exceeded the observed rainfall amounts within the 24-hour lead time. In this regard, it raises awareness of potential extreme events. However, the NAM variability was consistently the greatest for the 6 UTC (11 pm MST) and 18 UTC (11 am MST) model runs, and always less precipitation is forecast at those runs without updated upper-air initial boundary conditions. This large fluctuation reduces the confidence in the NAM predictions, suggesting a frequent "false alarm" situation.
- The RDPS has the shortest forecast period of 48 hours, and this severely limits its ability to forecast total rainfall for events >48 hours. At 0, 12, and 24 hr lead times, the RDPS consistently predicted the least rainfall.

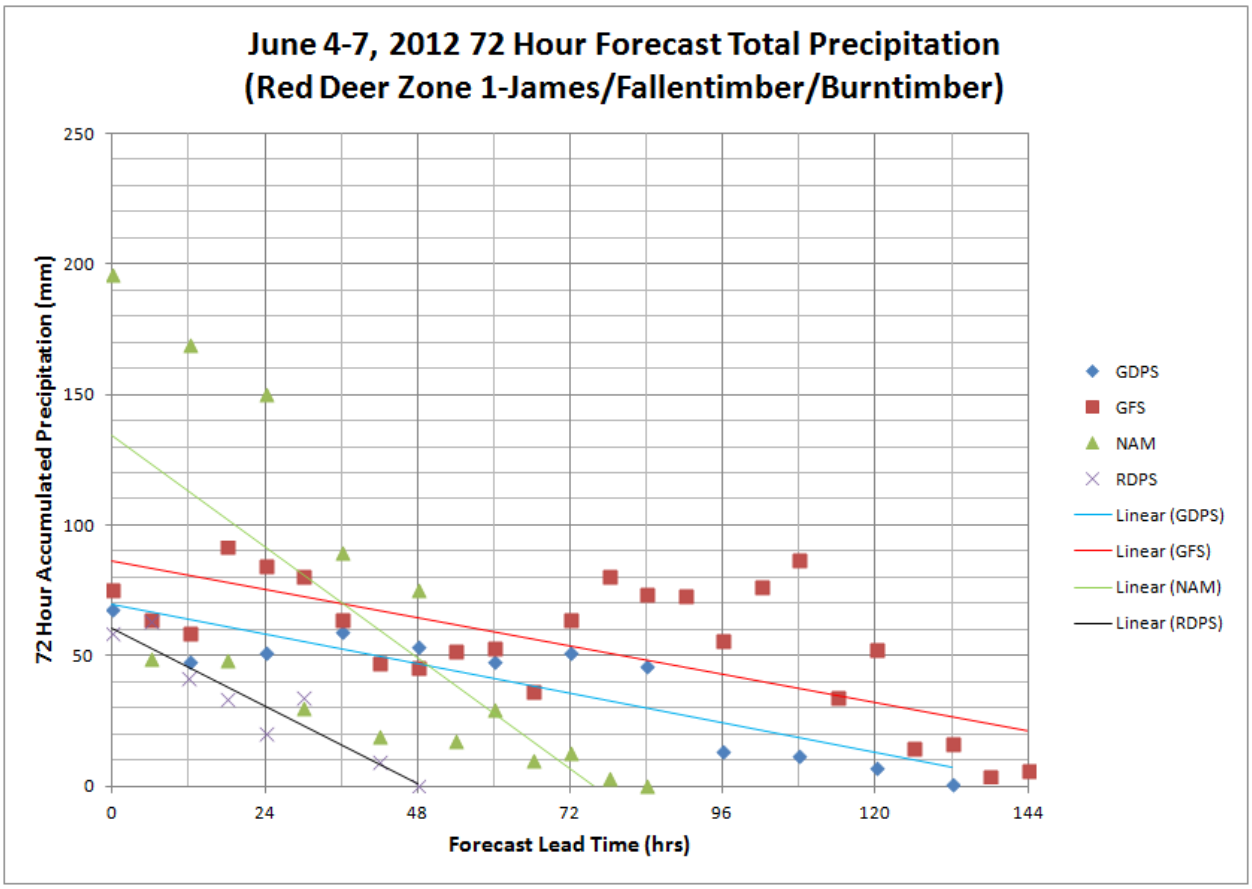


**Figure 71: 4 to 7 June 2012 72-hour Area-averaged Forecast Precipitation Versus Forecast Lead Time for Red Deer Zone #1 James/Fallentimber/Burntimber.**

## 17.4 July 2011 Central Alberta Numerical Weather Prediction Forecast Assessment

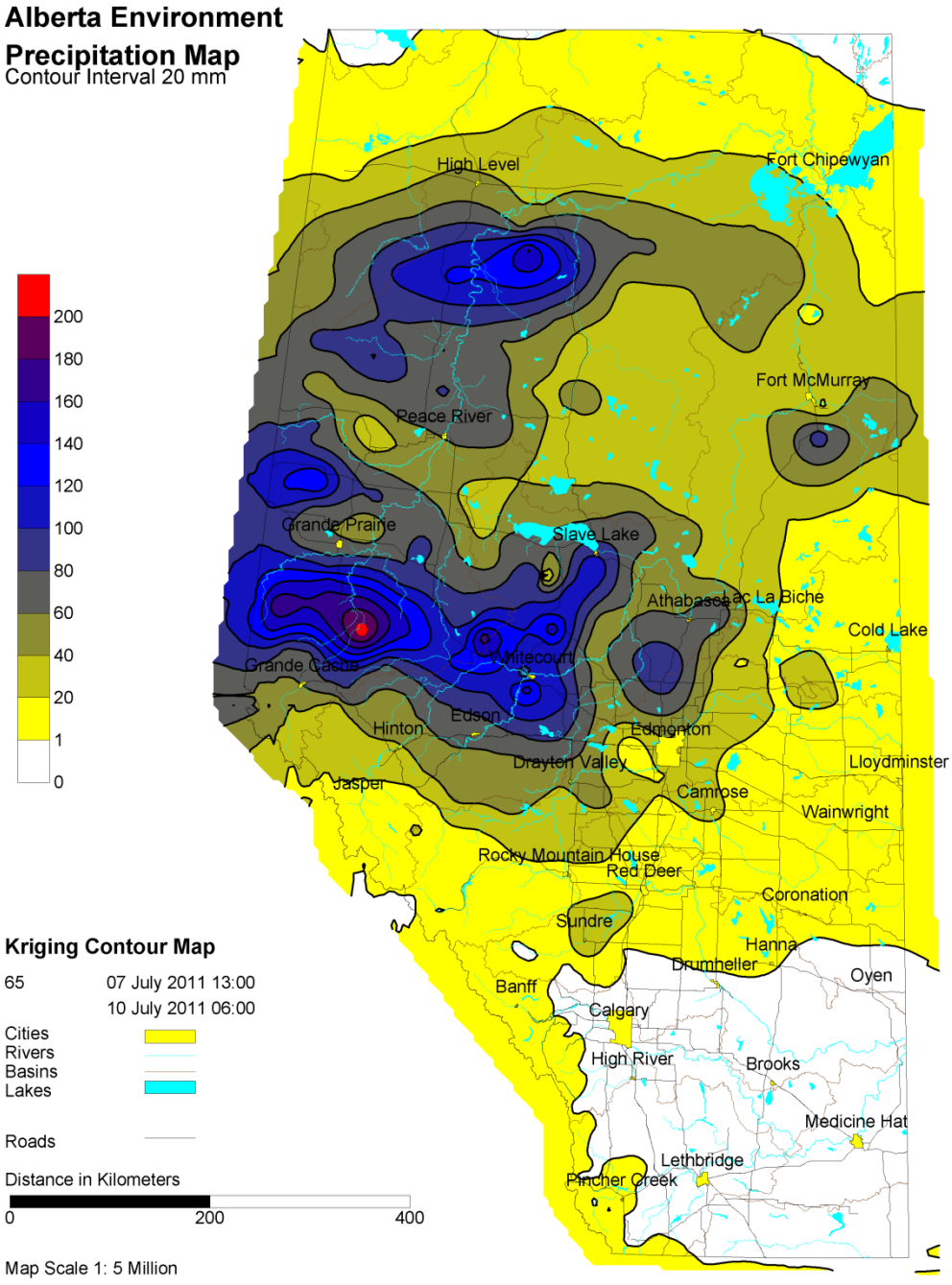


Courtesy Alberta Environment

**Figure 72: Precipitation Map for July 7 to 10, 2011**

The total precipitation that fell in Alberta between July 7 and 10, 2011 is shown in **Figure 72**. The total rain accumulations reported by rain gauge stations within the precipitation zone of

interest to the RFC are shown in **Table 2**. The maximum rainfall reported from this event was 125.6 mm at Little Paddle Headwaters station. The average rainfall reported over the zone of interest was 75.2 mm.

**Table 2:**
**Total Rain Accumulation Reported at Rain Gauges for the 7 to 10 July 2011 Extreme Rainfall Event**

| Station 7 and 10 July 2011 | Total (mm) |
|---|---|
| Ft Assiniboine | 48.6 |
| Busby | 70.8 |
| Schwartz Creek | 56.64 |
| Violet Grove | 37.3 |
| Tomahawk | 57.8 |
| Evansburg | 85.7 |
| Mayerthorpe | 111.7 |
| Paddle River Headwaters | 122.6 |
| Whitecourt | 90.6 |
| Little Paddle Headwaters | 125.6 |
| Greencourt | 116.2 |
| Paddle Dam Precip Site | 103.1 |
| Glenevis | 57.2 |
| Twin Lakes | 65.2 |
| Barrhead | 53.2 |
| | |
| Carrot Creek | 62 |
| Brazeau | 40.8 |
| Lovett | 48 |
| | |
| Maximum reported amount | 125.6 |
| Average | 75.2 |

The model QPF 72-hour accumulated precipitation for the July 7 to 10, 2011 event, area-averaged for Smokey zones #4 and #5 according to forecast lead time are shown in **Figures 73 and 74**. A close examination of Figures 73 and 74 reveals the following.

- The GFS consistently predicted the greatest rainfall amounts at the longest lead times (2 to 3 days in advance). The rainfall predictions 4 and 5 days in advance were considerably less and generally poor. The GFS generally predicts less rainfall at the 6 UTC (11 pm MST) and 18 UTC (11 am MST) model runs, but the variability is less than the NAM model.
- The GDPS rainfall predictions were consistently less than the GFS at all lead times up to 3 days for the 2011 case study for the two precipitation zones of interest. The GDPS is only available at the 0 UTC (5 pm MST) and 12 UTC (5 am MST) time periods.
- The NAM model consistently predicted the greatest rainfall amounts within 36 hours lead time. The NAM QPF predictions greatly exceeded the observed rainfall amounts within

36-hour lead time, with forecast amounts in the range of 200 mm to >500 mm. In this regard, it raises awareness of a potential extreme event. However, once again the NAM variability is consistently the greatest for the 6 UTC (11 pm MST) and 18 UTC (11 am MST) model runs, and always less precipitation is forecast at those runs without updated upper air initial boundary conditions. It is truly disconcerting to see the NAM forecast 280 to 320 mm at 24-hour lead time, and then only 100 to 120 mm 6 hours later. This large fluctuation reduces the confidence in the NAM predictions, suggesting a frequent "false alarm" situation.

- The RDPS has the shortest forecast period of 48 hours, and this severely hampers its ability to forecast total rainfall for events of 48 hours or more. This was the first case study where the RDPS predicted greater rainfall than the GDPS within 12 hours lead time of the event, but consistently less rainfall than the GFS and NAM.

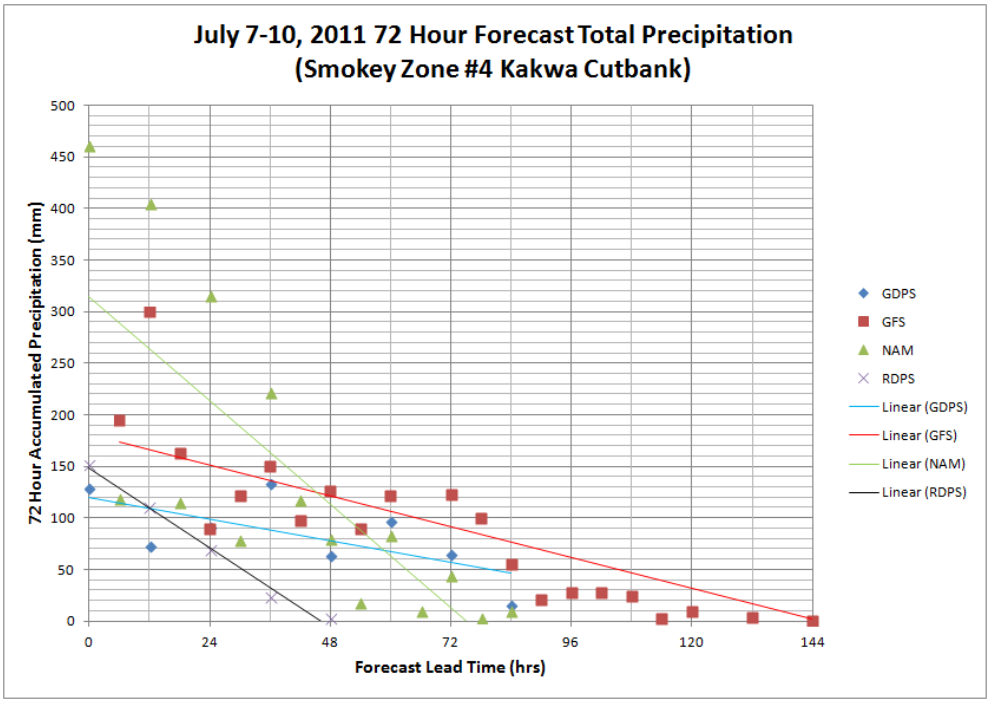


**Figure 73: 7 to 10 July 2011 72-hour Area-averaged Forecast Precipitation Versus Forecast Lead Time for Smokey Zone #4 Kakwa Cutbank**

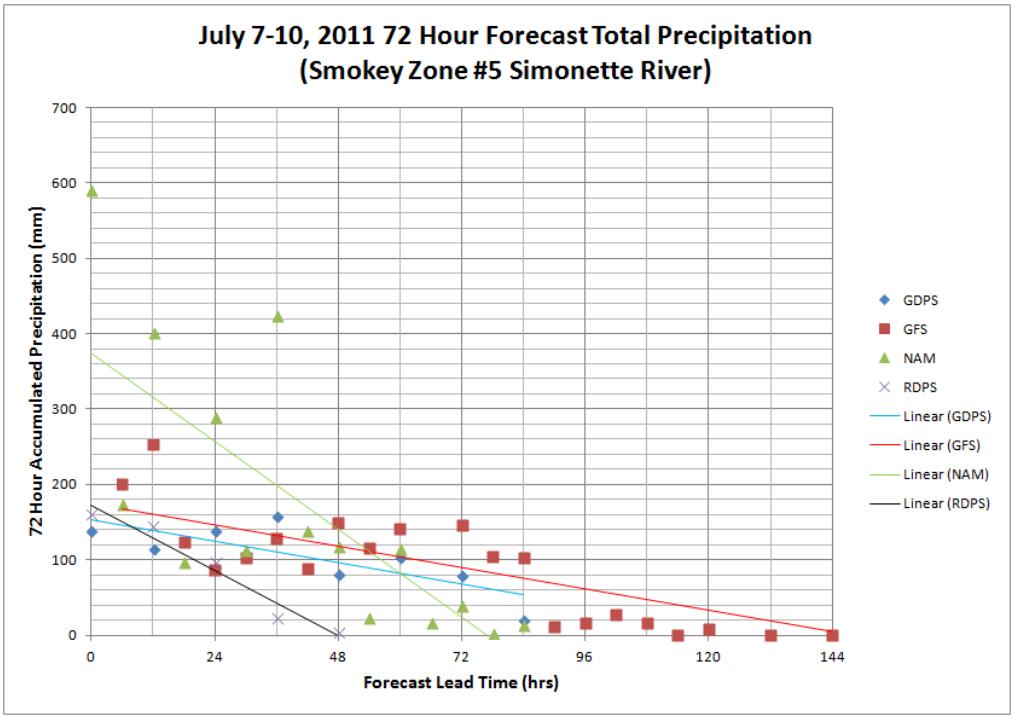


**Figure 74: 7 to 10 July 2011 72-hour Area-averaged Forecast Precipitation Versus Forecast Lead Time for Smokey Zone #5 Simonette River**

## 17.5 June 2010 Cypress Hills Numerical Weather Prediction Forecast Assessment

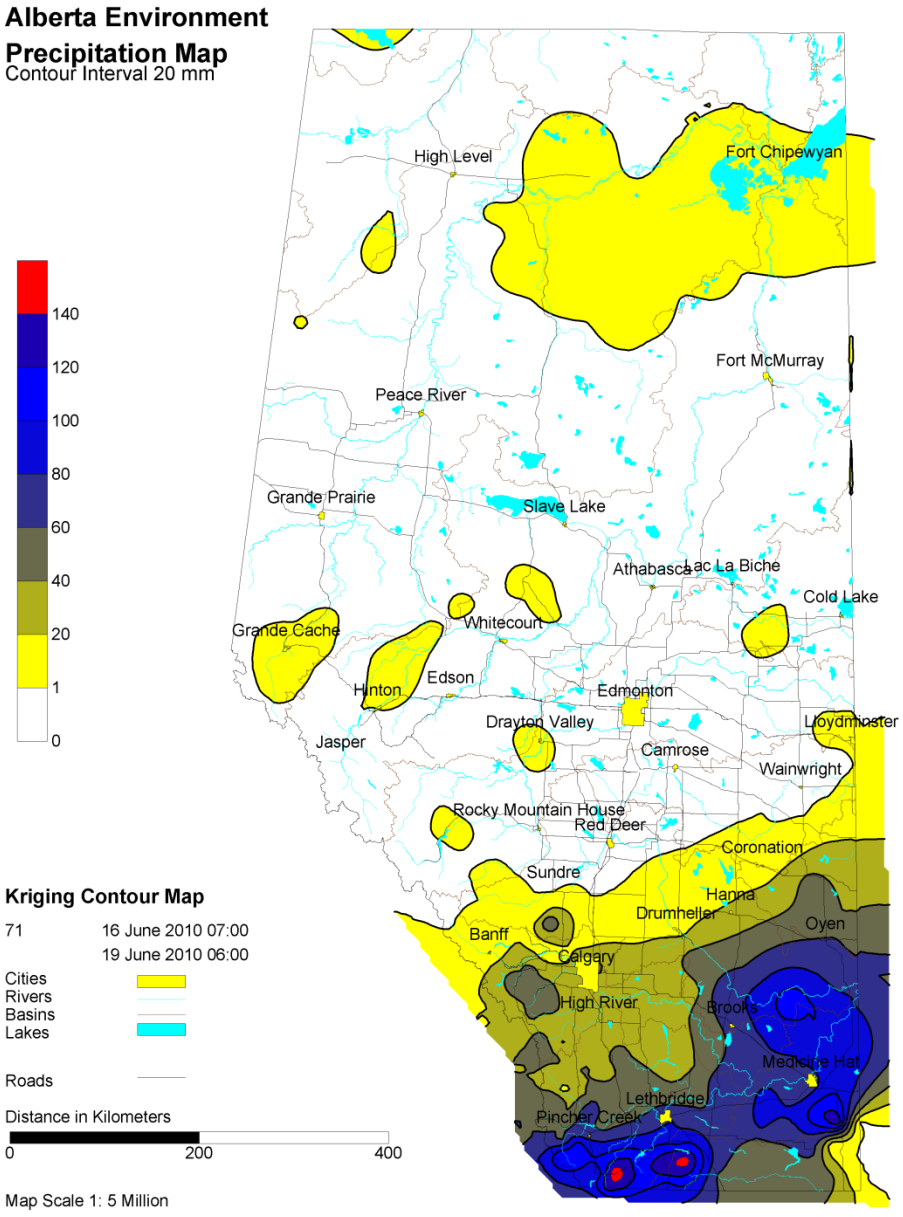


Courtesy Alberta Environment

**Figure 75: Precipitation Map for 16 to 19 June 2010**

The total precipitation that fell in Alberta between 16 and 19 June 2010 is shown in **Figure 75**. The total rain accumulations reported by rain gauge stations within the Cypress Hills precipitation zones of interest to the RFC are shown in **Table 3**. The maximum rainfall reported from this event was 139.93 mm at Medicine Lodge Lookout station. The average rainfall reported over the zone of interest was 79.1 mm.

**Table 3:**
**Total Rain Accumulation Reported at Rain Gauges for the 16 to 19 June 2010 Extreme Rainfall Event**

| Station 16 and 19 June 2010 | Total (mm) |
|---|---|
| Bow Island MSC | 83.7 |
| Pakowki Lake | 45.4 |
| Etzicom | 67.4 |
| Manyberries | 63.3 |
| One-Four Manyberries | 50.17 |
| Bare Creek Res near Elkwater | 1 |
| Cypress Hills | 124.44 |
| Medicine Lodge Lookout | 139.93 |
| Rush Lake | 113.3 |
| Bow Island | 87.2 |
| Seven Persons | 69 |
| Medicine Hat | 67.7 |
| Irvine | 96.4 |
| Schuler | 98.5 |
| | |
| Maximum reported amount | 139.93 |
| Average | 79.1 |

The model QPF 72-hour accumulated precipitation for the 16 to 19 June 2010 event, area-averaged for Cypress zones #1 and #2 according to forecast lead time are shown in **Figures 76** and **77**. This is an interesting case study because the target precipitation region is the Cypress Hills, and not central, southern, or northern Alberta. Only the 12-hour model run data was available for this case study. This presents an opportunity to see if the models behave differently in a different region. A close examination of **Figures 76** and **77** reveals:

- The GFS and GDPS did not predict rainfall >50 mm more than 72 hours (3 days in advance).
- The NAM model was the first to forecast the possibility of an extreme rain event (>100 mm) 60 hours (2.5 days) in advance. The NAM predicted > 150 mm 36 hours in advance.
- The GFS consistently predicted less rain than the NAM but more rain than the GDPS.
- The RDPS predicted more rain than the GDPS at 0 hours lead time (the day the event started).

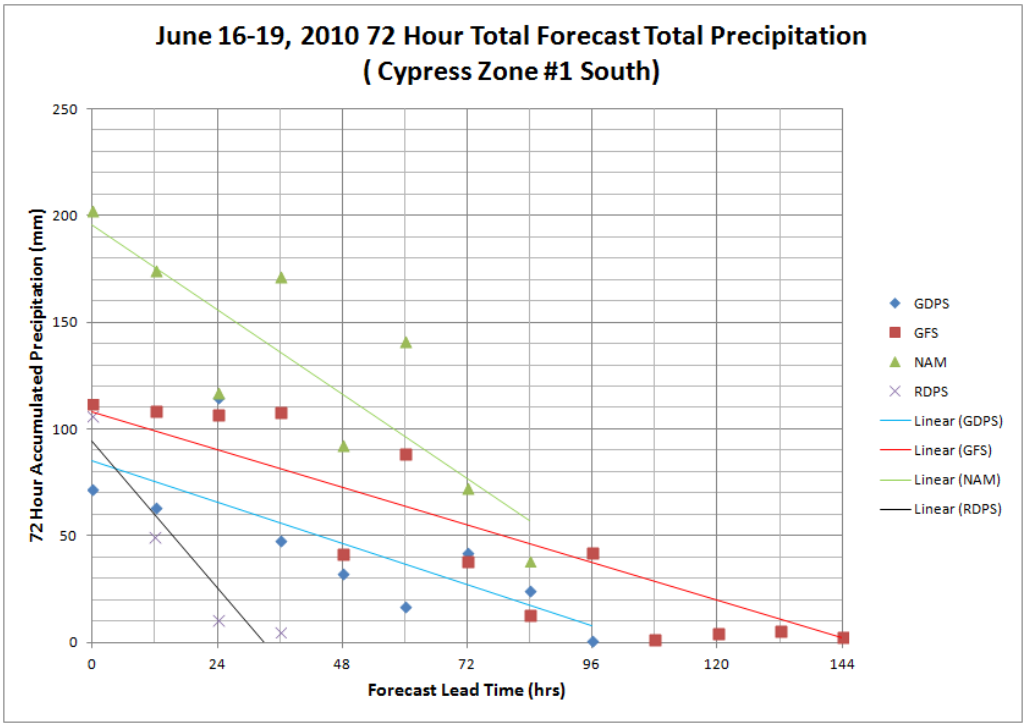


**Figure 76: 16 to 19 June 2010 72-hour Area-averaged Forecast Precipitation Versus Forecast Lead Time for Cypress Zone #1 South.**

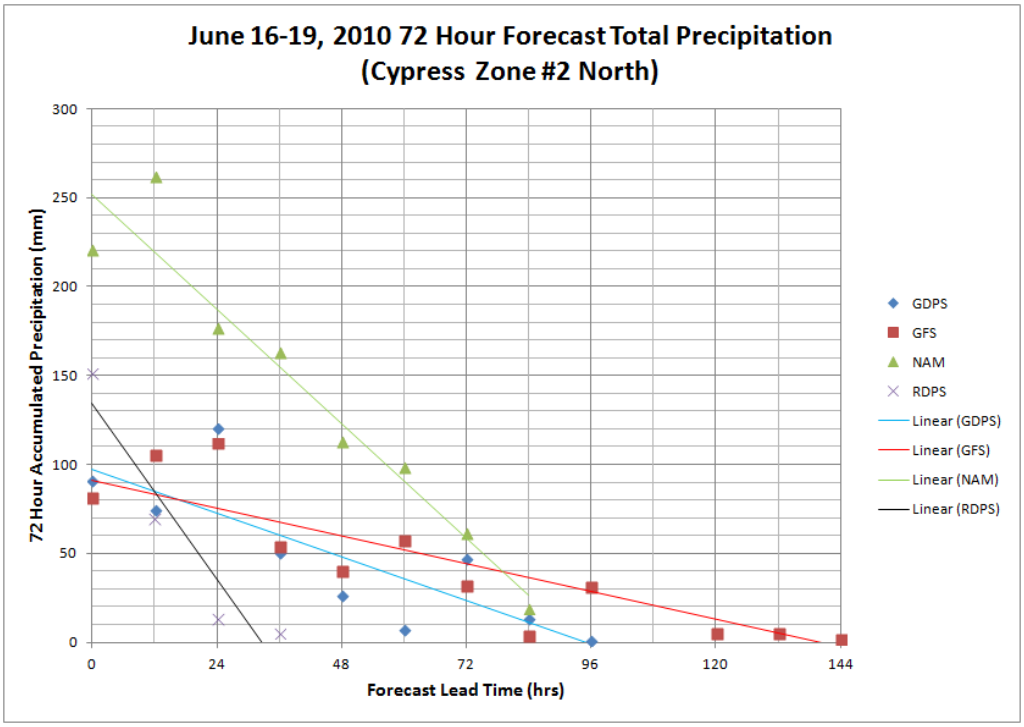


**Figure 77: 16 to 19 June 2010 72-hour Area-averaged Forecast Precipitation Versus Forecast Lead Time for Cypress Zone #2 North.**

## 17.6 May 2007 Swan Hills Numerical Weather Prediction Forecast Assessment

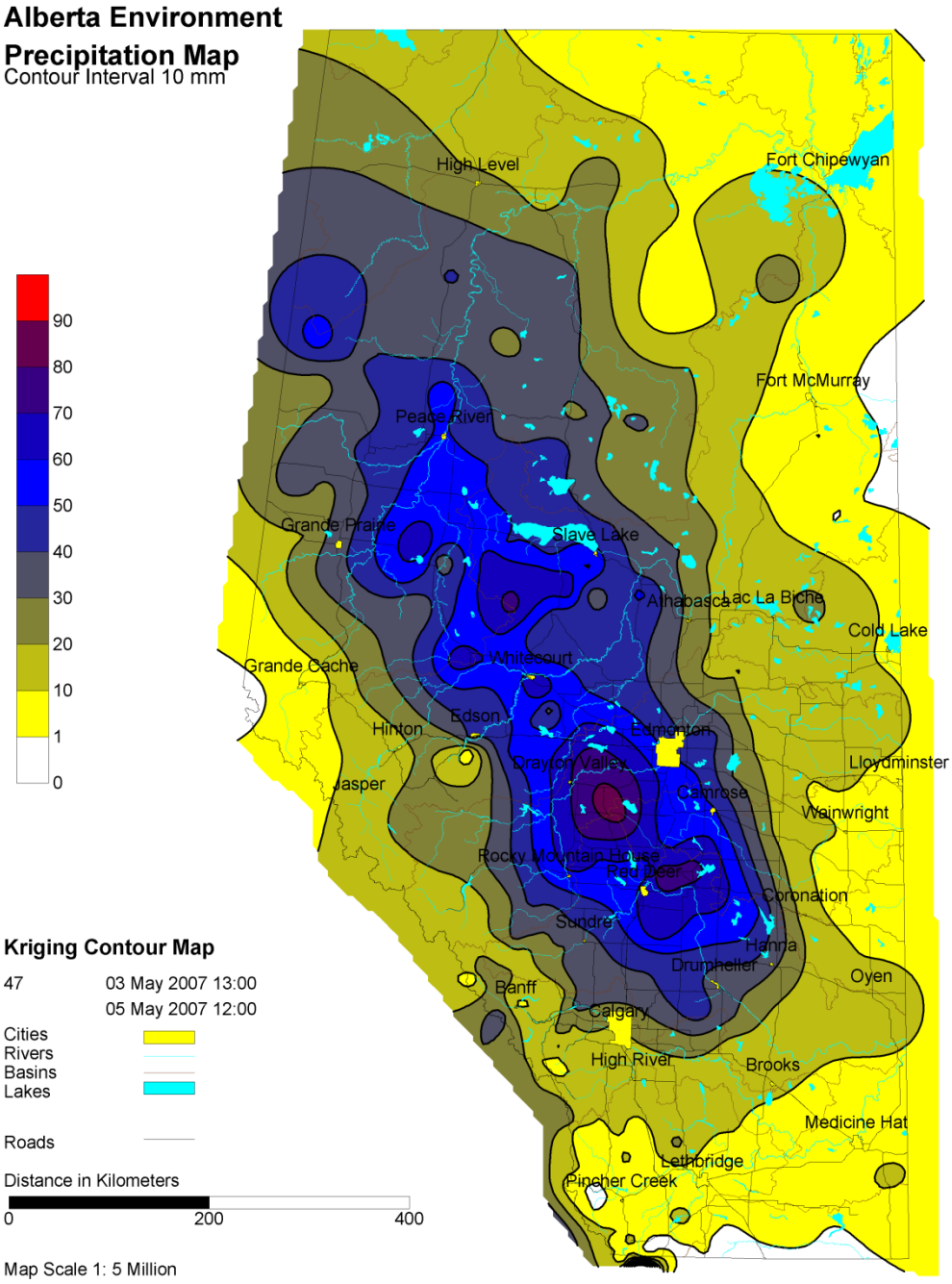


Courtesy Alberta Environment

**Figure 78: Precipitation Map for 3 to 5 May 2007**

The total precipitation that fell in Alberta May 3 to 5, 2007 is shown in **Figure 78**. (Note that the map only covers 48 hrs May 3 to 5). The total rain accumulations reported by rain gauge

stations within the precipitation zone of interest to the RFC are shown in **Table 4**. The maximum rainfall reported from this event was 73.8 mm at Goose Mountain Lookout station. The average rainfall reported over the zone of interest was 52.1 mm.

**Table 4:**
**Total Rain Accumulation Reported at Rain Gauges for the 3 to 6May 2007 Extreme Rainfall Event**

| Station May 3 to 6, 2007 | Total (mm) |
|---|---|
| Timue Creek | 43.67 |
| Freeman | 40.64 |
| Goose Mountain Lookout | 73.8 |
| Martin Hills | 41.37 |
| High Prairie Airport | 57.9 |
| High Prairie (Banana Belt) | 65.2 |
| Kinuso | 45.42 |
| Flattop Lookout | 62.1 |
| House Mountain Lookout | 64.8 |
| Salteaux | 33.78 |
| Vega | 54.41 |
| Ft Assiniboine | 38 |
| Imperial | 44.01 |
| Swan Dive | 51.7 |
| Deer Mountain | 69.4 |
| Enilda | 52.01 |
| Sweathouse | 57.31 |
| Chisholm | 62.1 |
| Meridian | 39.01 |
| Slave Lake Merchant MSC | 45.5 |
| | |
| Maximum reported amount | 73.8 |
| Average | 52.1 |

The model QPF 72-hour accumulated precipitation for the 3 to 6 May 2007 event, area-averaged for Swan Hills zone #1 according to forecast lead time is shown on **Figure 79**. A review of the available gauge data showed a maximum rain amount of 73.8 mm, and an average rain amount of approximately 52 mm. The target precipitation zone was the Swan Hills #1 zone. Only 12-hour model run data was available for this event. Some common observations and general conclusions can be made regarding this case study.

- The GFS and GDPS were in relatively close agreement out to 96 hrs (4 days lead time).
- The GFS and GDPS forecast reasonable average zone precipitation amounts between 40 and 80 mm, 48 hours in advance.
- The NAM model was the first to forecast the possibility of an extreme rain event (>100 mm) 24 hours in advance. The NAM predicted >140 mm, 24 hours in advance, and 190 mm,

12 hours in advance. The NAM predicted the greatest rainfall within 36 hours of the event start.

- The GFS generally predicted slightly more rain than the GDPS, and closer to the observed rainfall amounts.
- The RDPS predicted similar rain amounts to the GDPS within 12 hours lead time, but once again is limited by its 48-hour forecast period..

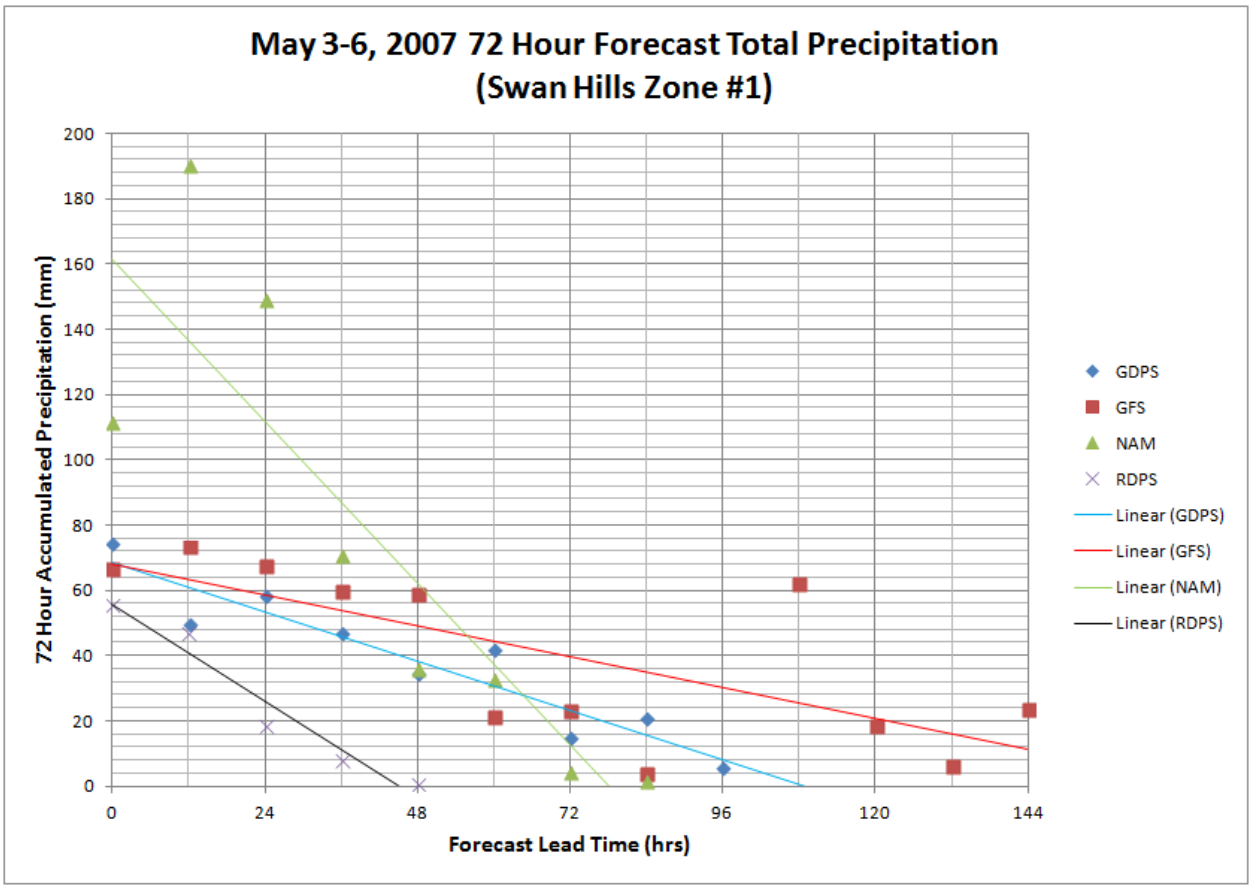


**Figure 79: 3 to 6 May 2007 72-hour Area-averaged Precipitation Versus Forecast Lead Time for Swan Hills Zone #1**

## 17.7 June 2005 Central Alberta Numerical Weather Prediction Forecast Assessment

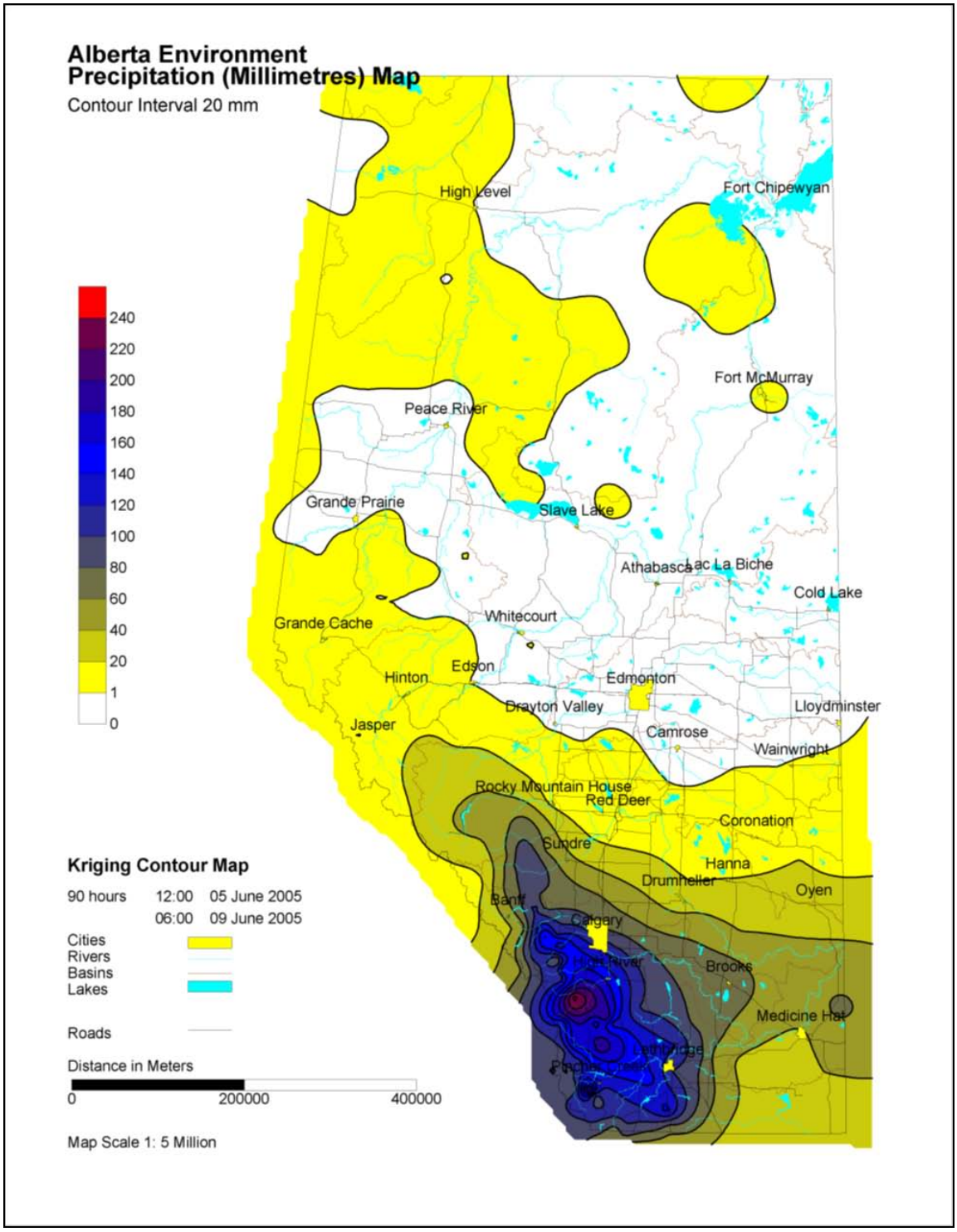


Courtesy Alberta Environment

**Figure 80: Precipitation Map for 5 to 9 June 2005**

The total precipitation that fell in Alberta 5 to 9 June 2005 is shown on **Figure 80**. The model QPF 72-hour accumulated precipitation for the 5 to 9 June 2005 event, area-averaged for the Bow-Oldman zones #4 and #5 according to forecast lead time are shown on **Figures 81** and **82**.

The Canadian model data (GDPS and RDPS) is no longer available for the 2005 event. Therefore, their QPF forecast verification results could not be derived and are not shown on **Figures 81** and **82** for that reason. The 6-hour model run data was not available for this event. A close examination of **Figures 81** and **82** reveals the following:

- The GFS and NAM only predicted rainfall amounts >50 mm, 48 hours (2 days) in advance, except for one GFS prediction of ~90 mm, 108 hours in advance.
- The NAM model predicted rainfall >100 mm, 24 hours in advance.
- The NAM and GFS predicted similar rainfall within 48 hours lead time but the predicted average rainfall across the both zones was considerably less than the observed rainfall of >200 mm, except for the NAM prediction at 12 hours lead time for 225 mm for Zone #4. In this regard, the NAM alerted to the possibility of an extreme rainfall event.

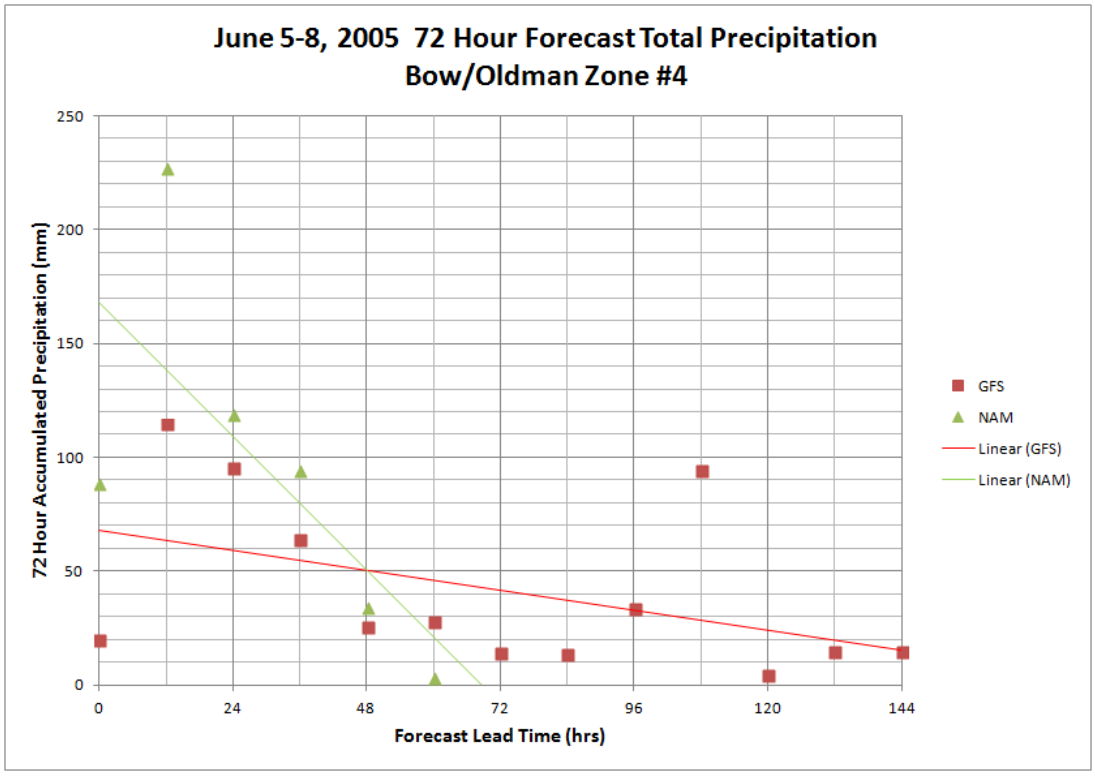


**Figure 81: 5 to 8 June 2005 72-hour Area-averaged Precipitation Versus Forecast Lead Time for Bow/Oldman Zone #4**

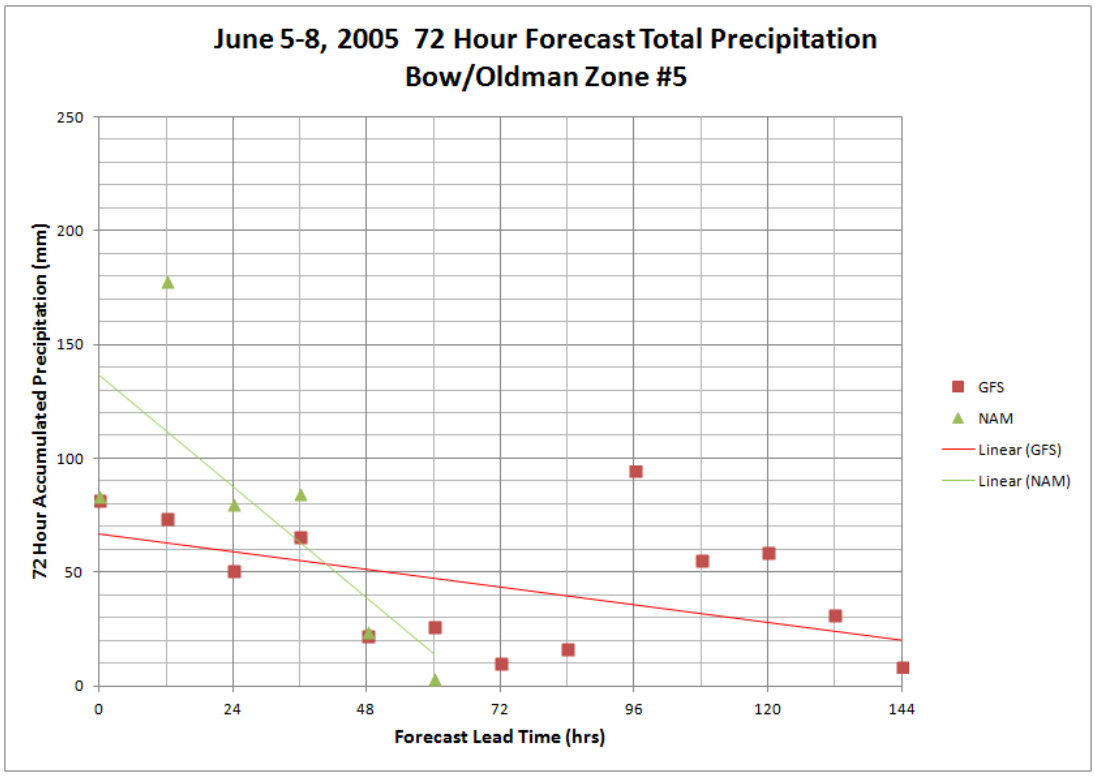


**Figure 82: 5 to 8 June 2005 72-hour Area-averaged Precipitation Versus Forecast Lead Time Bow/Oldman Zone #5**

## 18.0 DISCUSSION OF RESULTS

The purpose of this project was to develop an understanding of the uncertainties in weather forecasting and propose a method of how the RFC can manage those uncertainties when modeling rainfall scenarios and issuing flood advisories. The ultimate needs of any RFC are accurate forecasts of rainfall amount, location, timing, and intensity. This project was designed to assess how well these rainfall forecast requirements are currently being met by the current suite of popular NWP models, for the extreme events in Alberta, when they are needed the most. Specifically discussed is exactly how well the existing NWP models perform in these severe flood situations and what their variability is leading up to the event.

Extreme rainfall events that affected Albertans in 2013, 2012, 2011, 2010, 2007, 2005, and 2002, were analyzed in order to:

- Document the specific meteorological factors that caused the extreme rainfall amounts;
- Assess the performance of several NWP models in their ability to forecast the amount, location, and temporal and spatial variability of the precipitation; and
- As a function of forecast lead time.

The four NWP models analyzed for this project were the Canadian GEM Global model, GEM Regional model, and the US GFS and NAM models. Between 2011 and 2013 all the operational NWP models have received upgrades and improvements to their physics parameterizations and their horizontal and vertical resolution. Due to these recent changes to the NWP models, more emphasis was placed on the analyses and assessments of model performance for the most recent 2013 events, which occurred after the latest changes.

Numerical prediction of summertime convection over Alberta is very challenging due to the spatial distribution of the convective precipitation and orographic effects. High resolution model details can look amazingly realistic; however, the entire event may be misplaced, occur sooner or later, or may not occur at all. Careful examination of the situation is required to assess how plausible the prediction is, and other model runs, even coarser-resolution runs with less detailed physical parameterizations may give a sense of how likely an event is to occur or where and when it is more likely to occur.

A major obstacle to accurate weather forecasts, especially in western Canada, comes from the lack of observational data to provide adequate and accurate initial and boundary conditions for the input to the weather models. If a weather model is incorrectly initialized at a certain location, advection will transport this faulty situation downwind. The lack of detailed upper-air observations off the Pacific Coast and the coarse network of upper atmosphere sounding stations in western Canada is a serious limitation for proper modeling of the extreme events in Alberta, especially evident at the longer forecast lead times that are desired by hydrologic modellers. Upper air soundings are available only two times a day at 0 and 12 UTC (5 pm and 5 am MST). It is very evident that the model forecasts at 06 UTC (11 pm MST) and 18 UTC (11 am MST) have greater error and significant variability, most likely associated with the lack of updated radiosonde data at 06 and 18 UTC for their initialization conditions. Surface station observations are also sparse in the mountains and foothills, northern Alberta, and

Saskatchewan; therefore, there is a general lack of data to provide the necessary initial and boundary conditions required to achieve optimal model performance.

Verification of QPFs presents many scientific challenges that are associated with the characteristics of the forecasts as well as the observations. Precipitation is a highly discontinuous variable in both time and space. Statistics were computed for average depths over target precipitation zones (sub-basins) used as inputs for the hydrological modeling, using thresholds more representative of potentially dangerous amounts (e.g., >25 and >100 mm).

All of the NWP models did a relatively poor job in forecasting the most extreme observed precipitation amounts, locations, and the spatial and temporal variability more than 24 hours in advance. Automated, high-resolution temporal and spatial QPF forecasts that may be automatically input into operational hydrologic models are now possible; however, this study indicates that this level of sophistication may not lead to improved flood forecasts and warnings more than 24 hours in advance. For example, none of the NWP models accurately forecast the June 2013 extreme rainfall amounts and extent in southern Alberta. Burns Creek reported ~350 mm rainfall over a 72-hour period for this event. The GFS model had forecast 72-hour accumulations for that area of ~320 mm, 5 days in advance; however, subsequent model forecasts were all less and highly variable, thereby reducing the confidence in the earlier forecast. The GFS and NAM models forecast the most rain; >150 mm, 48 hours before the start of the 3-day flood event, within the target basin. However, the NAM forecast greater amounts in other sub-basins, and their forecasts at 6 and 18 UTC fluctuated considerably, with significantly lower values, which once again lowers the confidence in the higher amounts at the time they were forecast. The GFS model produced the most consistent high values of precipitation extending out to 48 hours lead time. Precipitation >100 mm was consistently forecast 72 hours (3 days) in advance over the sub-basin near the Burns Creek station; however, there were also significant deviations at the 6-hour intervals. The GDPS model had one high (~290 mm) forecast value 3.5 days in advance, and then consistently forecast about 100 to 150 mm (<50% of the maximum observed) in the period 2 to 3 days before the event. The RDPS model is limited by its maximum 48-hour forecast period, and consistently forecast the lowest precipitation the day before the event started.

The latest, advanced version of the WRF was run for the June 2013 event. The forecasts of total 72-hour precipitation, 2-days in advance and 1-day in advance were disappointing. There were no obvious differences or advantages to using the WRF, in spite of its very high spatial resolution (4 km), the latest physics parameterization schemes, and explicit convection. The WRF simulation was conducted in the same manner in which it would have been run in real-time, with initialization using the available GFS model data 48 hours in advance for initial and boundary conditions. The WRF model results in this study suffered from the errors and limitations introduced by the erroneous real-time GFS initialization, which just happened to be a very poor performance simulation.

Extreme precipitation often is the result of surface convergence and meso-scale features that cannot be predicted unless local surface data is assimilated into a high-resolution model run. Even then, it is extremely challenging to predict these conditions at long lead times

(e.g., several days). To a certain extent it isn't surprising that the synoptic scale lead times tended to predict less precipitation than what actually occurred.

We must conclude that considerable uncertainty is inherent in the current state-of-the-art precipitation forecasting process. Quantifying this uncertainty is important to the decision making processes associated with flood forecasting. This study supports the current trend in using ensemble-based approaches. Using ensembles is popular because they allow effects of a wide range of "inherent" uncertainties to be incorporated. The main sources of modeling uncertainty are associated with the following main groups:

- Random or systematic errors in the model input boundary and initial conditions;
- Uncertainties due to less than optimal model parameter values; and
- Uncertainties due to incomplete or biased model processes.

Small differences in the initial state of the atmosphere have been shown to result in large differences in the forecast, especially during extreme events. Therefore, forecasting precipitation should be thought in terms of probabilities. Ensemble statistics from several models can be used to provide a better estimate of the likelihood of future events. The best recommendation is that QPF should be probabilistic, especially at longer projection times.

Ensemble approaches appear to hold the greatest potential (at this time) for operational hydrologic forecasting. As demonstrated with atmospheric ensemble forecasts, the estimates of predictive uncertainty provide forecasters and users with objective guidance about the level of confidence that they may place in the forecasts. In summary, when assessing forecast uncertainty, the departure of each individual model from the ensemble mean is an indication of higher uncertainty. Ensemble spread is an indication of uncertainty and confidence:

- Small ensemble spread indicates higher confidence and higher predictability.
- Large ensemble spread indicates lower confidence and lower predictability.

The ensemble distribution should be considered when assessing possible scenarios as it can provide insights into the probability of occurrences of extreme events given that the ensemble mean may not always provide the best forecast. The end users can decide to take action based on the probability of occurrence, and prioritized according to their risk tolerance, on an event by event basis.

Future ensemble forecasts will likely include some of the latest generation, high resolution models like the WRF and the upcoming 2.5 km HRDPS, that have shown to have better capabilities for modeling convection over complex terrain, and therefore, are better at simulating extreme precipitation events. However, these higher resolution models are still limited by their computing requirements, shorter simulation periods, and the quality and quantity of data assimilation for initial and boundary conditions.

## 19.0 CLOSURE

This report has been prepared for the exclusive use of Alberta Environment and Sustainable Resource Development. This report is based on, and limited by, the interpretation of data, circumstances, and conditions available at the time of completion of the work as referenced throughout the report. It has been prepared in accordance with generally accepted industry practices. No other warranty, express or implied, is made.

Yours truly,

**AMEC Environment & Infrastructure**

Terry Krauss, Ph.D
Senior Consulting Meterologist, Met-Ocean Services
Direct Tel.: (403) 318-0400
E-mail: terry.krauss@amec.com

*Reviewed by:*

Shawn Allan, M.Sc.
Manager, Met-Ocean Services

TK/RA/elf

**Permit to Practice No. P-4546**

## 20.0 REFERENCES

Ament, F., and C. Simmer, 2006: Improved representation of land-surface heterogeneity in a non-hydrostatic numerical weather prediction model. *Boundary-Layer Meteorol.*, **121**, 153–174

Barlage, M., Chen, F., Tewari, M., Ikeda, K., Gochis, D., Dudhia, J., Rasmussen, R., Livneh, B., Ek, M. and Mitchell, K. (2010). Noah land surface model modifications to improve snowpack prediction in the Colorado Rocky Mountains. Journal of Geophysical Research 115: doi: 10.1029/2009JD013470. issn: 0148-0227

Brimelow, J. C. and G. W. Reuter, 2005: Transport of Atmospheric Moisture during Three Extreme Rainfall Events over the Mackenzie River Basin. J. Hydrometeo. Vol. 6, 423-440

Cheng, W.Y.Y., and W. J. Steenburgh, 2005: Evaluation of Surface Sensible Weather Forecasts by the WRF and the Eta Models over the Western United States, Wea. Forecasting, 20, 812-821

Chow, F. K., A. P. Weigel, R. L. Street, M. W. Rotach, and M. Xue, 2006: High-resolution large-eddy simulations of flow in a steep alpine valley. Part I: Methodology, verification and sensitivity studies. *J. App. Meteor.*, **45**, 63–86

Chung, Y. S., K. D. Hage, and E. R. Reinelt, 1976: On lee cyclogenesis and airflow in the Canadian Rocky Mountains and the East Asian Mountains. Mon. Wea. Rev., 104, 879-891

Dartmouth University, 2005: 2005 Global Register of Major Flood Events - 2005 Flood Archive. http://www.dartmouth.edu/~floods/Archives/2005sum.htm

Davis, C., B. Brown, R. Bullock, 2006: Object-Based Verification of Precipitation Forecasts. Part I: Methodology and Application to Mesoscale Rain Areas, Mon. Wea. Rev.,134, 1772-1784

Deacu, D., V. Fortin, E. Klyszejko, C. Spence, P.D. Blanken, 2012: Predicting the Net Basin Supply to the Great Lakes with a Hydrometeorological Model, Journal of Hydrometeorology,doi: http://dx.doi.org/10.1175/JHM-D-11-0151.1

Deardoff, J. W., 1980: Stratocumulus-capped mixed layers derived from a 3-dimensional model. *Bound.-Layer Meteorol.*, **18**, 495–527

Done, J., C.A. Davis, M. Weisman, 2004: The next generation of NWP: explicit forecasts of convection using the weather research and forecasting (WRF) model, Atmos. Sci. Let., 5, 110-117

Doswell, C. A., H.E. Brooks, and R.A. Maddox, 1996: Flash flood forecasting: An ingredients-based methodology. Wea. Forecasting, 11, 560-581

Erfani, A., A. Méthot, R. Goodson, S. Bélair, K.-S.Yeh, J. Côté, and R. Moffet, 2003: Synoptic and mesoscale study of a severe convective outbreak with the nonhydrostatic Global Environmental Multiscale (GEM) model. Meteor. Atmos. Phy., 82, 31-53

Flesch, T.K., and G.W. Reuter, 2012: WRF Model Simulation of Two Alberta Flooding Events and the Impact of Topography, J. of Hydrometeor., 13, 695-708

Fritsch, J.M. and C.F. Chappell, 1980: Numerical Prediction of Convectively Driven Mesoscale Pressure Systems. Part I: Convective Parameterization, J. Atmos. Sci., 37, 1722-1733 47

Grubišic, V., R.K. Vellore, A.W. Huggins, 2005: Quantitative Precipitation Forecasting of Wintertime Storms in the Sierra Nevada: Sensitivity to the Microphysical Parameterization and Horizontal Resolution, Mon. Wea. Rev., 133, 2834-2859

Kain, J.S. and J.M. Fritsch, 1993: Convective Parameterization for Mesoscale Models: The Kain-Fritsch Scheme, The Representation of Cumulus Convection in Numerical Models, Meteor. Monogr., No 46, Amer. Meteor. Soc., 165-170

Lin, Y., S. Chiao, T. Wang, M. Kaplan, L. Michael, and R.P. Weglarz, 2001: Some common ingredients for heavy orographic rainfall. Wea. Forecasting, 16, 633-660

Liu, C., K. Ikeda, G. Thompson, R. Rasmussen, J. Dudhia, 2011: High-Resolution Simulations of Wintertime Precipitation in the Colorado Headwaters Region: Sensitivity to Physics Parameterizations. *Mon. Wea. Rev.*, **139**, 3533–3553

Mesinger, F., G. DiMego, E. Kalnay, K. Mitchell, P.C. Shafran, W. Ebisuzaki, D. Jovic, J. Woollen, E. Rogers, E.H. Berbery, M.B. Ek, Y. Fan, R. Grumbine, W. Higgins, H. Li, Y. Lin, G. Manikin, D. Parrish, W. Shi, 2006: North American Regional Reanalysis, Bull. Amer. Meteor. Soc., 87, 343-360

Michalakes, J., J. Dudhia, D. Gill, J. Klemp, W. Skamarock, 1999: Design of a Next- Generation Regional Weather Research and Forecast Model, Towards Teracomputing, World Scientific, River Edge, New Jersey, 117-124

Michalakes, J., S. Chen, J. Dudhia, L. Hart, J. Klemp, J. Middlecoff, W. Skamarock 2001: "Development of a Next Generation Regional Weather Research and Forecast Model" in Developments in Teracomputing: Proceedings of the Ninth ECMWF Workshop on the Use of High performance Computing in Meteorology. Eds. Walter Zwieflhofer and Norbert Kreitz. World Scientific, Singapore. 269- 276

Milbrandt, J.A. and M.K. Yau, 2006: A Multimoment Bulk Microphysics Parameterization. Part III: Control Simulation of a Hailstorm, J. Atmos. Sci.63, 3114-3136

Moeng, C. H., 1984: A large-eddy simulation model for the study of planetary boundary layer turbulence. *J. Atmos. Sci.*, **41**, 2052–2062

Molders, N., and A. Raabe, 1996: A comparison of two strategies on land surface heterogeneity used in a mesoscale β meteorological model. Tellus, 48A(733-749)

Molod, A., H. Salmun, and S. W. Waugh, 2003: A new look at modeling surface heterogenety. *Journal of Hydrometeorology*, **4**, 810–825

Ou, A.A., 2008: Meteorological analysis of four rainstorms that caused severe flooding in Alberta during June 2005. MSc. Thesis. Univ. of Alberta, Edmonton, Canada

Palmer T. N., R. Buizza, M. Leutbecher, R. Hagedorn, T. Jung, M. Rodwell, F. Vitart, J. Berner, E. Hagel, A. Lawrence, F. Pappenberger, Y-Y. Park, L von Bremen, and I Gilmour, 2007: The ECMWF ensemble prediction system:Recent and on-going developments ECMWF research department technical memorandum no. 540, ECMWF: Shinfield Park, Reading,U.K.

Pennelly, G. Reuter, and T. Flesch, 2014: Verification of the WRF model for simulating heavy precipitation in Alberta. Atmospheric Research. 135–136, 1/2014:172–192

Phillips, D., 2013. Canada's Top 10 Weather Stories for 2013. Environment Canada. Available at http://www.ec.gc.ca/meteo-weather/default.asp?lang=En&n=5BA5EAFC-1

Reuter, G. W. and C. D. Nguyen, 1993: Organization of the Cloud and Precipitation in an Alberta Storm. Atmospheric Research, 30, 127-141

Roberts, N.M. and H.W. Lean, 2008: Scale-Selective Verification of Rainfall Accumulations from High-Resolution Forecasts of Convective Events, Mon. Wea. Rev., 136, 78-97

Rodwell, M. J., D. S. Richardson, T. D. Hewson, and T. Haiden, 2010: A new equitable score suitable for verifying precipitation in numerical weather prediction, Q. J. R. Meteorol. Soc., 136, 1344–1363

Roebber, P.J. and L.F. Bosart, 1998: The Sensitivity of Precipitation to Circulation Details. Part I: An analysis of Regional Analogs, Mon. Wea. Rev.,126, 437-455

Rotach, M. W., and D. Zardi, 2007: On the boundary-layer structure over highly complex terrain: Key findings from MAP. *Quart. J. Roy. Meteor. Soc.*, **133**, 937–948

Skamarock, W.C., J.B. Klemp, J. Dudhia, D.O. Gill, D.M. Barker, M.G. Duda, X.Y. Huang, W. Wang, J.G. Powers, 2008: A Description of the Advanced Research WRF Version 3, NCAR technical note NCAR/TN-475+STR, 113 pp

Smagorinsky, J., 1963: General circulation experiments with the primitive equations. *Monthly Weather Review*, **91**, 99–164

Smith, S. B., and M. K. Yau, 1987: The mesoscale effect of topography on the genesis of Alberta Hailstorms. Beitr. Phys. Atmosph., 60, 371-392

Szeto, K.K., W. Henson, R. Stewart and G. Gascon. 2011. "The Catastrophic June 2002 Prairie Rainstorm." *Atmosphere-Ocean*, 49:4, 380-395

Thompson, G., P.R. Field, R.M. Rasmussen, and W.D. Hall, 2008: Explicit forecasts of winter precipitation using an improved bulk microphysics scheme. Part II: Implementation of a new snow parameterization. Mon. Weather Review., 136, 5095-5115

Verschuren, J. P., and L. Wojtiw, 1980: Estimate of the maximum probable precipitation for Alberta river basins. Alberta Environment, Hydrology Branch, RMD-80/1, Edmonton, Alberta, 307 pp.

Wang, W. and N. S. Seaman, 1997: A Comparison Study of Convective Parameterization Schemes in a Mesoscale Model, Mon. Wea. Rev., 125, 252-278

Warner, L. A., 1973: Flood of June 1964 in the Oldman and Milk River basins, Alberta. Environment Canada. Technical Bulletin No. 73 (Inland Water Directorate). 89 pp.

Weigel, A. P., F. K. Chow, and M. W. Rotach, 2007a: On the nature of turbulent kinetic energy in a steep and narrow alpine valley. *Bound.-Layer Meteor.*, **124**, 269–290

Weigel, A. P., F. K. Chow, and M. W. Rotach, 2007b: The effect of mountainous topography on moisture exchange between the "surface" and the free atmosphere. *Bound.-Layer Meteor.*, **125**, 227–244

Xue, M., K. K. Droegemeier, and V. Wong, 2000: The advanced regional prediction system (ARPS) - a multi-scale non-hydrostatic atmospheric and prediction tool - Part I: Model dynamics and verification. *Meteor. Atmos. Phys.*, **75**, 161–193

Xue, M., K. K. Droegemeier, V.Wong, A. Shapiro, K. Brewster, F. Carr, and D.Weber, 2001: The advanced regional prediction system (ARPS) - a multi-scale non-hydrostatic atmospheric and prediction tool - Part II: Model physics and applications. *Meteor. Atmos. Phys.*, **76**, 143–165

Yu, L., X. Jin, and R. A. Weller, 2008: Multidecade Global Flux Datasets from the Objectively Analyzed Air-sea Fluxes (OAFlux) Project: Latent and sensible heat fluxes, ocean evaporation, and related surface meteorological variables. Woods Hole Oceanographic Institution, OAFlux Project Technical Report. OA-2008-01, 64pp.